Norwegian University
of Life Sciences

Master's Thesis 2019   60 ECTS
Faculty of Chemistry, Biotechnology and Food science (KBM)

Discovery, expression, and characterization of novel laccases derived from marine bacteria

Priscilla Cassandra Neeraas

Biotechnology

Discovery, expression and characterization of novel laccases derived from marine bacteria

Master Thesis
Priscilla Cassandra Neeraas

SINTEF Industry, Department of Biotechnology and
Nanomedicine

Department of Chemistry, Biotechnology and Food Science

The Norwegian University of Life Sciences

2019

Acknowledgements

Priscilla Cassandra Neeraas

Ås, 14.05.19

Abstract

Lignocellulose is the most abundant biomass on Earth and is primarily composed of three organic polymers; cellulose, hemicellulose, and lignin. Established technology exists to produce useful products such as fuels and chemicals from cellulose and hemicellulose. However, lignin has today still limited use for value creation. Every year, vast amounts of lignin is produced as an industrial byproduct, especially in the pulp and paper industry where about 98% of the material is burned to produce energy. The dependence on fossil resources to make fuels, chemicals and consumer goods has devastating effects on the environment, and growing concerns have resulted in an increasing demand for greener and more sustainable products. In a biorefinery setting, lignin has the potential to be used for the production of a range of bio-based chemicals and materials, and the use of enzymes for lignin valorization is considered a promising approach in the biorefinery industry.

Laccases are multi-copper oxidases that catalyze the one-electron oxidation of a variety of small phenolic substances, with simultaneous reduction of molecular oxygen to water. Bacterial laccases have been shown to depolymerize lignin through mediator substances, in so-called laccase-mediator systems (LMS). Mediators are thereby small phenolic substances that can be oxidized by laccase followed by non-enzymatic oxidation and breakdown of lignin. Despite of their advantages, known bacterial laccases still lack behind their fungal counterparts with respect to potency to degrade lignin. Therefore, discovery of new and engineering of known bacterial laccases are needed to efficiently apply them in lignin depolymerization and upgrading at large scale.

This study targeted both the discovery and description of new, and the engineering of a well-established bacterial laccase for potential future uses in this field. The work performed has resulted in in-depth knowledge about four newly discovered laccases from marine *Actinobacteria* with high thermotolerance and the potential to act as lignin degraders in a laccase-mediator system. Following substrate screening of a variety of small phenolic substances, one candidate, P20-F12, was observed to oxidize four potential mediator compounds. In efforts to develop a spectrophotometric assay for lignin degradation by LMS, the use of two mediators (ABTS and sinapic acid) was attempted. However, conversion of both mediators interfered with the spectrophotometric detection of lignin oxidation. Further work is

needed to establish a reliable assay to monitor lignin oxidation, e.g. involving mass spectrometry.

Vanillin has been observed to be directly derivable from Kraft lignin, and can hence function as a potential laccase mediator in lignin depolymerization. The highly thermostable laccase CotA, originating from *Bacillus subtilis*, underwent site-directed mutagenesis in an attempt to make the enzyme active against vanillin. Several amino acid mutations were suggested based on the substrate-binding of sinapic acid, which shares structural similarities with vanillin. Combining the two amino acid mutations P226M and L386A in CotA resulted in loss of activity towards the synthetic substrate ABTS, while each single mutation allowed the enzyme to retain its activity towards ABTS. The CotA variants were still not active against vanillin but lay the basis for further engineering on the way to the final aim of efficient vanillin oxidation by CotA.

The findings from the research performed, underline that bacterial laccases have potential to be used as lignin degraders in a laccase-mediator system. However, further research is necessary to characterize the four *Actinobacteria* laccases more extensively in terms of their stability in efficient enzyme systems for lignin degradation. Further research should in particular include the search for and engineering of bacterial laccases with higher enzymatic efficiency, and the four newly discovered *Actinobacteria* laccases could represent new basis for enzyme engineering through site-directed mutagenesis and molecular evolution. For that, it would also be expedient to develop new lignin assays that allow the rapid detection of lignin oxidation and breakdown.

Sammendrag

Lignocellulose er den mest rikelige formen for biomasse på jorda og er primært bygget opp av tre organiske polymerer; cellulose, hemicellulose, og lignin. Veletablerte teknologier eksisterer for å produsere nyttige produkter slik som brensel og kjemikalier fra cellulose og hemicellulose. Lignin, derimot, har i dag begrenset bruk som nyttelses produkter. Hvert år produseres det store mengder lignin som industrielt biprodukt, spesielt i papir industrien hvor omtrent 98% av materialet blir brent for energiproduksjon. Avhengigheten av fossile ressurser for å lage brensel, kjemikalier, og forbruksvarer har ødeleggende effekt på miljøet, og økende bekymring har resultert i økt etterspørsel etter grønnere og mer bærekraftige produkter. I en bioraffineri setting har lignin potensiale til å bli brukt i produksjonen av en rekke bio-baserte kjemikalier og materialer, og bruk av enzymer for lignin foredling er sett på som en lovende tilnærming i bioraffineri industrien.

Lakkaser er multi-kobber oksidaser som katalyserer enkelt-elektron oksidering av en rekke små fenoliske substanser, samtidig som molekylært oksygen blir redusert til vann. Bakterielle lakkaser har blitt påvist evnen til å de-polymerisere lignin gjennom mediator substansers i et såkalt lakkase-mediator system. Mediatorer er små fenoliske substanser som kan bli oksidert av lakkaser og som deretter kan bryte ned lignin gjennom en ikke-enzymatisk reaksjon. Til tross for deres fordeler, er ikke bakterielle lakkaser like potente lignin-nedbrytere som fungale lakkaser. Derfor er oppdagelse av nye, og utvikling av allerede kjente lakkaser nødvendig for å effektivt kunne utnytte de i lignin depolymerisering.

Denne studien tar for seg både oppdagelse og beskrivelse av nye lakkaser, samt utvikling av vell-etablerte bakterielle lakkaser for potensiell bruk i dette feltet. Arbeidet som har blitt utført har resultert i økt kunnskap og forståelse om fire nylig oppdagede lakkaser fra marine *Actinobacteria* med høy thermotoleranse og potensialet til å fungere som lignin nedbrytere i et lakkase-mediator system. Etter screening av små fenoliske forbindelser ble det observert at en av de fire lakkase kandidatene, P20-F12, kunne oksidere fire av disse potensielle mediatorene. I et forsøk på å utvikle et spektrofotometrisk assay for lignin degradering i et lakkase-mediator system ble to mediatorer (ABTS og sinapinsyre) forsøkt brukt. Oksidering av begge mediatorene forstyrret spektrofotometrisk deteksjon av lignin oksidasjon. Videre arbeid er derfor nødvendig for å kunne etablere et pålitelig assay som tillater overvåkning av lignin oksidasjon, for eksempel ved å involvere masse spektrometri.

Vanillin har blitt observert som en av bestanddelene i Kraft lignin, og kan derfor fungere som en potensiell lakkase mediator i lignin nedbrytning. Den thermostabile lakkasen CotA, med opphav fra *Bacillus subtilis*, undergikk sete-spesifikk mutagenese i et forsøk om å gjøre CotA aktiv mot vanillin. Flere aminosyre-mutasjoner ble foreslått basert på substrat-binding med sinapinsyre, som har strukturelle likheter med vanillin. En kombinasjon av de to aminosyre mutasjonene P226M og L386A resulterte i at CotA mistet aktivitet mot det syntetiske substratet ABTS, mens hver enkeltmutasjon resulterte i at CotA fortsatt hadde aktivitet mot ABTS. Ingen av CotA variantene hadde blitt aktive mot vanillin, men la grunnlaget for videre utvikling i veien mot effektiv vanillin oksidasjon av CotA.

Funnene som ble gjort i denne studien understreker at bakterielle lakkaser har potensiale til å bli brukt som lignin nedbrytere i et lakkase-mediator system. Videre undersøkelser er derimot nødvendige for å karakterisere de fire *Actinibacteria* lakkasene mer omfattende, i form av deres stabilitet i effektive enzym systemer for lignin nedbrytning. Videre arbeid burde særdeles inkludere søk etter og utvikling av bakterielle lakkaser med høyere enzymatisk effektivitet, og de fire nylig oppdagede *Actinobacteria* lakkasene kan representere grunnlaget for enzym utvikling gjennom sete-spesifikk mutagenese, og molekylær utvikling. Det et også være hensiktsmessig å utvikle lignin assay som tillater rask deteksjon av lignin oksidasjon og nedbrytning.

Abbreviations

ABTS	2,2-azino-bis(3-ethylbenzothiazoline-6-sulphonic acid)
ddH$_2$O	Double distilled water
HRP	Horse-radish peroxidase
IPTG	Isopropyl β-D-1-thiogalactopyranoside
IMAC	Immobilized metal affinity chromatography
kDa	Kilo Dalton
LMCO	Laccase-like multi-copper oxidase
LMS	Laccase-mediator system
MCO	Multi-copper oxidase
MW	Molecular weight
PDB	Protein Data Bank
SDS-PAGE	Sodium dodecyl sulphate-polyacrylamide gel electrophoresis
SLAC	Small laccase
V	Volt

Table of contents

1. Introduction

1.1. The need for renewable resources

Fossil resources have contributed to higher living standards for the human population, which in turn have made it possible for the population to expand from 1 billion in 1820 to approximately 7.6 billion today. Throughout history the human society has built infrastructure that is heavily dependent on fossil resources in order to function properly, including daily activities of industry, commerce, and private life ("Oil and Natural Gas Depletion and Our Future" 2007).

The main resources for the world energy and chemical building block supply are the finite fossil resources crude oil, coal and gas, and the dilemma concerning when the fossil reserves will be depleted is a fundamental question that needs to be answered (Shafiee and Topal 2009). Conventional oil production must eventually decline to near zero, and maintaining growth and supply has been a reoccurring concern for over 50 years (Miller and Sorrell 2014). Shafiee and Topal presented in 2009 calculations concerning expected time perspectives of when the three fossil resources will be completely depleted. The depletion times for oil, coal and gas were found to be approximately 35, 107, and 37 years, respectively, meaning that coal reserves will be available up to year 2112 and will be the only fossil fuel available after 2042 (Shafiee and Topal 2009). However, the development of renewable alternatives could further prolong availability of oil coal and gas.

The dependence and development of society built on the use of petroleum to make fuels, chemicals and consumer goods has a devastating effect on the environment, releasing large amounts of greenhouse gases through combustion, contributing to temperature rise of the atmosphere and the ocean(Oreskes 2004), massive plastic pollution threatening the marine environment (Xanthos and Walker 2017), and air pollution from motor traffic, industry, power plants, and domestic fuels which can cause adverse human health effects (Mayer 1999). The detrimental effects of greenhouse gas emissions from fossil fuels are well documented, and the need for novel sources of energy and chemicals that can replace petroleum is of the highest necessity to preserve the planet and retain societal development. Mass consumption of materials based on petroleum has given environmental problems that also threatens human beings. This growing concern has resulted in society demanding green and sustainable products. Alternative

solutions need to be utilized to develop sustainable products, like new bio-based polymers for bioplastics, derived from renewable resources in order to decrease the dependence on fossil resources (Isikgor and Becer 2015). Biomass and biomass derived materials are considered to be one of the most promising alternatives, because they are generated from available CO_2 through photosynthesis. Therefore, biomass is considered to be a sustainable source for organic carbon with net zero carbon emission (Isikgor and Becer 2015). The most abundant and bio-renewable resource is lignocellulose which can be processed in different ways to give a variety of products that can replace petroleum-based products (Chio, Sain, and Qin 2019).

Biorefining is a process that integrates biomass conversion to produce fuels, power and chemicals from biomass (Luo, van der Voet, and Huppes 2010). The development of biorefining combining genetics, biotechnology, process chemistry and engineering has made it possible to convert renewable biomass to valuable fuels, chemicals and products(Yang et al. 2014). Petroleum-based refineries that produce petrochemicals are fed with crude oil, whereas in the future it is anticipated that biorefineries will produce many bio-based products from plant biomass (FitzPatrick et al. 2010) (Figure 1.1). In order to reach this future perspective, cheap and effective biotechnological processes capable of plant biomass hydrolysis and target chemical production must be developed (Hasunuma et al. 2013).
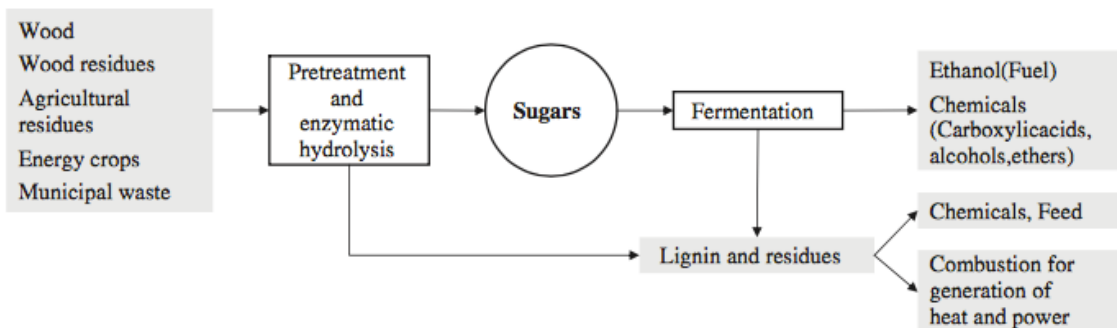
Figure 1.1. Overview of a biorefinery producing fuel, chemicals and energy from various lignocellulosic materials. Adapted from (Jørgensen, Kristensen, and Felby 2007).

2

1.2. Plant biomass

Plant biomass is formed through photosynthesis and one of the dominant photosynthetic products are carbohydrates. These carbohydrates can be converted to biofuels and chemicals through different approaches, and efficient methods for converting sugars or starch-based biomass to hydrocarbons have already been developed (Dusselier, Mascal, and Sels 2014). The main advantage of hydrocarbon products is that they are already well integrated as fuels in today's automotive infrastructure. However, industrially produced ethanol and biodiesel derived from sugars and starches, also referred to as first generation biofuels, competes with the demand for human consumption and animal feed. The non-edible plant biomass lignocellulose, has therefore been suggested as an alternative sustainable 2nd generation feedstock for biofuel and chemical industries (Kang and Lee 2015).

1.2.1. Lignocellulose

Wood and other plant biomass contains a composite material called lignocellulose which is the most abundant form of biomass on Earth (Zhang, Song, and Han 2016). Lignocellulose is primarily constructed from three organic polymers; cellulose, hemicellulose, and lignin (Figure 1.2) and smaller amounts of pectin, protein, extractives and ash. Cellulose, hemicellulose and lignin are found in varying relative compositions in different plants depending on the plant species, age and growth conditions, forming the structural framework of the plant cell wall (Jørgensen, Kristensen, and Felby 2007). In general, the weight percentage of wood biomass contains 30-50% cellulose, 20-35% hemicellulose, and 15-30% lignin (Anwar, Gulfraz, and Irshad 2014). Cellulose is the main component in plant cell walls forming a crystalline microfibril that consists of β-1,4-linked D-glucose chains. Hemicellulose is a branched polymer made up of different types of monosaccharide sugars including pentoses, hexoses and uronic acids. The hemicellulose backbone consists of either a homo- or heteropolymer with branches linked by β-1,4-glycosidic bonds and occasionally β-1,3-glycosidic bonds (Bajpai 2016). Lignin is a large, complex molecular structure built up of cross-linked polymers of phenolic monomers. In plant cell walls, lignin provides a rigid resistance layer against microbial attacks and for structural support (Bajpai 2016).

Lignocellulose is made up of an average of 75% carbohydrates, which in the near future will become an essential source for fermentable carbohydrates which may form the basis of liquid

biofuel production for the transport sector as well as a variety of commodity chemicals and bio-based and biodegradable materials (Jørgensen, Kristensen, and Felby 2007).
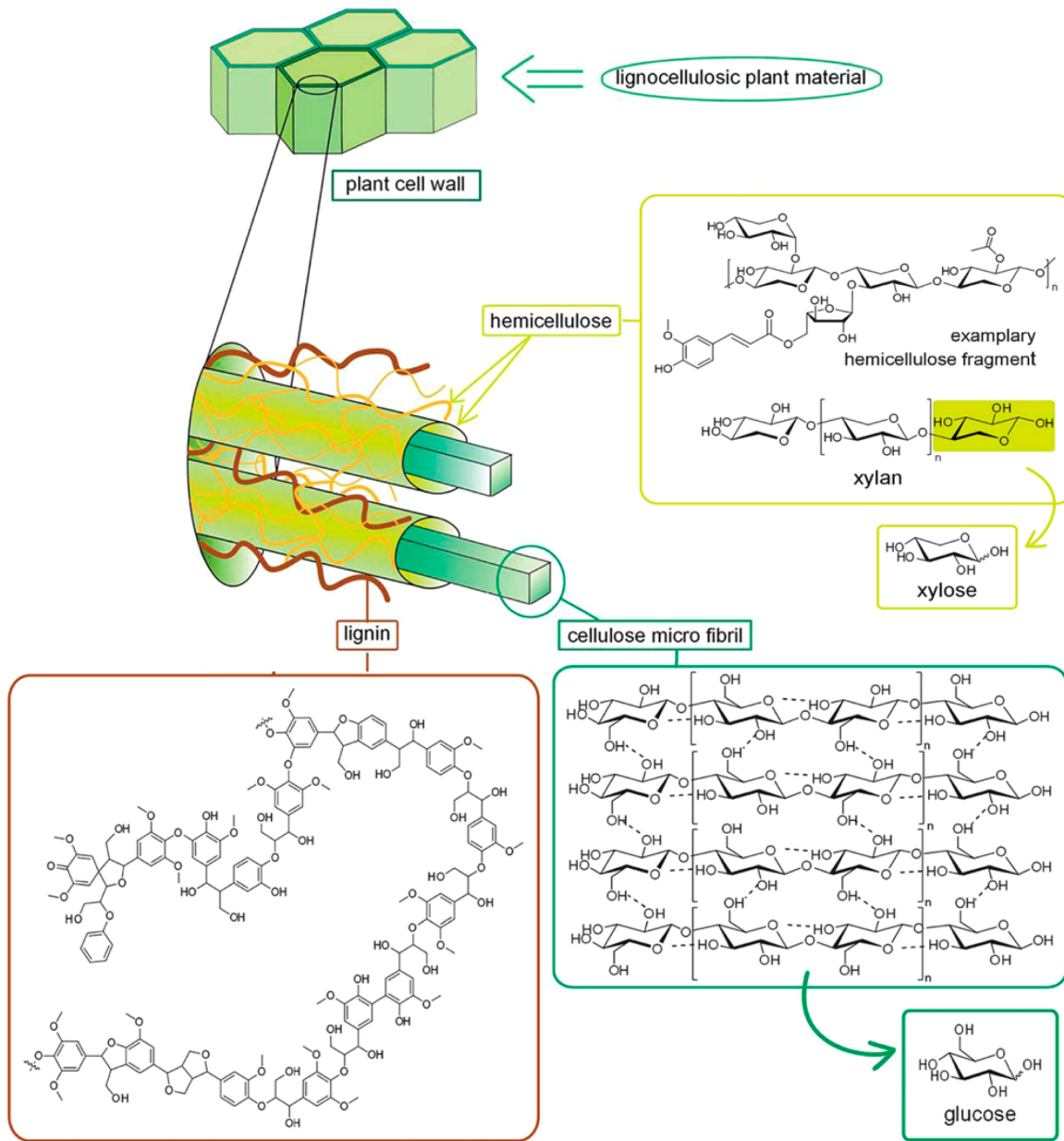
Figure 1.2: Illustration of the three different main components of lignocellulose, **i.e. cellulose, hemicellulose and lignin.** Adapted from (Zhang, Song, and Han 2016)

1.3. Lignin

Lignin is an aromatic polymer found in all terrestrial plants and is the most complex biopolymer found in plant cell walls. This phenolic polymer is derived from three aromatic alcohols, also called monolignols, namely *p*-coumaryl alcohol, coniferyl alcohol and sinapyl alcohol (Figure 1.3) (Lu and Ralph 2010). These three building blocks are linked together in a variety of ether

and carbon-carbon intermolecular linkages or bonds creating a complex and highly branched network. Unlike cellulose and hemicellulose that have a distinct structure, lignin has no repeating multiunit structure and its composition varies depending on their origins, which makes it difficult to give lignin a definition based on its structural features. Lignin is difficult to decompose with a single chemical, enzymatic or microbiological method, traits that provides lignin with high capacity to withstand mechanical, chemical and biological degradation in nature (Fang and Smith, 2016). Lignin does not only provide the plant cell wall with mechanical strength, but it also contributes to hydrophobicity in cell walls of xylem in woody biomass, a feature that is considered to be important for the process of water transport, binding and encrusting (Anwar, Gulfraz, and Irshad 2014).
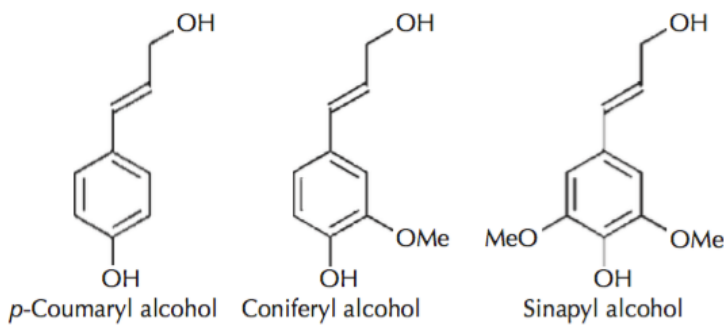
Figure 1.3. The three lignin monomers p-coumaryl alcohol, coniferyl alcohol, and sinapyl alcohol. Adapted from (Lu and Ralph 2010)

1.3.1. Applications of lignin

Decomposing lignin with a single enzyme or chemical is not an easy task due to its macromolecular structure that is highly irregular as well as having different types of ether and carbon-carbon linkages (Parthasarathi et al. 2011) (Figure 1.4). In a biorefinery, lignin has the potential to be used for the production of chemicals and lignin-based materials. Technical lignin is highly underexploited and can for instance be found in the paper and pulping- and biofuels industries.
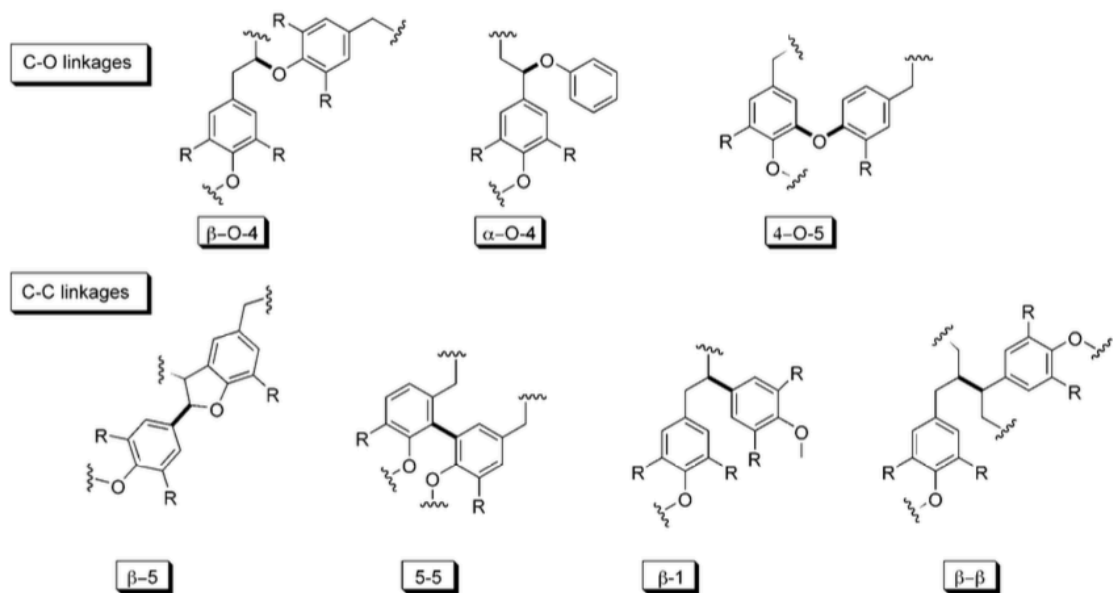
Figure 1.4. Overview of C-O and C-C linkages between monolignols. Adapted from (Calvo-Flores and Dobado 2010).

The paper industry produces a vast amount of lignin every year, and about 98% of the material is burned as an energy recovery step in the same factories as it is produced (Calvo-Flores and Dobado 2010). There are several lignin preparations that are commercially available, and the main lignin preparations are Kraft lignin, lignosulfonates, organosolv lignin, and steam-exploded lignin. Kraft lignin is generated during the conversion of wood into pulp in the pulp and paper industry, where the *Kraft* process results in a black liquor typically containing 30-34% lignin (Silva et al. 2009). This stream, in a conventional process, is burned to provide energy used in mill operations and to recover chemicals used during the *Kraft* process. Burning the black liquor results in loss of organic compounds, including lignin, that has the potential to be converted to many valuable substances or materials, such as activated carbon, dispersing agents, synthetic tannins, vanillin, vanillic acid, etc. (Silva et al. 2009). Waste liquid from softwood are used to produce lignosulfonates, using salts or sulfurous acids to extract the lignin from wood during a sulfite-pulping procedure. Lignosulfonates are soluble in water and chemically modified with sulfonate groups, carbohydrates, inorganic compounds, and small amounts of wood extracts. They are mainly prepared as calcium, ammonium, and magnesium salts. Lignosulfonates are non-hazardous and can be used as binders, dispersant agents for pesticides, and emulsifiers (Calvo-Flores and Dobado 2010). Organosolv lignin is the product when lignin is extracted from biomass with the use of organic solvent or water mixtures at high temperature/pressure. The obtainment of organosolv lignin with the Organosolv process is

especially attractive as it provides lignin that is highly fluid, which can easily be fed into oven combustion chambers for energy production. In addition, organosolv lignin contains less ash compared to other types of technical lignin, which facilitates its combustion (de la Torre et al. 2013). When wood biomass is treated with steam at high temperature and pressure followed by decompression, lignin is partially hydrolyzed, resulting in steam-exploded lignin, a water-soluble material with low levels of carbohydrate and wood-extractive impurities. Steam-explosion can be combined with enzymatic hydrolysis, resulting in carbohydrates that can be used for fermentation (Calvo-Flores and Dobado 2010).

The renowned biorefinery Borregaard, located in Sarpsborg, Norway, is one of the world's leading suppliers of lignin-derived vanillin supplied from wood, in addition to commercializing a range of other lignin-derived products, including lignosulfonates for the concrete industry. The vanillin product is primarily used in foods like chocolate, dairy products and bakery products, but also as raw material in the pharmaceutical industry. Today lignin has limited applications, but there are three main areas where end-uses of technical lignin or lignin derivatives are applied: energy, renewable chemicals, and materials and additives (Amezcua-Allieri and Aburto 2017).

In a biorefinery context lignin is regarded as a recalcitrance factor, but it is also considered to be an important component of the economic aspects of a biorefinery. Depolymerization of lignin has the potential to enable higher value-added products for various industries, but in order to achieve properties desirable for industrial applications, lignin needs to be fragmented to a lower molecular weight. The main obstacles of lignin valorization are its diverse structure and poor solubility. Enzymatic degradation of lignin has long been considered to be applied in the industry, because the catalytic process performed by enzymes occurs in water and under mild conditions, which in turn avoids high pressure and temperatures, and toxic and expensive chemicals. The utilization of enzymes for lignin depolymerization gives rise to new opportunities for biorefinery lignin valorization with economic feasibility (Hämäläinen et al. 2018).

1.3.2. Fungal and bacterial degradation of lignin

Wood is naturally degraded by organisms in nature through different catabolic pathways that involve enzymes. Not many organisms have the ability to degrade lignin, but certain fungi and bacterial species have been found to do so with different levels of efficiency where fungi are more efficient in lignin delignification than bacteria, where it occurs slower and more limited (Janusz et al. 2017).

Wood degrading fungi are mainly divided into three main groups; white-rot fungi, brown-rot fungi and soft-rot fungi. Most of them come from the phyla Basidiomycota and Ascomycota. Basidiomycetous white-rot fungi can selectively degrade lignin without breaking down cellulose and hemicellulose and are therefore the most studied lignin-degrading organism (Fang and Smith, 2016). Lignin degrading bacteria are represented in Actinomycetes, α-Proteobacteria and γ-Proteobacteria. These microbial groups are widely distributed in ecosystems worldwide and can be found in both terrestrial and aquatic habitats. An interesting trait is their resemblance with filamentous fungi due to their apical and branching growth, morphogenic development, and production of aerial or substrate mycelia. Production of secondary metabolites and extracellular enzymes makes these bacterial species considered to be major decomposers of lignocellulose in soil (Janusz et al. 2017).

Four enzyme systems have over the years been reported to depolymerize lignin in decaying plant cell walls, including lignin peroxidases (LiPs), manganese peroxidases (MnPs), versatile peroxidases (VP), and laccases, gaining attention for being considered potential biological catalysts for lignin degradation (Pollegioni, Tonin, and Rosini 2015).

LiPs have a very high redox potential at 1.2 V at pH 3.0 compared to laccases that has a redox potential of 0.8 V at pH 5.5 which enables LiP to catalyze the oxidation of non-phenolic aromatic compounds. MnP is a heme protein and represents the most common peroxidase produced by almost all wood-colonizing basidiomycetes. In the presence of 0.2 mM manganese at pH 4.5 and 37 °C, MnP was able to depolymerize and repolymerize synthetic lignin molecules. VP has a broad substrate preference and shares typical features of fungal MnP and LiP. The activity of VP has been identified in white-rot fungi, and has a high redox potential of >1.4 V. Laccase enzymes have moderately low redox potentials varying from 0.42-0.79 V and oxidize phenolic compounds through a four-electron substrate oxidation reaction using

molecular oxygen (O_2) as final electron acceptor with the simultaneous production of H_2O as the only side-product (Pollegioni, Tonin, and Rosini 2015).

Due to its properties, lignin processing often requires harsh chemical treatments which would require enzymes that are capable of withstanding such conditions in order to have industrial applications. Fungal laccases are usually not stable in harsh conditions such as extreme temperatures, pH, high salt concentrations, etc. The production of fungal laccases is also challenging due to the accumulation of large amounts of fungal biomass. Bacterial production of laccases is preferred because they have several significant properties that are not characteristic for fungi, such as stability at high temperatures and pH, salt tolerance etc. (Sondhi et al. 2014).

1.3.2.1.   *Psychrobacter* species

The genus *Psychrobacter* comprises of Gram negative bacteria that have a spherical to rod-shaped form, are strictly aerobic, and are chemotrophic, nonmotile, osmotolerant, and cold-adapted (Bowman 2006). Since the description of the first *Psychrobacter* species, *Psychrobacter immobilis* in 2003, several species have been isolated from natural environments including sea ice and krill, deep-sea environments, and Antarctic ornithogenic soils (Bozal et al. 2003), showing that cold environments constitute their ecological niche. They can grow at low temperatures and tolerate a wide range of salt concentrations.

Cold-adaptive enzymes have a high potential in biotechnological applications, with high k_{cat} at low temperatures, high thermolability at rising temperatures and ability to be active in organic solvents. (Cavicchioli et al. 2011). These enzymes can minimize unwanted chemical reactions that could occur at higher temperatures, they can be used with substrates that are heat sensitive, and they are quickly inactivated with heating, properties that can be used in the food industry and in molecular biosciences. A recent study (Moghadam et al. 2016) describes the discovery of four arctic marine *Psychrobacter* strains that exhibit extracellular laccase activity and their potential as cold-active biocatalysts. There is little to no information regarding studies of lignin degradation by *Psychrobacter* species, but Moghadam et al. 2016 have discovered and sequenced four new *Psychrobacter* strains where a total of six laccase like multicopper oxidase (LMCO) genes were identified in the sequences of the new *Psychrobacter* strains. Analysis of

the amino acid sequences of the six LMCOs revealed the presence of conserved copper binding sites of 3-domain laccases (see section 1.4.1) Work on the production and characterization of three of these *Psychrobacter* laccases, P2G3, P11G3 and P11F6, is included in this study.

1.3.2.2. Actinobacteria

Actinobacteria is one of the largest bacterial phyla and consist of Gram-positive bacteria with a high G+C content ranging from 50% up to more than 70% (Ventura et al. 2007). They exhibit a wide morphological variety from coccoid to fragmenting hyphal forms, and they have diverse metabolic and physiological properties such as the formation of different secondary metabolites and the production of extracellular enzymes. Many of the metabolites are potent antibiotics. The genus *Streptomyces* of the *Actinobacteria* is being widely exploited by the pharmaceutical industry due to its antibiotics producing traits. *Actinobacteria* can be found in both terrestrial and aquatic ecosystems, and have adapted to a wide range of ecological environments, making them a very diverse phylum (Barka et al. 2016). Most of them are saprophytic, soil-dwelling organisms spending most of their lives as semi-dormant spores, but they are also adapted to live in soils, fresh and saltwater, and even air. *Actinobacteria* are mostly mesophilic with an optimum growth temperature between 25 to 30 °C, but some are thermophilic and can grow at temperatures as high as 50 and 60 °C.

It is considered that *Actinobacteria* are of great importance in degradation of recalcitrant and complex polymers that are found naturally in litter and soil, such as humic acid and lignin (Fernandes et al. 2014). Studies concerning laccases from *Actinobacteria* are scarce, but several two-domain small laccases (see section 1.4.3.3) have been characterized in a variety of *Streptomyces spp*. In addition to possessing unique antibiotic biosynthetic pathways, it has been stated that *Actinobacteria* have the ability to produce enzymes attractive for biotechnological applications, with one area of focus being the production of laccases for potential degradation of lignin (Fernandes et al. 2014).

1.4. Multi-copper oxidases

The protein super family of multi-copper oxidases (MCOs) comprises multi-copper proteins that catalyze the one electron oxidation of different aromatic and non-aromatic compounds

while simultaneously generating two water molecules by the reduction of molecular oxygen (Claus 2004). The oxidation occurs in a mononuclear copper center T1, and the electrons are then transferred to a trinuclear copper center T2/T3 where dioxygen is reduced, yielding two water molecules (Figure 1.5). MCOs are classified according to the number of domains in their structure, either as three-domain, six-domain or two-domain structures (Figure 1.6) (Komori and Higuchi 2015).
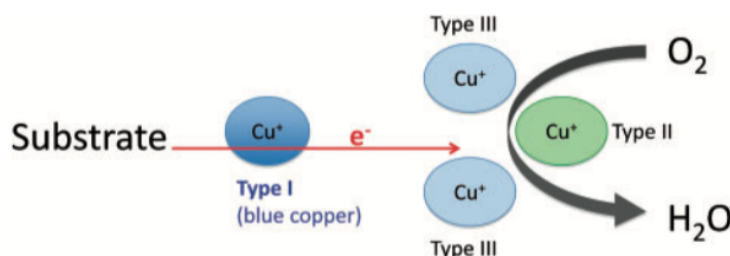
Figure 1.5: Schematic overview of the one electron oxidation of MCO substrate, simultaneously reducing molecular oxygen to water. Adapted from (Komori and Higuchi 2015).
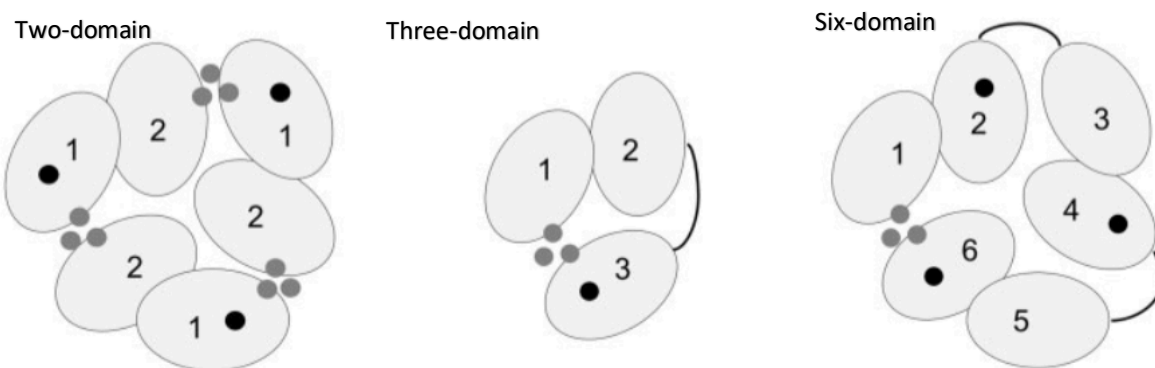
Figure 1.6. Overview of the structures of two-domain, three-domain, and six-domain MCOs. The two-domain MCOs forms a trimer of two domain subunits. The three-domain and six-domain MCOs are single chain proteins. The black circles indicate the type I copper center, and the grey circles indicate the type II and III copper centers. Adapted from (Komori and Higuchi 2015).

The sequence homology among MCOs is low, but the overall structure and the active site is highly conserved. There are four copper molecules in the active site responsible for the substrate oxidation. They are organized in four strictly conserved motifs in the primary amino acid sequence HXHG, HXH, HXXHXH and HCHXXXHXXXXM/L/F (Reiss et al. 2013). The T1 copper atom is coordinated by two histidine residues and one cysteine residue, forming a metallo-organic bond. In close proximity to the T1 copper site, the side chains of a methionine,

a leucine or isoleucine can be found. The T2 copper is coordinated by two histidine residues, and the two T3 copper atoms are coordinated by a total of six histidine residues (Figure 1.7).
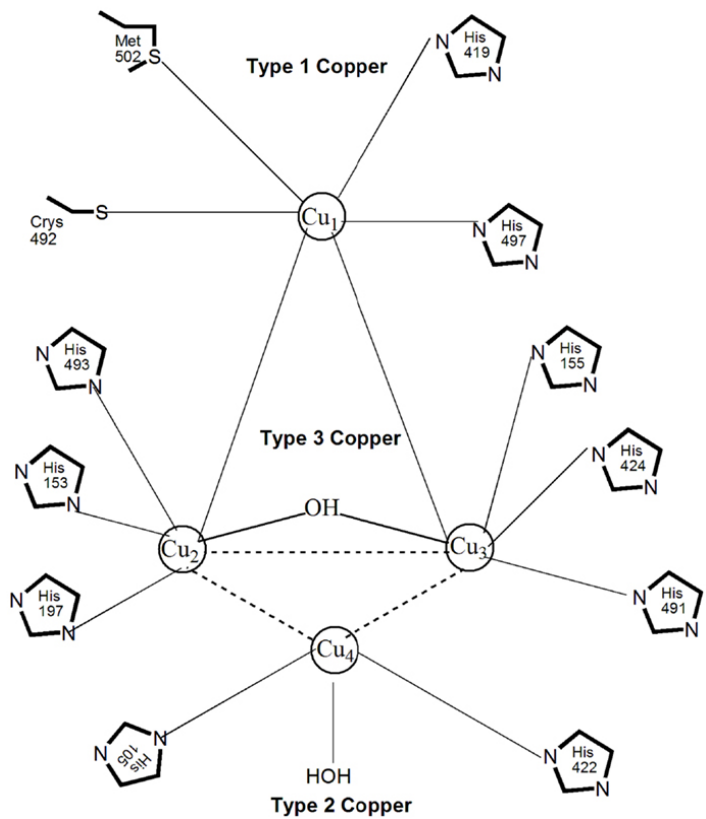
Figure 1.7. Schematic overview of the coordination of the T1, T2 and T3 copper atoms in a multi-copper oxidase. Adapted from (Christopher, Yao, and Ji 2014).

The reduction of molecular oxygen to water is thought to occur through two different reaction intermediates; a peroxide intermediate (intermediate I) and a native intermediate (intermediate II) (Komori and Higuchi 2015). Substrate oxidation occurs in the T1 copper site as a one-electron oxidation. In order to reduce all the copper atoms in the active site, four one-electron oxidations must occur. The fully reduced MCO transfers two electrons to molecular oxygen, forming a peroxide intermediate. The other two electrons are then transferred to the peroxide intermediate, forming the native intermediate (Figure 1.8). The native intermediate is then converted to H_2O via proton assisted steps (Figure 1.8) (Vashchenko and MacGillivray 2013).
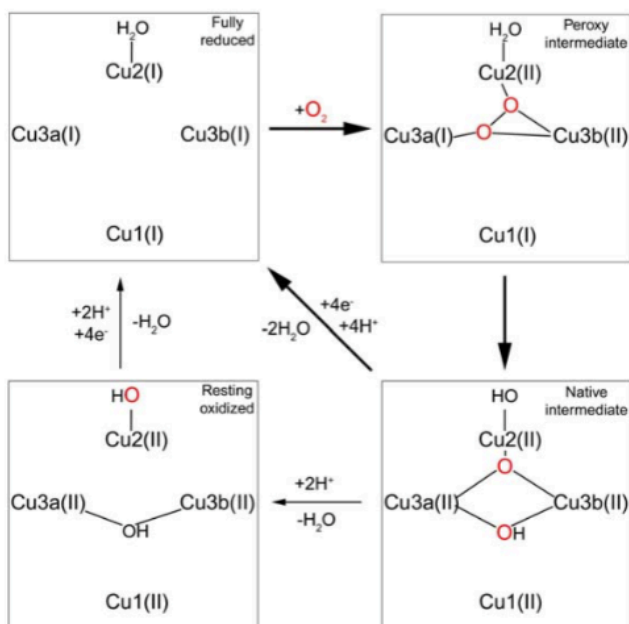
Figure 1.8. Schematic overview of the reaction mechanism of the reduction of molecular oxygen to water in the MCO active site. The broad arrows represents the steps occurring in the catalytic cycle of MCOs, and the thinner arrows represents steps that can be experimentally observed, and is not part of the catalytic cycle (Vashchenko and MacGillivray 2013).

1.4.1. Laccases and laccase-like multi-copper oxidases (LMCOs)

Laccases are the largest subgroup of MCOs and was first studied in 1849 in the exudates of the Japanese lacquer tree *Rhus vernicifera*, hence the name laccase (Alcalde 2007). They catalyze the one electron oxidation of a variety of phenolic compounds, but also diamines and aromatic amines, while simultaneously reducing molecular oxygen to water. Laccases are usually found in higher plants and fungi but also exists in bacteria and insects (Vashchenko and MacGillivray 2013). Many suggestions have been made concerning laccases biological functions. These include plant wounding response, development of fruiting bodies in fungi, reconstitution of cell walls, and metabolic turnover of soil humic matter. They are also believed to play a role in pathogenesis, sporulation, spore pigmentation, and fungal morphogenesis. Laccases play important roles in several commercial areas such as the food industry, paper and pulp industry, synthetic chemistry, textile industry, cosmetics, and biodegradation of environmental pollutants. (Alcalde 2007).

Bacterial laccases have not yet been shown to depolymerize lignin directly, but it has been demonstrated that they can depolymerize lignin through mediators. Mediators are small phenolic molecules that can be oxidized by laccases followed by non-enzymatic oxidation of lignin (section 1.5). Laccases have been observed to have broad substrate specificity, giving them the potential to degrade lignin in many ways, creating renewable materials from a source that today is usually burned for energy (Bugg et al. 2011).

Today, despite its formal grouping in Enzyme Commission number EC 1.10.3.2, there is no definition of what a true laccase is. The definition is complicated because laccases are a very diverse subgroup of MCOs that spans from plant to fungal to bacterial taxonomic genera (Reiss et al. 2013). Laccases also have a broad range of substrates, both natural and synthetic compounds, making a definition based on substrate inadequate. There has also been made attempts to classify laccases based on sequence analysis, but there are so far no unifying amino acid patterns that can be used for laccase identification. Reiss et al. therefore propose to introduce the term laccase-like MCOs (LMCOs) accounting for the potential multiplicity of the laccase's biological functions.

1.4.2. Fungal laccases

Fungal laccases are involved in several biological functions such as pigment biosynthesis, development of fruiting bodies, sporulation, pathogenesis, and depolymerization of lignin (Gianfreda, Xu, and Bollag 1999). The active site of laccases is relatively conserved with four copper atoms bound to three redox sites (see section 1.4). Laccases are generally divided in three groups concerning their redox potential at the T1 copper site: low (0.4-0.5 V), medium (0.5-0.6 V) and high (0.7-0.8 V), and representative fungal laccases have been characterized for all three groups. The difference in redox potential may be explained by the varying electronic environment of the T1 copper, such as substitution of the methionine side chain by a leucine found in close proximity to the T1 copper site. As a result of the relatively low redox potential of fungal laccases they are only able to oxidize polyphenols, monophenols, amino-phenols and aromatic amines. Previous studies have demonstrated that laccases can oxidize the phenolic units of lignin, by studies on model molecules (Sigoillot et al. 2012).

White-rot fungi are among of the few fungi that can degrade lignin, which results in bleached decayed wood. Fungal lignin degradation involves extracellular heme-peroxidases and laccases

that use H_2O_2 and O_2 as electron acceptors, respectively, where peroxidases oxidize the non-phenolic lignin components and laccases oxidize the phenolic lignin components, indicating a cooperative relationship in order to depolymerize lignin (Sigoillot et al. 2012). The fungus *Trametes versicolor* expresses a laccase that has one of the highest redox potentials among known laccases and is one of the major components of the lignin-degrading system of *T. versicolor*. The redox potential of the extracellular laccase has been found to be 785 mV, and a specific activity of 170 U/mg with the synthetic substrate 2,2-azino-bis(3-ethylbenzothiazoline-6-sulphonic acid) (ABTS) has been measured (Iimura, Sonoki, and Habe 2018).

Fungal laccases have, in previous studies, been shown to mineralize Kraft lignin to significant extent, compared to bacterial laccases where partially degraded and modified lignin occurred (Asina et al. 2016). However, practical challenges concerning fungal protein expression, fungal genetic manipulation, and enzymatic performance loss when exposed to harsh chemicals (Bugg et al. 2011) makes utilization of bacteria laccases for industrial applications more desirable as they are easily genetically modified, more easily produced, and in several cases stable at elevated temperatures (Sondhi et al. 2014).

1.4.3.   Bacterial laccases

1.4.3.1.   CotA

Bacillus subtilis is a spore-forming bacterium that synthesize a protein coat around the developing endospore. The *cotA* gene codes for a protein (CotA) with a size of 65 kDa that is a part of the outer spore coat of *B. subtilis*. The exact function of CotA is not fully understood, but the absence of the protein results in the loss of the brownish pigmentation of the colonies. The CotA protein shows similarities with MCOs, containing the four copper-binding sites with the T1 mono-nuclear copper site and the T2/T3 trinuclear cluster. It has also been reported to be a classical laccase (Hullo et al. 2001).

Copper-incorporation into the CotA laccase has been shown to be a sequential process, with the type 1 copper center being the first, followed by the type 2 and type 3 copper centers (Durão et al. 2008). When CotA laccase from *B. subtilis* is recombinantly produced by *Escherichia coli*, microaerobic conditions have shown to accumulate up to 80-fold more copper than cells

grown aerobically. Even though the total protein content produced under microaerobic conditions is a two-fold lower, the enzymatic activity towards the substrate ABTS is a remarkable nearly 100-fold higher than from cells grown under aerobic conditions.

The CotA laccase has been observed to follow Michaelis-Menten kinetics (see section 1.6) with ABTS at pH 4.0, exhibiting a high turnover number (k_{cat}) = 16.8 s^{-1} at 37 °C. In a temperature stability analysis of recombinant CotA with 1 mM ABTS a temperature optimum at 75 °C was observed. The CotA laccase has also been observed to have high alkali stability, in addition to the high thermal stability, traits that are desirable for industrial applications (Wang et al. 2016).

1.4.3.2.   *Psychrobacter* LMCOs/laccases

Four *Psychrobacter* species with laccase-positive phenotypes have previously been described (Moghadam et al. 2016). Beyond this, information concerning *Psychrobacter* laccases is scarce. A total of six LMCO genes from *Psychrobacter* species has been identified and annotated as copper resistance proteins (CopA), and amino acid sequence analysis revealed the presence of the three conserved T1, T2 and T3 copper binding sites of a three-domain laccase. It was also observed that these laccases did not solely rely on copper for their activity due to the presence of other metal ions in the medium that could possibly also serve as cofactors for laccases, but the highest activities have been observed in the presence of 0.25 mM CuCl$_2$. The four characterized *Psychrobacter* laccases share high amino acid sequence similarity, but considerable differences in the amino acids that form the predicted substrate binding pocket, suggesting that they exhibit different substrate preferences. Further studies are required to evaluate the role of the identified *Psychrobacter* laccases, as well as their biochemical characterization and their potential in biotechnological applications (Moghadam et al. 2016).

1.4.3.3.   Small laccases (SLAC)

Laccases are usually constructed of three domains, where domain one and three contains the copper sites and domain two often helps to form a substrate-binding cleft. The genome of *Streptomyces coelicolor* was found to encode for a laccase, but in contrast to the usual construction of three domains, this laccase was a small, four-copper oxidase that was missing

the second domain(Machczynski et al. 2004). This gave rise to a new family of enzymes known as the two-domain laccases, also called small laccases (SLAC).

Even though SLACs are missing the second domain, they still exhibit significant activity. SLACs have also shown some interesting characteristics such as resistance to detergents and high thermal stability. Its activity towards the substrate 2,6-minethoxyphenol (DMP) reaches its maximum at pH 9.4, suggesting that the enzyme can be suitable for industrial processes. There is still limited information on SLACs from *Streptomyces spp.,* and the enzyme family is still quite underexplored (Dubé et al. 2008).

1.5. Mediators

Laccases have relatively low redox potentials (≤ 0.8 V), restricting oxidation to the phenolic compounds of lignin. Oxidation of non-phenolic lignin moieties can be performed via redox mediators (Pollegioni, Tonin, and Rosini 2015). Mediators are small aromatic molecules which can be oxidized by laccase. The enzyme uses molecular oxygen to oxidize the mediator which subsequently can act as a chemical, non-enzymatic oxidants for lignin (Figure 1.9). This mechanism hinders steric limitations that usually hinders the enzymes oxidation of larger molecules. Mediators also lets laccases overcome their phenolic-substrate restriction which in turn expands the range of lignin units to be oxidized. A few typical laccase mediators are vanillin, syringaldehyde, and 2,2´-azinobis(3-ethylbenzthiazoline-6-sulphonate) (ABTS).
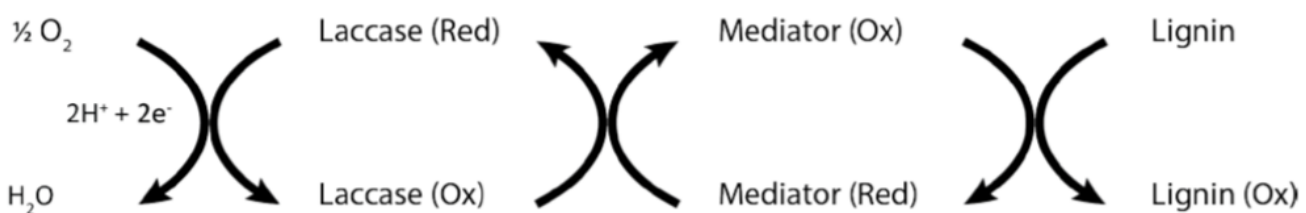
Figure 1.9. The catalytic cycle of laccase and mediator for lignin depolymerization. Adapted from (Longe et al. 2018)

The ideal redox mediator is a good laccase substrate that has a stable form both when reduced and oxidized, and does not inhibit the enzyme reaction (Morozova et al. 2007). Its redox conversion should also be cyclic and perform many cycles without degradation. Laccase alone

oxidizes small phenolic compounds and can with the help of mediators oxidize non-phenolic subunits in lignin. This is possible because oxidized mediators become strong oxidizing intermediates, and their redox potential exceeds the redox potential of non-phenolic subunits in lignin (Munk et al. 2015). However, the mechanisms for lignin degradation through a mediator is insufficiently understood in many cases, but it is the redox potential of the substrate that is oxidized by the laccase and the T1 copper that is the driving force of the reaction (Morozova et al. 2007). In the first reaction step, the mediator is oxidized by the laccase to a stable intermediate with high redox potential. The oxidized mediator then follows a diffusion-controlled reaction, where it diffuses away from the enzyme and penetrates the pore of the plant cell wall (due to its small size) to reach the target substrate. This results in the substrate, which could be lignin, aromatic compounds etc., to become oxidized by the mediator. The mediator is then reduced to its initial form (Christopher, Yao, and Ji 2014). Many compounds have been described to work as laccase mediators, and they are usually divided in two groups; natural and synthetic. Natural mediators are compounds that are products of lignin degradation, but their existence makes it difficult to distinguish between laccase oxidation and laccase mediator system (LMS) oxidation. Synthetic mediators are chemically synthesized substrates added together with the laccase, such as ABTS. However, many synthetic laccase mediators are quite expensive, which restricts their applicability in industrial processes and demands for cheaper alternatives, e.g. derivable from abundant bio-resources.

In biotechnology there are several articles and patents dedicated to the use of laccases and LMSs, as well as commercial formulations. One example is the Danish company Novozymes who manufactures a commercial formulation that utilizes a LMS for fabric bleaching (Munk et al. 2015). Laccases uses O_2 as the final electron acceptor, unlike lignin peroxidases that uses H_2O_2. This makes laccases more industrial applicable, because addition of hydrogen peroxide is currently not feasible as it contributes to corrosion of process equipment.

1.6. Enzyme kinetics

The study of enzyme kinetics comprises of factors that influence the rates of enzyme-catalyzed reactions. The two scientists Leonor Michaelis and Maud Menten were the first to demonstrate that these reactions take place in two stages (Figure 1.10). The reaction begins with the substrate binding to the enzyme, forming the enzyme-substrate complex (ES, Figure 1.10) which occurs quickly in a reversible fashion, where k_1 and k_2 are the rate constants for these processes.

Following the ES formation, the substrate is converted into a product that dissociates from the enzyme in a reversible fashion. The rate constants for this process are k_3 and k_4 (Engelking 2015)

$$E + S \underset{k_2}{\overset{k_1}{\rightleftharpoons}} ES \underset{k_4}{\overset{k_3}{\rightleftharpoons}} E + P$$
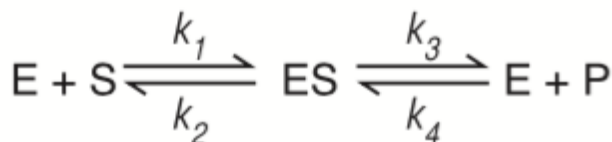
Figure 1.10. Two-step reaction occurring during enzyme-catalyzed reactions. E = Enzyme, S = substrate, ES = Enzyme-substrate complex, P = Product, k_1 to k_4 = rate constants. Adapted from (Engelking 2015).

An enzyme´s catalytic power on a given substrate involves the two variables K_m and V_{max}, where K_m is a measurement of the enzyme's affinity for the given substrate and V_{max} is a measurement of the enzyme's maximum velocity during catalysis. Substrate concentration can affect the reaction velocity, which can be described by the Michaelis-Menten equation;

$V = V_{max}[S]/ (K_m + [S])$

Where:
V = Reaction velocity
[S] = Substrate concentration
V_{max} = Maximal reaction velocity
K_m = [S] at ½ V_{max}

The Michaelis-Menten equation is based on four assumptions: 1) [S] is larger than the enzyme concentration, so the formation of ES does not alter [S], 2) The product concentration is insignificant, so the k_4 reaction rate can be ignored, 3) The rate where ES is converted to E + P (Figure 1.10) is rate-limiting, and 4) Formation of the ES complex is fast and reversible, so that the formation rate is equal to the disappearance rate (Engelking 2015).

At high substrate concentrations, the reaction rate will asymptotically approach a plateau where the enzyme becomes saturated with substrate and cannot catalyze the reaction any faster. This point is referred to as the enzyme's maximal reaction velocity, also referred to as V_{max}. Another important constant is the Michaelis-Menten constant, also referred to as K_m, which is the

substrate concentration where ½ V_{max} is reached. Low K_m values indicate high substrate affinity, while high K_m values indicates low substrate affinity (Engelking 2015).
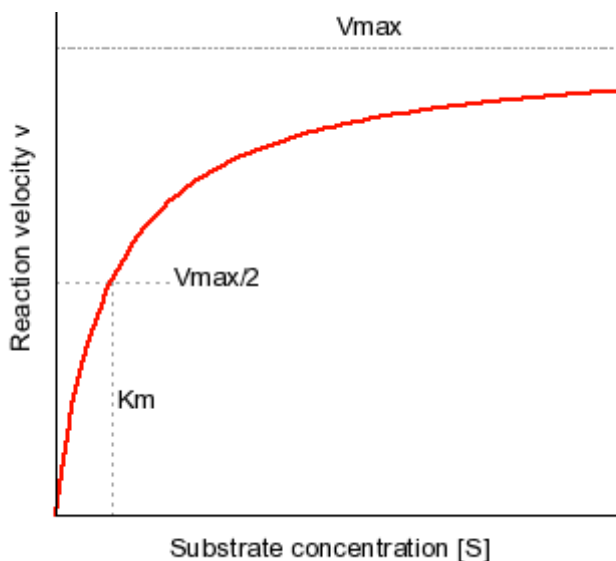
Figure 1. 11. Hyperbola curve that follows the Michaelis-Menten equation. Adapted from ("Michaelis-Menten Kinetics and Briggs-Haldane Kinetics" n.d.).

1.6.1.   Enzyme activity

An enzymes activity is the measurement of the enzymes ability to convert a substrate to a product (Baltierra-Trejo, Márquez-Benavides, and Sánchez-Yáñez 2015). An important parameter used to describe an enzymes catalytic activity is k_{cat} which is the turnover number, also referred to as the catalytic constant. The turnover number represents the number of catalytic cycles that each active site undergoes per unit time (usually expressed in s^{-1}) (Jambovane et al. 2009), a parameter that describes the catalytic efficiency for an enzyme with a given substrate.

The enzyme unit (U) has throughout many years been given different definitions. The International Union of Biochemistry defines U as "the amount of enzyme required to convert 1 µmol substrate per minute at 30 °C", while the International System of Units defines U in terms of katal, where 1 U = 0,000000016666 kat, and 1U is "the amount of enzyme that converts 1 mol substrate per second." Some authors refer to U as "the amount of enzyme that converts 1µmol substrate per minute per unit volume, expressed as U L^{-1} or U mL^{-1}." In this study, the enzyme unit has been used to characterize enzymatic activity as specific activity (U/mg) by using the substrates molar absorption coefficient (see section 3.6), giving U = µM/min.

20

Some enzyme assays are quantified using spectrophotometric methods where the concentration of the product is determined using the molar extinction coefficient of the product. These calculations are thus based on the Lambert-Beer Law that states "absorbance of light is directly proportional to the thickness of the media through which it is being transmitted, as well as to the concentration of a chromophore in the media":

A= ε*C*d

Where

A: Absorbance, ε: molar extinction coefficient ($M^{-1}cm^{-1}$), C: Enzyme concentration (M) and d: optical trajectory (cm).

During the enzymatic reaction, the substrate is converted to product according to the total assay volume (V_t) and volume of the enzyme stock solution (V_s) added. Incorporation of these elements requires a modification of the Lambert-Beers Law:

C= $\frac{A}{\varepsilon*d}*\frac{Vt}{Vs}$

Where C = U/L (Baltierra-Trejo, Márquez-Benavides, and Sánchez-Yáñez 2015).

1.7. Aim of the study

The scientific study represented by this master's degree project is an integrated part of the OXYMOD project (Optimized oxidative enzyme systems for efficient conversion of lignocellulose to valuable products), which is funded by the Norwegian Research Council (project no. 269408). OXYMOD is a research project that, through a transdisciplinary approach, aims to develop, define, and demonstrate new enzyme systems for efficient conversion of Norwegian lignocellulosic biomass into valuable products, focusing on the very much underexplored class of redox enzymes. The main objective for the present study was to characterize newly discovered laccase enzymes for the depolymerization of lignin, using a laccase-mediator system. The main aims were to 1) Clone, express and purify chosen laccases from recently sequenced *Actinobacteria,* 2) Characterize the enzymes in terms of pH, catalytic

activity, and temperature stability, 3) Screen for enzymatic activity towards small phenolic substrates, and 4) Attempt to develop a possible lignin assay based on laccase-mediator systems.

Three *Psychrobacter* laccases, P2G3, P11G3 and P11F6 were used as a reference for characterizing a set of newly discovered actinobacterial laccase enzymes described in the OXYMOD project, with the ambition of producing the enzymes inhouse and obtain knowledge and experience of the preparation regimes and methods that would be used later for characterization of the new laccases.

Bacterial enzymes have not shown to be active towards the phenolic substrate vanillin. Vanillin is one of the most abundant monomers in Kraft lignin (see section 4.4) and has the potential to be used as a low-cost mediator for lignin degradation. On the basis of this, the last part of this study involved mutagenesis on the well-known thermostable CotA laccase from *B. subtilis*. The objective was to obtain insight into protein engineering by generating specific amino acid changes with the goal to provide CotA with activity towards vanillin.

2. Materials

2.1. Chemicals

Table 2.1. Chemicals

Chemical	Supplier
2,2´-azino-bis(3-ethylbenzothiazoline-6-sulphonic acid) (ABTS)	Sigma-Aldrich
2-Morpholinethanesulfonic acid sodium salt (MES Na)	Merck KGaA
3,4-Dihydrobenzoic acid	Sigma-Aldrich
4-Hydrobenzoic acid	Sigma-Aldrich
5-bromo-4-chloro-3-inodyl-**β**-D-galacto-pyranoside (X-gal)	Sigma-Aldrich
Acetic acid glacial	Fisher Scientific
Agar powder	Oxoid
Bacto™ Yeast extract	Becton, Dickinson and Company
Bacto™ Tryptone	Becton, Dickinson and Company
Catechol	Sigma Aldrich
Copper (II) Chloride ($CuCl_2$)	Sigma-Aldrich
D-(+)-glucose monohydrate	Sigma-Aldrich
Dimethylformamid (DMF)	J. T. Baker
Dimethyl sulfoxide (DMSO)	J. T. Baker
Ethanol 96%	Antibac AS
Ferulic Acid	Sigma-Aldrich
Formic acid	Sigma-Aldrich
Glycerol 99.5%	VWR
Guaiacol	Sigma-Aldrich
Imidazole	Merck KGaA
Instant Blue™ Protein Stain	Expedon

Isopropyl β-D-1-thiogalactopyranoside (IPTG)	Sigma-Aldrich
Lignin, alkali	Sigma-Aldrich
Magnesium Chloride hexahydrate ($Cl_2Mg.6H_2O$)	Sigma-Aldrich
Magnesium Sulphate heptahydrate ($MgSO_4.7H_2O$)	Sigma-Aldrich
Methanol	VWR
NZ amine	Sigma-Aldrich
Sinapic acid	Sigma-Aldrich
Sodium Chloride (NaCl)	Merck KGaA
Sodium phosphate dibasic (Na_2HPO_4)	Sigma-Aldrich
Sodium phosphate dibasic dihydrate ($Na_2HPO_4.H_2O$)	Sigma-Aldrich
Sodium phosphate monobasic monohydrate ($NaH_2PO_4.H_2O$)	Merck KGaA
Trizma Base	Sigma-Aldrich
Vanillic acid	Sigma-Aldrich
Vanillin	Sigma-Aldrich

2.2. Kits

Table 2.2. Kits used during the study and the content of each kit

Kit	Supplier	Contents
Wizard® Plus SV Miniprep DNA purification Systems kit	Promega	Cell resuspension solution Cell lysis solution Alkaline protease solution Neutralization solution Wash solution Nuclease-free water Wizard® SV minicolumns and collection tubes
QuikChange II Site-Directed Mutagenesis Kit	Stratagene	*PfuUltra* High-fidelity DNA polymerase (2.5 U/μL) 10x reaction buffer

		Dpn I restriction enzyme (10 U/µL)
		Oligonucleotide control primer #1 [34-mer (100 ng/µL)]
		5´CCA TGA TTA CGC CAA GCG CGC AAT TAA CCC TCA C 3´
		Oligonucleotide control primer #2 [34-mer(100 ng/µL)]
		5´GTG AGG GTT AAT TGC GCG CTT GGC GTA ATC ATG G 3´
		pWhitescript 4.5-kb control plasmid (5 ng/µL)
		dNTP mix
		XL1- Blue supercompetent cells
		pUC18 control plasmid (0.1ng/µL in TE buffer)
Qubit Protein Assay Kit	Thermo Fisher	Qubit protein buffer
		Qubit protein reagent
		Qubit protein standard #1 (0 ng/mL)
		Qubit protein standard #2 (200 ng/mL)
		Qubit protein standard #3 (400 ng/mL)

Qubit DNA Assay Kit	Thermo Fisher	Qubit dsDNA BR Buffer
		Qubit dsDNA BR Reagent
		Qubit ds DNA BR standard #1
		Qubit ds DNA BR standard #2

2.3. Primers for site-directed mutagenesis

Table 2.3. Primers for the suggested site-directed mutagenesis of CotA, provided by Eurofins Genomics

Oligo name	Sequence
cotA_P226M_fw	5´ ACTGCCTAATCCTTCAATCGTTATGGCTTTTTGCGGAGAAA 3´
cotA_P226M_rv	5´ TTGACGAGTATGGTTTCTCCGCAAAAAGCCATAACGATTGAA 3´
cotA_L386A_fw	5´ AGGACGAATACGGCAGACCCGTCGCACTGCTTAATAACAAA 3´
cotA_L3861_rv	5´ TCGTGCCAGCGTTTGTTATTAAGCAGTGCGACGGGTCTGCCGT 3´
cotA_A471P_fw	5´ TGGAAAGACACCATTCAAGCGCATCCAGGTGAAGTCCTGAGA 3´
cotA_A471P_rv	5´ TGTCGCCGCGATTCTCAGGACTTCACCTGGATGCGCTTGA 3´
cotA_A376S_G377V_fw	5´ ATCAGAACGTTAAAACTGTCAGTCACCCAGGACGAATACGGCA 3´

cotA_A376S_G377V_ rv	5´ GCGACGGGTCTGCCGTATTCGTCCTGGGTGACTGACAGT TTTA 3´

2.4. Buffers

Table 2.4 : Buffers with respective pH values and their purpose

Buffer	pH	Purpose
0.1 M Acetate buffer	3.8, 4.2, 4.6, 5.0	Activity assay
0.1 M Format buffer	3.4	Activity assay
20 mM MES buffer (0.1 M NaCl)	5.4	Activity assay and regeneration of His-Pur™ Ni-NTA Resin for His-tag purification
0.1 M Sodium Phosphate buffer	5.8, 6.2, 6.6, 7.0, 7.4, 7.5, 7.8	Resuspension of cell pellet, enzyme storage, buffer exchange, activity assay
0.1 M Tris buffer	8.2, 8.6	Activity assay

2.5. Plasmids

Table 2.5. Plasmids

Plasmid	Antibiotic resistance gene	Laccase	Source
pET-21a(+)	*AmpR*	N-His P01-C03 N-His P01-E07 N-His P06-A08 N-His P20-F12	GenScript®
pET-30a	*KanR*	P2G3 P11G3 P11F6	GenScript®
pET-22b(+)	*AmpR*	CotA	UNKNOWN

3. Methods

3.1. Buffer preparation

Buffers are partially neutralized solutions consisting of weak acids or weak bases with the ability to resist pH changes, a concept called "buffering" (Stoll and Blanchard 1990). The quality of a buffer depends on its buffer capacity, which is its ability to resist pH changes when a strong acid or base is added. The buffers ability to maintain a stable pH during dilutions and addition of neutral salts are also characteristics of a high-quality buffer. Some buffer systems work better at certain pH values than others, therefore it is important to use a buffer that works well at the desired pH value. An overview of all buffers and their purposes in this study is displayed in section 2.4.

The pH for all buffers was verified using a sensION™ pH multimeter from Hach. Necessary pH adjustments were made by adding either NaOH or HCl from suitable stock solutions (e.g. 1 M) until the desired pH was reached. Calibration of the pH multimeter was done prior to use, using Certipur® Buffer solutions from Merck KGaG with known pH values of 4.0, 7.0 and 10.0 to verify the accuracy of the multimeter. All buffers were sterile filtered using 500 mL flow filter units with 0.2 μm aPES membrane from Thermo scientific and a vacuum gas pump from VWR after the desired pH was reached.

3.1.1.   Sodium phosphate buffer

Materials
- 1 M $NaH_2PO_4.H_2O$ (Monobasic stock solution)
- 1 M Na_2HPO_4 (Dibasic stock solution)
- ddH_2O
- sensION™ pH multimeter (Hach)

Procedure

Preparation of 0.1 M sodium phosphate buffer with different pH values was done by mixing monobasic and dibasic stock solution according to Table 3.1 obtained from www.benchling.com, and adjusting the pH using either NaOH or HCl while monitoring the pH using a sensION™ pH multimeter.

Table 3.1. Volumes of monobasic and dibasic stock solution that need to be mixed together to achieve 500 mL of 0.1 M sodium phosphate buffer with the respective pH values

pH	Monobasic (mL)	Dibasic (mL)	ddH$_2$O (mL)
5.8	45.75	4.25	450
6	43.4	6.6	450
6.2	40.4	9.6	450
6.4	36.1	13.9	450
6.6	30.95	19.05	450
6.8	25.15	24.85	450
7.0	19.25	30.75	450
7.2	14.15	35.85	450
7.4	9.9	40.1	450
7.6	6.7	43.3	450
7.8	4.6	45.4	450
8.0	3	47	450

3.1.2. Tris buffer

<u>Materials</u>

- 6.057 g of Trizma base
- ddH$_2$O
- sensION™ pH multimeter (Hach)

<u>Procedure</u>

Tris buffer was prepared by adding Trizma base to a 500 mL Pyrex glass bottle, dissolving it in 450 mL of ddH$_2$O. After dissolving the Trizma base, the pH was measured and adjusted to the desired pH (see section 2.4) using NaOH or HCl. After pH adjustment, ddH$_2$O was added to a final volume of 500 mL.

3.1.3. Acetate buffer

<u>Materials</u>

- 4.473 mL Acetic acid, glacial
- ddH$_2$O
- sensION™ pH multimeter (Hach)

<u>Procedure</u>

Acetate buffer was prepared by adding Acetic acid glacial to a 500 mL Pyrex glass bottle and dissolving it in 450 mL of ddH$_2$O. After dissolving the Acetic acid, glacial, the pH was measured and adjusted to the desired pH (see section 2.4) using NaOH or HCl. After pH adjustment ddH$_2$O, was added to a final volume of 500 mL.

3.1.4. Formate buffer

<u>Materials</u>

- 2.807 mL Formic acid
- ddH$_2$O
- sensION™ pH multimeter (Hach)

<u>Procedure</u>

Formate buffer was prepared by adding Formic acid to a 500 mL Pyrex glass bottle and dissolving it in 450 mL ddH$_2$O. After dissolving the Formic acid, the pH was measured and adjusted to the desired pH (see section 2.4) using HCl. After pH adjustment, ddH$_2$O was added to a final volume of 500 mL.

3.1.5. MES buffer

<u>Materials</u>

- 10.86 g 2-Morpholinethanesulfonic acid sodium salt (MES Na)
- ddH$_2$O

- sensION™ pH multimeter (Hach)

<u>Procedure</u>

MES buffer was prepared by adding MES Na to a 500 mL Pyrex glass bottle dissolving it in 450 mL ddH$_2$O. After dissolving the MES Na, the pH was measured and adjusted to the desired pH (see section 2.4) using NaOH or HCl. After pH adjustment, ddH$_2$O was added to a total volume of 500 mL.

Tris, acetate, format and MES buffers were made using recipes generated from www.liv.ac.uk/buffers.

Sodium phosphate buffers are best suited in the pH range from 5.7-8.0 (Stoll and Blanchard 1990). Tris buffers are best suited in the pH range from 8.4-9.0, acetate buffers works best at pH ranging from 3.6-5.6, and format buffers works best at lower pH values (Stoll and Blanchard 1990).

3.2. Cultivation

Most bacteria are able to grow and multiply under different conditions in nature, but to be able to study them in pure cultures, bacteria need to be cultivated in artificial media (Vollum, Jamison, and Cummins 1970). The media may be in either solid or liquid form and needs to be customized according to the bacteria's nutritional needs.

3.2.1.   Cultivation media

Lysogeny broth (LB)

Liquid media (for 1 L volume)

<u>Materials</u>
- 10 g tryptone
- 5 g yeast extract
- 10 g NaCl

- ddH$_2$O

Procedure

All ingredients were first added to a 1 L Pyrex glass bottle and deionized water was added to a final volume of 1 L. All ingredients were dissolved using an AM4 Multiple Heating Magnetic Stirrer (Velp scientifica) followed by autoclaving using a HICLAVE HV-85L (HMC Europe).

Agar selection plates (for 1 L volume)

Materials

- 10 g tryptone
- 5 g yeast extract
- 10 g NaCl
- 20 g agar
- ddH$_2$O

Procedure

All ingredients were first added to a 1 L Pyrex glass bottle and deionized water was added to a final volume of 1 L. All ingredients were dissolved using an AM4 Multiple Heating Magnetic Stirrer (Velp scientifica) followed by autoclaving using a HICLAVE HV-85L (HMC Europe). After autoclaving, the media was cooled down with a magnetic mixer until it was cool enough to touch. To make selection plates ampicillin or kanamycin was added to a final concentration of 50 μg/mL or 30 μg/mL, respectively, depending on the antibiotic resistance marker of the transformed bacteria (see section 3.2.2). Working in a laminar flow workbench, the medium was then poured into sterile single-use plastic petri dishes. After allowing the agar to cool until solid, all plates were stored at 4 °C.

NZY+ broth (for 1 L volume)

Materials

- 10 g NZ amine (casein hydrolysate)
- 5 g yeast extract
- 5 g NaCl

- 12.5 mL 1 M MgCl$_2$
- 12.5 mL 1 M MgSO$_4$
- 10 mL 2 M glucose
- ddH$_2$O

Procedure

NZ amine, yeast extract and NaCl were first added to a 1 L Pyrex bottle and deionized water was added to a final volume of 1 L. All ingredients were dissolved using an AM4 Multiple Heating Magnetic Stirrer (Velp scientifica). The pH was then adjusted to 7.5 using NaOH while monitoring the pH using a multi-pH meter. After achieving the correct pH, the solution was autoclaved using a Certoclav-Tisch Autoclave CV-EL 12L/18L. MgCl$_2$, MgSO$_4$ and glucose were sterile filtered and added prior to use.

3.2.1.1.   Liquid LB with antibiotics

Medium used for cultivation of transformed bacteria was added with either ampicillin or kanamycin to a final concentration of 50 μg/mL or 30 μg/mL, respectively, depending on the antibiotic resistance marker of the transformed bacteria (see section 3.2.2).

3.2.2.   Antibiotics

Ampicillin is a broad spectrum β-lactam penicillin antibiotic with bactericidal activity. Ampicillin binds covalently to penicillin-binding proteins (PBPs) found in the inner membrane of the bacterial cell wall (Chudobova et al. 2014). This covalent binding inhibits enzymes responsible for vital stages in the synthesis of the bacterial cell wall, leading to cell lysis upon cell growth.

Kanamycin is an aminoglycoside antibiotic that inhibits normal protein synthesis in Gram-negative bacteria by binding irreversibly to the 30S ribosomal subunit, which prevents elongation of peptide chains during protein synthesis (Forge and Schacht 2000).

In this study, ampicillin was used to select for *E. coli* bacteria containing the pET-21a(+) plasmid, used for expression of newly discovered *Actinobacteria* laccases, or the pET-22b(+)

plasmid used for expression of the cotA laccase. Both plasmids contain the *AmpR* gene which codes for the enzyme β-lactamase. β-lactamase is an enzyme that hydrolyzes the β-lactam ring in penicillin antibiotics consequently deactivating its antimicrobial function (Zeng and Lin 2013), making *E. coli* cells that have taken up the plasmid and expressing the *ampR* gene resistant towards ampicillin. Kanamycin was also used to select for transformed *E. coli* bacteria. Kanamycin resistant *E. coli* contained variants of the pET-30a(+) plasmid used for expression of the three different *Psychrobacter spp.* laccases included in this study. The pET-30a derived plasmids contain the *kanR* gene coding for the enzyme aminoglycoside phosphotransferase. Aminoglycoside phosphotransferase is an aminoglycoside modifying enzyme that carries out the phosphorylation of specific hydroxyl groups of the aminoglycoside by using ATP as a co-factor (Fong, Burk, and Berghuis 2005), resulting in loss of the kanamycin´s antimicrobial effect, thus allowing all *E. coli* that have taken up the plasmid during transformation and expressing the *kanR* gene to become resistant towards kanamycin.

3.2.3.   Transformation of *E. coli* BL21 (DE3)

Bacteria are able to acquire new genetic information in three different ways; conjugation, transduction and transformation. Transformation involves the uptake of DNA from the extracellular surroundings (Chen and Dubnau 2004). Since the discovery of transformation, biologists have transformed *E. coli* using procedures that alter the cells permeability, making it more receptive, also referred to as competent, to uptake of foreign DNA.

Materials

- BL21 (DE3) competent *E. coli* cells (BioLabs Inc.)
- Super Optimal broth with Catabolite repression (S.O.C) outgrowth medium (BioLabs inc.)
- pUC19 control DNA
- Plasmid DNA containing gene of interest (see section 3.2.2)
- LB-ampicillin (50 µg/mL) or kanamycin (30 µg/mL) agar selection plates

Procedure

To transform BL21 (DE3) competent *E. coli* cells with the plasmid vector, the transformation protocol from BioLabs was used. For each transformation, one vial of competent cells was used.

Vials containing BL21 (DE3) competent *E. coli* cells were thawed on ice for 10 minutes before adding 1-5 µL of the DNA miniprep containing 1 pg – 100 ng of plasmid DNA, depending on the concentration of DNA miniprep. In this study, 100 ng of plasmid DNA was added to each vial. The DNA concentration of the miniprep was first measured using a DS-11 FX$^+$ spectrophotometer/fluorometer and the appropriate volume of DNA was added based on the concentration. DNA samples with high concentrations were diluted with nuclease-free water.

After adding an appropriate volume of DNA miniprep, the content in the vial was carefully mixed by flicking it 4 to 5 times and incubated on ice for 30 minutes. After incubation, the vial was exposed to heat shock at 42 ℃ for exactly 10 seconds, using a preheated Isotemp® GPD2S water bath, before being placed back on ice and incubated for 5 minutes. After incubation, 950 µL of room temperature S.O.C was added to each vial followed by incubation at 37 ℃ and 250 rpm for 1 hour. Following the incubation each sample was diluted 10 x and 100 x with room temperature S.O.C outgrowth medium, before spreading 100 µL of the original sample and each dilution on separate LB-ampicillin agar plates preheated to 37 ℃. All selection plates were incubated overnight at 37 ℃ for at least 16 hours (Alternatively at 30 ℃ for 24-36 hours or at 25 ℃ for 48 hours).

3.2.4.   Overnight culture

Overnight cultures were prepared by scraping a single colony from an LB agar selection plate or the surface of a frozen bacterial glycerol stock using a sterile pipette tip, releasing the pipette with the desired bacteria in a sterile 50 mL Greiner test tube with a conical bottom containing 5 mL (for small scale cultivation) or 12 mL (for large scale cultivation) of LB with either ampicillin (50 µg/mL) or kanamycin (30 µg/mL). The bacterial suspension was then incubated at 37 ℃ and 160 rpm overnight, for at least 16 hours.

3.2.5.   Cultivation of *E. coli* BL21 (DE3) for protein expression

In this study BL21 competent *E. coli* cells, provided by BioLabs, were used for transformation and expression of heterologous proteins.

Escherichia coli is a facultative anaerobe, Gram-negative bacterium that is naturally found in the lower intestine of warm-blooded animals, including humans (Nataro and Kaper 1998). *E. coli* is widely used as a host to produce heterologous proteins, and its genetics are one of the most characterized (Baneyx 1999). There are many systems capable of heterologous protein expression, but *E. coli* is the most attractive due to its ability to grow rapidly at high density using inexpensive substrates, its highly characterized genetics, and ability to be easily transformed.

Different strains of *E. coli* are used to produce a variety of heterologous proteins. This is done by inserting the gene coding for the desired protein in a plasmid specifically designed for expression of a target gene. The *E. coli* expression host is then transformed with the plasmid containing the target gene and cultivated to generate large numbers of transformed *E. coli* cells. With the addition of an inducer, the target protein is expressed and can subsequently be purified.

All media and reagents used for cultivation were autoclaved (20 min at 121 °C) or sterile filtered before use, and all bacteria cultures were made under sterile conditions using a laminar flow workbench and/or a Flameboy handheld bunsen burner. Used cultures were inactivated by autoclaving for at least 20 min at 121 °C.

3.2.5.1. Small scale cultivation

Materials
- 500 mL shake flasks
- Sterile 50 mL Greiner test tubes with a conical bottom
- LB ampicillin (50 µg/mL) or LB kanamycin (30 µg/mL) media
- Fresh overnight culture (see section 3.2.4)
- 1 M Isopropyl β-D-1-thiogalactopyranoside (IPTG)
- 2.5 M $CuCl_2$
- Shimadzu UV-1700 spectrophotometer

Procedure

In a 500 mL shake flask 100 mL of liquid LB medium with either ampicillin (50 µg/mL) or kanamycin (30 µg/mL) was inoculated with 1:50 fresh overnight pre-culture. The shake flask was incubated at 30 °C and 160 rpm for approximately 2 hours in a Minitron rotating incubator (INFORS) until and OD_{600} of 0.4-0.5 was reached. The OD_{600} was measured by pipetting 1 mL of the bacteria culture to a 10 x 4 x 45 mm polystyrene cuvette (SARSTEDT), keeping the shake flask sterile by using a handheld Bunsen burner, placing the cuvette in a Shimadzu UV-1700 spectrophotometer. Liquid LB was used as blank. After the appropriate OD_{600} was reached protein expression was induced by adding IPTG to a final concentration of 1 mM, and $CuCl_2$ was added to a final concentration of 0.25 mM in order to ensure sufficient cofactor supply for the produced laccase enzymes. After induction, the shake flask culture was incubated at 15 °C and 100 rpm for 4 hours before shifting to static incubation for overnight expression >16 hours, keeping the temperature at 15 °C. Static incubation leads to oxygen limited growth which has been shown to increase the yield of fully copper loaded bacterial LMCO´s in *E. coli* (Reiss et al. 2013). After overnight expression, bacterial cells were harvested by transferring the shake flask cultures to sterile 50 mL tubes, followed by centrifugation at 18 514 x g at 4 °C for 20 minutes using an Eppendorf centrifuge 5810R. The culture medium was discarded, and the cell pellet stored at -20 °C until further use.

3.2.5.2. Large scale cultivation

Materials

- 2 L shake flasks
- LB medium
- Ampicillin (50 mg/mL)
- Fresh overnight culture (see section 3.2.4)
- 1 M Isopropyl β-D-1-thiogalactopyranoside (IPTG)
- 2.5 M $CuCl_2$
- Shimadzu UV-1700 spectrophotometer

Procedure

In a 2 L shake flask, 500 mL of liquid LB media added with ampicillin to a final concentration of 50 µg/mL ampicillin was inoculated with 1:50 of fresh overnight pre-culture. The shake flask

was incubated at 30 °C and 160 rpm in an Innova®44 (New Brunswick) rotating incubator until and OD_{600} of 0.4-0.5 was reached. This would take approximately 2.5 hours. OD_{600} was measured by pipetting 1 mL of the bacteria culture to a 10 x 4 x 45 mm polystyrene cuvette (SARSTEDT), keeping the shake flask sterile by using a handheld Bunsen burner, placing the cuvette in a Shimadzu UV-1700 spectrophotometer. Liquid LB was used as blank. After the appropriate OD_{600} was reached protein expression was induced by mixing IPTG and $CuCl_2$ together prior to induction and adding it to the shake flask culture to a final concentration of 1 mM and 0.25 mM respectively. After induction, the shake flask culture was incubated at 15 °C and 100 rpm for 4 hours before shifting to static incubation for overnight expression >16 hours, keeping the temperature at 15 °C. After overnight expression the bacterial cells were harvested by transferring the cell culture to a plastic container placed in a 1000 mL polypropylene tube and centrifuged using an Avanti™ HP-20 XPI centrifuge (Beckman coulter) at 4 °C and 12 227 x g (7000 rpm) for 30 minutes. After centrifugation the media was discarded, and the cell pellet stored at -20 °C until further use.

3.3. Protein extraction

3.3.1. Sonication

In order for cells to release cellular content to its exterior environment, the cell wall needs to be disrupted and the cells lysed. This can be done physically e.g. by sonication. The principle of sonication is the use of sound waves to break the cell wall. This leads to the release of soluble proteins to the surrounding environment (usually a suitable buffer solution), which can be further separated from the cell debris e.g. by centrifugation, leaving the soluble proteins in the supernatant.

Materials
- Cell pellet generated from cultivation
- 0.1 M Sodium phosphate buffer pH 7.5
- Sonic Dismembrator ultrasonic processor (Fisher Scientific)

Procedure

Sonication was performed using a Sonic Dismembrator ultrasonic processor from Fisher Scientific. Prior to sonication, the cell pellet was resuspended in 0.1 M Sodium Phosphate buffer, pH 7.5. The program was set to 40% amplitude, 20s ON, 30s OFF with a total of 2 minutes, which is the standard program for sonication of *E. coli* cells that is used in the lab where the study was performed. All samples were kept on ice before, during, and after sonication to prevent heating and denaturation of proteins. After sonication, the samples were immediately centrifuged at 4 ℃ and 18 514 x g using an Eppendorf centrifuge 5810R to remove insoluble cell debris. The supernatant was transferred to a new tube and kept in an ice box placed in a 4 ℃ storage room until further use.

3.3.2.   BugBuster (Merck)

The BugBuster reagent is used for protein extraction by gently disrupting the cell wall of *E. coli*. This results in the liberation of soluble proteins. The BugBuster reagent is a proprietary formulation that utilizes a mixture of non-ionic detergents capable of perforating the cell wall without denaturing soluble proteins. Certain components of the BugBuster are unstable at low pH, and it is therefore expedient to avoid dilution with buffers lower than pH 5.0. Salt concentrations above 1.0 M may result in precipitation of the BugBuster reagent. BugBuster is also known to be compatible with phosphate and Tris buffers, but in order to be sure that precipitation in other buffer systems does not occur, a small aliquot of BugBuster should be diluted in the buffer system in question.

BugBuster 10x protein extraction reagent was diluted to 1x BugBuster protein extraction reagent using 0.1 M Sodium phosphate buffer, pH 7.5. The cell pellet was resuspended in 1x BugBuster solution using 5 mL BugBuster per gram of wet weight cell pellet. The cell suspension was incubated at room temperature in an IKA®Trayster digital rotating mixer for 20 minutes at 30 rpm. After incubation the cell suspension was centrifuged at 4 ℃ and 16 000 x g in an Eppendorf centrifuge 5810R to remove insoluble cell debris. The supernatant was transferred to a new sterile tube and stored in an ice box placed in a 4 ℃ storage room until further testing.

3.4. Protein purification

3.4.1. Heat treatment

Thermostable proteins can be purified with heat treatment. Non-thermostable proteins in the cell extract are denatured at high temperatures, leaving the thermostable proteins intact in the supernatant. Heat treatment can result in the breaking up of the electrostatic and other interactions in the protein structure, which expose the hydrophobic core to the solute. Upon cooling, intermolecular hydrophobic interactions forms aggregates that are insoluble, which can easily be separated from the soluble proteins (e.g. by centrifugation) that have not been denatures.

Samples were placed in a Julabo F20 water bath at 90 °C for 10 minutes, followed by centrifugation at 4 °C to remove denatured proteins.

3.4.2. Immobilized metal affinity chromatography (IMAC)

Immobilized metal affinity chromatography, also called His-Tag purification, is a method based on the fusion of a target protein to an affinity tag (Scheich, Sievert, and Büssow 2003), a method that has become standard practice in molecular biology. A His-Tag is an additional poly-Histidine chain extension (Ledent et al. 1997) at either the N- or the C-terminus of the peptide chain of a target protein. During purification, the imidazole moieties of the His-tag will bind to immobilized nickel or cobalt by forming a complex with the metal ions, separating the target protein from other non-His-tagged proteins with lower affinity to the metal affinity matrix. Elution of the target protein occurs by increasing the concentration of imidazole, which will compete with the imidazole ring of the histidine residues and result in release of the target protein (Galaev et al. 1997).

3.4.2.1. HisPur™ Ni-NTA Resin (Thermo Scientific)

Materials
- HisPur Ni-NTA resin
- Polypropylene columns (Qiagen)

- Equilibration buffer: 20 mM sodium phosphate, 300 mM sodium chloride with 10 mM imidazole, pH 7.4

- Wash buffer: 20 mM sodium phosphate, 300 mM sodium chloride with 25 mM imidazole, pH 7.4

- Elution buffer: 20 mM sodium phosphate, 300 mM sodium chloride with 250 mM imidazole, pH 7.4

- Stand and clamps to hold the polypropylene columns

- DS-11FX+ spectrophotometer/fluorometer

Procedure

The target proteins were purified by using HisPur™Ni-NTA Resin from Thermo scientific. The resin is composed of 6% crosslinked agarose with immobilized nickel-charged nitrilotriacetic acid (NTA), enabling immobilized metal affinity chromatography purification of his-tagged proteins from a soluble protein extract. Using 1 mL polypropylene columns from Qiagen an appropriate amount of resin was added, using 1 mL resin per 60 mg protein, and allowing the storage buffer to drain from the column by gravity flow. The column with the resin was then equilibrated using two resin volumes of equilibration buffer, allowing the buffer to drain by gravity flow. This step was repeated twice. The sample was prepared by mixing an equal volume of sample and equilibration buffer. The prepared sample was then added to the column, at 4 °C, and drained by gravity flow. Using two resin volumes of wash buffer, the column was washed until the protein concentration (280 nm) approached baseline using a DS-11FX+ spectrophotometer/fluorometer to measure the protein concentration. The his-tagged proteins were then eluted in two fractions using two resin volumes of elution buffer in each fraction. The elution fractions were stored in an ice box placed in a 4 °C storage room until further use.

3.4.2.2.   HIS-select® Spin columns (Sigma Aldrich)

The HIS-select spin columns contain spherical silica particles derivatized with a proprietary quadridentate chelate charged with nickel, allowing rapid purification of crude cell extract in a small scale. The binding capacity of each HIS-Select spin column is >500 µg determined with an ~30 kDa his-tagged protein recovered under high levels of protein expression.

Materials

- HIS-Select® Spin Columns and collection tubes (Sigma-Aldrich)

- Equilibration buffer: 50 mM sodium phosphate with 0.3 M sodium chloride, pH 8.0

- Wash Buffer: 50 mM sodium phosphate with 0.3 M sodium chloride and 5 mM imidazole, pH 8.0

- Elution buffer: 50 mM sodium phosphate with 0.3 M sodium chloride and 250 mM imidazole, pH 8.0

- MiniSpin plus, Eppendorf microcentrifuge

<u>Procedure</u>

To equilibrate the spin column, 600 μL equilibration buffer was added, and the column was centrifuged at 500 x g using a MiniSpin plus, Eppendorf microcentrifuge. The flow-through in the collection tube was discarded, and the spin column placed back into the collection tube, before loading the column with 600 μL of cell extract. The column was then centrifuged as previously described. The flow-through was saved for further testing, and the column placed in a new collection tube. To wash unbound protein from the spin column, 600 μL of wash buffer was added, and the spin column was centrifuged as previously described. The wash step was done twice. Using a new collection tube, the target protein was eluted with 500 μL elution buffer and placed in an ice box in a 4 °C cold storage room until further testing. The purification was performed at room temperature.

3.4.3.   Buffer exchange

The principle of buffer exchange is to replace one set of buffer in a solution of soluble protein with another (Phillips and Signs 2005). This is easily accomplished by size exclusion chromatography (SEC) allowing small molecules, such as salts, to be efficiently separated from higher molecular weight substances of interest, such as proteins/enzymes.

In this study, buffer exchange was performed to replace the elution buffer used during His-Tag protein purification with a pH neutral sodium phosphate buffer. The imidazole in the elution buffer interferes with measurements of protein concentration, making buffer exchange necessary to be able to measure the correct protein concentration of the solution.

3.4.3.1.   PD-10 Desalting columns (GE Healthcare)

Materials

- PD-10 desalting columns
- 0.1 M sodium phosphate buffer pH 7.5
- Sterile 5 mL Eppendorf tubes

Procedure

The storage buffer in the desalting columns was discarded and the sealed end of the column was clipped of. The column was filled up with 0.1 M sodium phosphate buffer, allowing the buffer to drain by gravity-flow. This was repeated four times, and the flow-through was discarded. After equilibration, the purified protein sample was added to the column followed by the addition of 0.1 M sodium phosphate buffer to a total volume of 2.5 mL, letting it drain by gravity flow. The proteins were eluted by adding 3.5 mL of 0.1 M sodium phosphate buffer to the column and letting it drain by gravity flow. The eluate was collected in a 5 mL Eppendorf tube. The purification was done at 4 °C, and the eluted sample was placed in an ice box in a 4 °C storage room until further use.

3.4.3.2.   Amicon® Ultra-0.5 Centrifugal filter devices (Milipore Ireland Ltd)

Amicon® Ultra-0.5 Centrifugal filter devices allow buffer exchange by concentrating the sample followed by a reconstituting to the original sample volume with the desired solvent. The sample can be "washed out" with the desired solvent until the concentration of the contaminating solute has been sufficiently reduced.

Materials

- Amicon® Ultra-0.5 Centrifugal filter devices (30K)
- Microcentrifuge tubes
- 0.1 M Sodium phosphate buffer pH 7.5
- MiniSpin plus, Eppendorf microcentrifuge

Procedure

The Amicon® Ultra-0.5 filter device was placed in a microcentrifuge tube, and 500 µL of purified protein solution was added to the filter device. The device was then centrifuged at 14 000 x g for 20 minutes to concentrate the protein solution, removing 450 µL of the undesired buffer and concentrating the protein in a 50 µL volume. The solution containing the concentrated purified protein was diluted with the new buffer by adding 450 µL 0.1 M sodium phosphate buffer and centrifuged at 14 000 x g for 10 minutes. The flow-through was discarded. To recover the concentrated solute containing purified proteins, the filter device was placed upside down in a new microcentrifuge tube and centrifuged for 2 minutes at 1000 x g, transferring the concentrated solute into the microcentrifuge tube. Then 450 µL 0.1 M sodium phosphate buffer was added to the concentrated solute and kept in an ice box placed at a 4 °C storage room until further analysis. The procedure was done in room temperature.

3.5. Qubit assay

The Qubit assay is used to determine the concentration of either protein, RNA or DNA by utilizing target-selected dyes that emits fluorescence only when bound to the specific target molecule. In contrast to UV-absorbance methods that measure the absorbance of light at 260 nm for nucleic acids and 280 nm for proteins, the Qubit assay uses fluorescent dyes to determine the concentration of the molecule of interest without interference from other contaminants tolerated by the assay. These include reducing reagents, salts, free nucleotides, amino acids, and solvents. UV-absorbance methods can be unreliable and inaccurate because the UV-absorbance readings indiscriminately measure anything that can absorb light at 260 nm or 280 nm, in contrast to the Qubit assay where the fluorescence is correlated with the sample concentration because of the specificity of the assay. In addition, the sensitivity of spectrophotometry is often insufficient as it prohibits quantitation of samples with low concentrations.

To determine the concentration in the Qubit assay it must remain linear and follow Beer´s law. This require a standard curve. Before measuring protein, RNA or DNA concentration a standard curve is made by measuring known concentrations and creating a linear graph. The assay is accurate for original protein sample concentrations from 12.5 µg/mL to 5 mg/mL, and original dsDNA sample concentrations from 100 pg/µL- 1,000 ng/µL for broad range measurement of

dsDNA. Samples concentrations too high for measurement in the fluorometer need to be diluted and re-measured.

Materials

- Qubit protein or DNA assay kit (Thermo scientific) (see section 2.2)
- 500 µL Qubit assay tubes (Thermo scientific)
- Invitrogen Qubit 4 Fluorometer (Thermo scientific)
- Plastic tubes for preparing the Qubit working solution

Procedure

Before preparing the Qubit working solution the number of 500 µL Qubit assay tubes needed for standards and samples were set up and labeled. The Qubit protein assay requires three standards and the Qubit dsDNA assay requires 2 standards. Each sample was prepared in triplicate. The Qubit working solution was prepared by diluting the Qubit reagent dye 1:200 in Qubit buffer using a clean plastic tube, preparing 200 µL for each standard and sample to be measured. The working solution should not be mixed in a glass container because the Qubit reagent dye might stain the glass permanently. For example, for seven samples and three standards a total volume of 2 mL Qubit working solution is required. To obtain this volume by diluting the Qubit reagent dye 1:200, 1,990 µL Qubit buffer needs to be mixed with 10 µL of Qubit reagent dye.

Each standard tube was prepared by adding 190 µL Qubit working solution and 10 µL of standard to a Qubit assay tube. Each sample was prepared by adding 195 µL Qubit working solution and 5 µL of the original sample to a Qubit assay tube. The sample tubes can be prepared with 180-199 µL Qubit working solution and 1-20 µL of the original sample to a total volume of 200 µL. All tubes were mixed by vortexing for 2-3 seconds and incubated at room temperature with 2-minute incubation for DNA and 15-minute incubation for protein. After incubation, the standards were read first to generate the standard curve before reading the sample Qubit assay tubes in the Invitrogen Qubit 4 Fluorometer.

3.6. Enzyme activity assay

The enzymatic activity of laccases is usually detected spectrophotometrically by its capacity to oxidize several aromatic compounds. The compound 2-2′-azinobis(3-ethylbenzthiazoline-6-sulfonic acid) (ABTS) is one of the most commonly used substrates for detecting laccase activity (Terrón et al. 2004). In an activity assay with laccase enzymes, ABTS is oxidized to the ABTS cation radical presented in Figure 3.1 (Chaurasia, Yadav, and Yadava 2013), that has a blue-green color which absorbs light without interference from non-oxidized ABTS (Solís-Oba et al. 2005). The blue-green cation radical concentration can be correlated to the activity of the laccase enzyme with an extinction coefficient of ε(420 nm) = 36,000 $M^{-1}cm^{-1}$ (Chaurasia, Yadav, and Yadava 2013), a measurement of how strongly a chemical substance or species absorbs light at a particular wavelength (here 420 nm). It should be noted that the extinction coefficient of ABTS was determined at specific pH and temperature, which could have an effect on the observed activity if the conditions during the performed assay differs from the conditions used to determine the extinction coefficient.

Originally, it was assumed that it was the $ABTS^+$ radical cation was responsible for oxidation of non-phenolic substrates, but it has recently been proved, through spectrochemical and electrochemical studies, that ABTS undergoes a two-step oxidation reaction when being oxidized by laccase. ABTS is first oxidized to $ABTS^+$ radical cation followed by a slow oxidation to $ABTS^{2+}$ di-cation. Both the radical cation and the di-cation are responsible for non-enzymatic substrate oxidation. Their redox potential was evaluates as 0.680 V for $ABTS^+$ and 1.09 V for $ABTS^{2+}$ (Chaurasia, Yadav, and Yadava 2013).
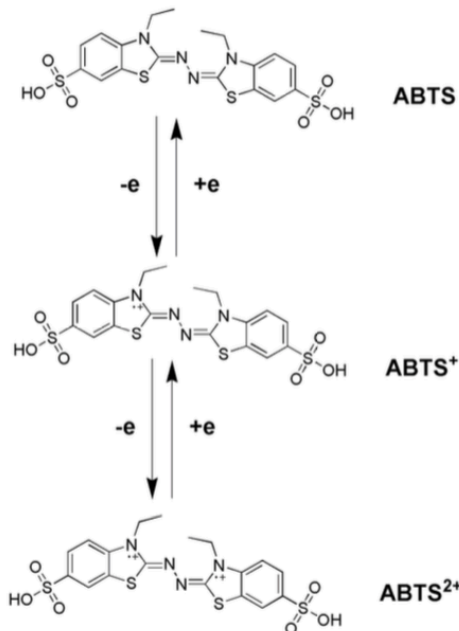
Figure 3.1. The oxidation of ABTS to the ABTS+ cation radical followed by the slow oxidation to ABTS²⁺ di-cation. Adapted from (Christopher, Yao, and Ji 2014)

Materials

- FLUOstar Omega microplate reader
- CORNING UV-transparent or GREINER Bio one 96-well microtiter plate (depending on the wavelength to be monitored during the assay)
- Assay solution

Procedure

The enzymatic activity was determined at room temperature using a FLUOstar Omega microplate reader from BMG labtech. The reaction was followed with different wavelengths depending on the substrate in the assay solution. The oxidation of ABTS was monitored at a wavelength of 420 nm (Reiss et al. 2013). Using a 96-well microplate, the assay volume for all reactions was 200 µL in each well. All activity measurements were done in triplicate using 5 µL of enzyme solution and 195 µL assay solution. For the oxidation of ABTS, the assay solution contained ABTS diluted in desired buffer with desired pH value. Enzymatic activity can be observed by the change in absorption over time. The enzyme activity was measured according to the linear initial velocity, and the region where linearity was maintained was used to measure absorbance over time, as described in previous studies (Iimura, Sonoki, and Habe 2018).

3.6.1. Temperature stability assay with ABTS

Materials

- Sterile 1.5 mL Eppendorf tubes
- Thermomixer comfort heat block
- 5 mM 2,2′-azino-bis(3-ethylbenzothiazoline-6-sulphonic acid) (ABTS)

Procedure

For determination of the thermostability of laccase, 100 μL of purified enzyme solution was incubated at different temperatures and time-periods before running an activity assay (see section 3.6) and calculating the specific activity in order to see how the activity would change after incubation at different temperatures. Four laccase enzymes (P01-C03, P01-E07, P06-A08 and P20-F12) were incubated at 30 ℃, 40 ℃, 50 ℃, 60 ℃, 70 ℃, 80 ℃, 90 ℃, and 99 ℃ for 30 minutes using a Thermomixer comfort heat block. In order to determine if time would have an impact on the enzymatic activity, all enzymes were incubated at 80 ℃, 90 ℃, and 99 ℃ for 1 hour, 1.5 hour, and 2 hours. After each incubation, activity assay was performed for each of the enzymes with 5 mM ABTS diluted in sodium phosphate buffer pH 5.7. The assay conditions were based on the pH optimal study of previously characterized bacterial laccases in the OXYPOL project (pH 5-6) (unpublished data). The temperature stability assay was performed prior to the pH optimum assay, hence pH 5.7 was used in the assay.

3.6.2. pH optimum assay with ABTS

The determination of the pH stability of the laccase enzymes P01-C03, P01-E07, P06-A08 and P20-F12 was performed with several activity assays (see section 3.6) to monitor the change in specific activity at different pH values. The substrate ABTS was diluted in the buffers listed in Table 3.2 to a final concentration of 5 mM and used as the assay solution.

Table 3.2. Buffers used for analysis of enzyme pH optimum at different pH values.

Buffer	pH
0.1M Formate buffer	3.4
0.1M Acetate buffer	3.8, 4.2, 4.6, 5.0
0.1M MES buffer	5.4

0.1M Sodium Phosphate buffer	5.8, 6.2, 6.6, 7.0, 7.4, 7.8
0.1M Tris buffer	8.2, 8.6

3.6.3. Substrate screening

<u>Materials</u>

- 0.1 M Ferulic acid
- 0.1 M Sinapic acid
- 0.1M 4-hydroxybenzoic acid
- 0.1 M 3,4-dihydrobenzoic acid
- 0.1 M Vanillic acid
- 0.1 M Catechol
- 0.1 M Guaiacol
- 0.05 M Syringealdehyde
- 0.05 M Vanillin
- 96 % Ethanol
- Dimethyl sulfoxide (DMSO)
- 0.1 M Sodium phosphate buffer pH 7.5

<u>Procedure</u>

Screening for potential laccase substrates, a variety of small phenolic substrates were selected based on previous substrate screenings done for CotA. Sinapic acid was dissolved in DMSO, *m*-coumaric acid, *p*-coumaric acid, 4-hydrobenzoic acid, 3,4-Dihydrobenzoic acid, vanillic acid, guaiacol, and syringealdehyde were dissolved in 96% ethanol, and ferulic acid, catechol and vanillin were dissolved in 0.1 M Sodium phosphate buffer pH 7.5 to generate stock solutions of the substrates. All stock solutions were diluted with 0.1 M Sodium phosphate buffer pH 7.5, and the obtained solutions were analyzed in a UV/visible scan to find the wavelength with the highest absorption value for each substrate (see 7.1, appendix A) to determine at which wavelength the oxidation of the substrate should be monitored during the activity assay. The activity assay was performed as described in section 3.6. All substrates were diluted to a final concentration of 0.05 mM prior to the activity assay, the same substrate concentration that was used in the UV/visible scan. Activity assays were run with the enzymes P01-C03, P01-E07, P06-A08 and P20-F12 and all the phenolic substrates chosen for screening.

3.7. Determination of K_m, V_{max}, and k_{cat}

In order for an enzymatic reaction to follow Michaelis-Menten kinetics the plot of the initial velocity, *v*, against the substrate concentration, [S], will give a hyperbola with the form of

$v = V_{max}[S]/(K_m + [S])$

Where V_{max} is the maximum initial velocity and K_m is the substrate concentration at half-maximal initial velocity (Dowd 1965). All four *Actinobacteria* laccase candidates were analyzed to evaluate if their enzymatic reaction followed Michaelis-Menten kinetics, by calculating the specific activity for each enzyme at different ABTS substrate concentrations. The specific activity was converted to the formation of oxidized ABTS (µM) per minute with the following equation;

$$\frac{\Delta E/d}{\varepsilon ABTS}$$

Where ΔE is the change in absorption per minute, d is the path length (depending on the microtiter plate that was used), and $\varepsilon ABTS$ is the molar absorption coefficient of ABTS at 420 nm wavelength, 36 000 $M^{-1}cm^{-1}$.

The following ABTS substrate concentrations were used; 20 mM, 15 mM, 10 mM, 5 mM, 2.5 mM, 1.25 mM, 0.625 mM, 0.32125 mM and 0.156 mM, diluted in acetate buffer pH 4.2, and activity assays with three replicates were run for each substrate concentration with P01-C03, P01-E07, P06-A08 and P20-F12.

To generate the hyperbola curve and calculate K_m and V_{max} the simple tool kit from http://ic50.tk/kmvmax.html was used. The K_m V_{max} toolkit allows the rate of an enzyme-catalyzed reaction to be plotted against the concentration of the substrate fitted to the Michaelis-Menten equation to give K_m and V_{max}. Based on the V_{max} generated from the tool kit, k_{cat} was calculated using the following equation:

$$kcat = \frac{Vmax}{[E]t}$$

Where $[E]_t$ is the total enzyme concentration used in the activity assay.

3.8. SDS-PAGE (Sodium dodecyl sulfate-polyacrylamid gel electrophoresis)

Polyacrylamide gel electrophoresis is used to separate molecules based on size and charge (Brunelle and Green 2014). SDS-PAGE is a type of gel electrophoresis that is used to separate protein molecules based on size. Heat incubation together with SDS will denature the proteins and coat them with a negative charge that will allow the protein to migrate in the gel towards the anode. Smaller protein fragments will migrate faster through the polyacrylamide gel, and larger fragments will migrate slower, separating different sized fragments from each other. SDS-PAGE is helpful in monitoring protein purification and determine the presence of the protein of interest.

Materials
- 3 x SDS loading dye
- 12% 10-well RunBlue™ SDS gel
- RunBlue™ 20x SDS Running Buffer
- Precision Plus Protein™ Dual Color Standard (Bio-Rad)
- InstantBlue™ Protein Stain
- Protein sample
- ddH$_2$O
- Sterile 1.5 mL Eppendorf tubes
- Thermomixer comfort heat block
- DCS-700 dual cool mini vertical electrophoresis unit
- PowerPac™Basic Power Supply
- Petri dishes for staining
- Chemidoc Imaging System/ImageLab™ Touch software

Procedure:
Samples were prepared by mixing 20 μL of protein sample with 10 μL 3 x SDS loading dye in a 1.5 mL Eppendorf tube followed by heat incubation at 95 ℃ for 10 minutes to denature the proteins. The 20x SDS running buffer was diluted to 1x SDS running buffer with ddH$_2$O. The SDS gel was placed in a DCX-700 dual cool mini vertical electrophoresis unit and filled with

1 x SDS running buffer. In order to make sure there were no air bubbles in the wells on the SDS gel, all wells were washed with 1 x SDS running buffer using a pipette. After heat incubation of the samples, 7 μL of the Precision Plus Protein™ Dual Color Standard and 15 μL of each sample was applied to separate wells on the SDS-gel. After application of all the samples, the program was set to 150 V for 65 minutes with constant voltage using a PowerPac™Basic Power Supply, which is the standard program used for SDS-PAGE in the laboratory where the work was performed. After running the program, the 1 x SDS running buffer was transferred to a Pyrex glass bottle for re-use, and the SDS-gel was stained overnight with InstantBlue™ Protein Stain at room temperature in a Titramax 1000 vibrating platform shaker at 50 rpm. After overnight staining the digital image of the gel was obtained using a Chemidoc Imaging System/ImageLab™ Touch software.

3.9. Site directed mutagenesis (QuikChange kit, Agilent technologies)

In vitro site-directed mutagenesis is a PCR-based technique used to mutate specific nucleotides of a sequence within a plasmid vector (Bachman 2013). To generate specific mutations to the protein sequence of interest, specifically designed primers containing the mutation is needed. The forward and reverse primers are centered on the desired nucleotide change(s), overlapping completely in both directions. The extension of these primers around the plasmid generates a template containing the inserted mutation.

The QuikChange kit from Agilent technologies, provides a three-step procedure that allows site-specific mutations in virtually any double-stranded plasmid. The first step is synthesis of the mutant strand which is done by thermal cycling. The DNA template is first denatured followed by annealing of the mutagenic primers. The primers are then extended with DNA polymerase. After mutant strand synthesis, the parental strands of DNA obtained from *E. coli* are digested using *Dpn*I, which cuts methylated and hemi-methylated DNA. The last step is transformation of competent cells with the mutated plasmid vector for nick repair.

Materials:

- QuikChange Site-Directed mutagenesis kit (see section 2.2)
- Forward and reverse oligo primers containing different mutations (see section 2.3)

- NZY+ broth (see section 3.2.1)
- LB-ampicillin agar plates (50 μg/mL)
- 80 μg/mL 5-bromo-4-chloro-3-inodyl-β-D-galacto-pyranoside (X-gal)
- 20 mM Isopropyl β-D-1-thiogalactopyranoside (IPTG)
- SimpliAmp Thermal Cycler (Thermo Fischer)

Procedure

Mutant Strand Synthesis Reaction (Thermal Cycling)

The control reaction was prepared as indicated below in a PCR tube to a final volume of 51 μL:

- 5 μL of 10 x reaction buffer
- 2 μL (10 ng) of pWhitescript 4.5-kb control plasmid (5 ng/μL)
- 1.25 μL (125 ng) of oligonucleotide control primer #1
- 1.25 μL (125 ng) of oligonucleotide control primer #2
- 1 μL of dNTP mix
- 38.5 μL nuclease-free water (to bring the final reaction volume to 50 μL)

Then add

- 1 μL of *PfuUltra* HF DNA polymerase (2.5 U/μL)

The sample reactions were prepared as indicated below in a PCR tube to a final volume of 51 μL:

- 5 μL of 10 x reaction buffer
- 25 ng of dsDNA template
- 125 ng of forward oligonucleotide primer
- 125 ng of reverse oligonucleotide primer
- 1 μL of dNTP mix
- Nuclease-free water to a final volume of 50 μL

Then add

- 1 μL of *PfuUltra* HF DNA polymerase (2.5 U/μL)

To determine the volume of dsDNA template needed in the sample reaction to obtain 25 ng of DNA a Qubit assay of the DNA miniprep was performed as described in section 3.5.

Each reaction was executed using the cycling parameters displayed in Table 3.3, where the number of cycles is set according to the type of mutation, which here is a single amino acid change.

Table 3.3. Cycling parameters used for mutant strand synthesis

Segment	Cycles	Temperature	Time
1	1	95 °C	30 seconds
2	16 (sample)	95 °C	30 seconds
	18 (control)	55 °C	1 minute
		68 °C	6 minutes (sample)
			5 minutes (control)

DpnI digestion of the Amplification products

After thermal cycling, 1 µL of *Dpn*I restriction enzyme was added to each amplification reaction. Each reaction mixture was thoroughly mixed and centrifuged for 1 minute at room temperature, followed by incubation at 37 °C for 1 hour to digest the parental DNA.

Transformation of XL1-Blue supercompetent Cells

XL1-Blue super-competent cells were thawed on ice prior to use. For each sample and control, 50 µL of supercompetent cells were aliquoted to a 1.5 mL Eppendorf tube with 1 µL of *Dpn*I treated DNA. As an additional control to verify the transformation efficiency of the XL1-Blue super-competent cells, 1 µL of the pUC18 control plasmid was added to a 50 µL aliquot of the super-competent cells. All reactions were mixed by carefully swirling the tubes, followed by incubation on ice for 30 minutes. After incubation, the transformation reactions were heat-pulsed for 45 seconds at 42 °C using an Isotemp® GDP25 water bath from Fisher scientific. After the heat pulse, all reactions were placed on ice for 2 minutes, and 0.5 mL of NZY$^+$ broth (see section 3.2.1) preheated to 42 °C was added to each reaction. All reaction mixtures were then incubated at 37 °C and 225 rpm for one hour. After incubation each transformation reaction was spread on LB-agar plates containing 50 µg/mL ampicillin as indicated in Table 3.4. The

two control reactions were spread on LB-ampicillin agar plates pre-spread with 80 µg/mL X-gal and 20 mM IPTG 30 minutes prior to use, for blue-white color screening. All transformation plates were incubated overnight at 37 ℃.

Table 3.4. Volume of transformation reaction to plate om LB-agar plates containing 50 $\mu g/mL$ ampicillin.

Reaction type	Volume to plate
pWhitescript mutagenesis control	250 µL
pUC18 transformation control	5 µL (in 200 µL of NZY⁺ broth)
Sample mutagenesis	250 µL on each of two plates (entire transformation reaction)

In this study, a total of five amino acid mutations were suggested to be performed on the plasmid vector containing the sequence of the CotA laccase. The mutations are listed in Table 3.5**.** Introducing several mutations on the same plasmid was done by using a mutated plasmid vector as template and introducing a second or third mutation by performing a new site-directed mutagenesis using oligo primers with the desired mutation.

Table 3.5. Amino acid mutations to be performed on the genomic sequence of the *cotA* gene from B. subtilis. A total of five mutations were planned, but only mutations 1, 2 were completed and analyzed. The last three mutations were not completed.

Amino acid mutation nr.	Mutation
1	P226M
2	L386A
3	A471P
4	A376S_G377V (Double mutation)

3.10. Plasmid isolation (Wizard® Plus SV Miniprep DNA purification Systems kit, Promega)

<u>Materials</u>

- Wizard® Plus SV Miniprep DNA purification Systems kit (see section 2.2)
- 1-10 mL fresh overnight culture (see section 3.2.4) containing plasmid to be isolated

- LB-ampicillin agar plates (50 μg/mL)
- Sterile 2 mL Eppendorf tubes
- Eppendorf minispin plus centrifuge

Procedure

Production of cleared lysate

A volume of 2 mL fresh overnight culture was transferred to a 2 mL Eppendorf tube and centrifuged at 14,100 x g for 5 minutes to harvest the cell culture, discarding the supernatant. The cell pellet was resuspended with 250 μL of cell resuspension solution. To lysate the cells, 250 μL of cell lysis was added, and the sample was carefully mixed by inverting the tube four times. To digest proteins in the cell lysate, 10 μL of alkaline protease solution was added. The sample was mixed by inverting the tube four times and incubated at room temperature for 5 minutes. After incubation 350 μL of neutralization solution was added and centrifuged at 14,100 x g for 10 minutes using an Eppendorf minispin plus minicentrifuge.

Binding of plasmid DNA

A Wizard®SV minicolumn was placed in a collection tube and the cleared lysate was transferred to the collection tube and centrifuged at 14,100 x g for 1 minute at room temperature. The flow-through was discarded, and the column reinserted in the collection tube. To wash the solution 750 μL of wash solution was added to the spin column and centrifuged at 14,100 x g for 1 minute at room temperature. This was repeated again using 250 μL of wash solution.

Elution of plasmid DNA

The plasmid was eluted from the spin column to a sterile Eppendorf tube by adding 50 μL of nuclease free water followed by centrifugation at 14,100 x g for 1 minute. The column was discarded, and the eluted DNA was stored at -20 °C.

3.11. Bacteria storage

For long-time storage of *E. coli* cells glycerol stocks were made to preserve the cells carrying either the pET-21a(+), pET-22b(+), or pET-30a(+) plasmids containing the gene of interest (see section 3.2.2). All plasmids were used for bacterial expression of the target genes. The pET-21a(+) and pET-22b(+) plasmids both provide bacterial resistance against ampicillin. The pET-

30a(+) plasmid provides resistance against kanamycin. The glycerol stabilizes the bacterial cells and prevents damage to the cell membrane upon ice crystal formation at freezing temperatures. Glycerol stocks were made by mixing 0.5 mL of fresh overnight culture (see section 3.2.4) with 0.5 mL 50% glycerol in a cryo-tube. All glycerol stocks were stored at -80 °C for long-time storage and -20 °C for making overnight cultures.

3.12. Sequence alignment and homology model building

SINTEF has recently sequenced approximately 1,200 genomes of marine *Actinobacteria* isolates collected from the Trondheim fjord. Analyzing these genomes has revealed several redox enzyme candidates of interest. The search for new laccase candidates for characterization was done using these recently sequenced *Actinobacteria* genomes.

The genes representing the laccase candidates used in the present MSc study were selected by Giang-Son Nguyen (SINTEF) and obtained through gene synthesis and cloning at a commercial supplier (GenScript) prior to the start of the project. In short, the following selection procedure was applied. The laccase candidates selected for characterization were obtained from a shortlist comprising of 18 sequences from the strain collection. The Multicopper Oxidase engineering database was used to search for SLAC-like laccases. A collection of SLAC-like laccases, HFAM 39, was found. As there were no Hidden Markov model (HMM) profiles for SLAC-like laccases in Pfam, new HMM profiles were generated using HMM-build in HMMR. The newly built HMM profiles were used in HMMscan to find SLAC-like candidates among the 1,200 actinobacteria genomes. This resulted in 439 hits, and after the selection the shortlist comprised of 18 different laccase candidate sequences. The shortlist was generated by Giang-Son Nguyen (SINTEF).

All 18 sequences from the shortlist were first uploaded in the program Geneious before running a BLAST search, using blastp, against the Protein databank (PDB) and Nucleotide collection (nr/nt) for each sequence. The sequence hit from the Nucleotide collection BLAST that had the highest query coverage percentage and pairwise identity percentage was aligned against the candidate sequence. In the alignment, the area of which the candidate sequence matched the sequence area of the BLAST hit was extracted, and the areas of the candidate sequences that did not align with the BLAST hit were left out. A homology model for each extraction was

generated by uploading the sequence in PHYRE.[1] The template that was used to generate the homology model was aligned in pyMol with the homology model and the best hit from PDB BLAST, to observe how much the homology model differed from the template. Sequence alignments and structural alignments were studied. Focusing on sequence alignment, candidates were chosen based on their similarity to known SLACs. For risk mitigation, some candidates were chosen based on their high sequence similarities, and some were chosen because of their low sequence similarity, in approximately equal numbers. In total, seven candidates were selected and sent to GenScript for gene synthesis.

3.13. Calculating specific enzymatic activity (U/mg)

An enzyme´s specific activity is a measurement of the purify of an enzyme solution. It is defined as the amount of substrate that is converted during the enzymatic process per unit of time and mass of the total protein (Foustoukos 2014). To calculate the specific activity of a protein solution containing the enzyme of interest, the enzyme activity (See section 1.6.1) is divided by the protein concentration (mg/mL) (Baltierra-Trejo, Márquez-Benavides, and Sánchez-Yáñez 2015), and is expressed as U mg^{-1}.

---

[1] http://www.sbg.bio.ic.ac.uk/phyre2/html/page.cgi?id=index

4. Results

In this study the three *Psychrobacter* laccases P2G3, P11G3 and P11F6 were expressed for the first time in-house at SINTEF to gain knowledge and insight in practical methods of heterologous enzyme production, prior to producing and characterizing the *Actinobacteria* laccase enzymes obtained in the OXYMOD project. During this part of the study, also the effect of adding $CuCl_2$ at different stages during protein expression was examined.

The four *Actinobacteria* laccases candidates P01-C03, P01-E07, P06-A08 and P20-F12 were successfully produced for the first time in *E. coli*, confirmed to be active laccases, and underwent extensive characterization including temperature stability, pH stability, substrate screening, and lignin assays.

The genetic sequence of the thermostable CotA laccase from *B. subtilis* underwent several amino acid mutations in order to evaluate if it would be possible to generate activity towards the potential mediator vanillin.

4.1. Expression of the three *Psychrobacter* laccases P2G3, P11G3 and P11F6

To verify the successful transformation of *E. coli* with different plasmids containing the genes representing the different enzymes, all three transformants were cultivated as described in section 3.2.5.1 followed by protein extraction, SDS-PAGE, activity assay, and purification.

In order to get insight into the stability of the enzyme´s activity and the influence of providing Cu^{2+} ions at different stages of enzyme production, the three recombinant *E. coli* strains encoding *Psychrobacter* laccases P2G3, P11G3 and P11F6 were cultivated, and respective cell extracts exposed to different soaking conditions (soaking indicates supplementation of $CuCl_2$ directly to the cell extract), shown in Table 4.3 and the specific activity was calculated according to the method described in section 3.13. The results are presented in Table 4.1. All three enzyme encoding strains were also cultivated without induction or addition of $CuCl_2$ as controls.

To investigate if storage at 4 °C would have an impact on the enzymatic activity, the specific activity of all laccases was determined once a day in a period of 8 days. Two different concentrations of CuCl$_2$, 0.25 mM and 1 mM, were applied during cultivation (see section 3.2.5.1) to see if it would have an effect on the enzymatic activity. The results of the cultivation with respect to protein yield and specific activity is presented below in section 4.1.4.

4.1.1.   Initial protein expression experiments

To investigate expression of laccases P2G3, P11G3 and P11F6 in *E. coli*, cell extracts (containing soluble proteins) and cell pellets (containing insoluble proteins and other cell debris) were analyzed using SDS-PAGE (Figure 4.1 and Figure 4.2). Expression of P2G3, P11G3 and P11F6 was done as described in section 3.2.5.1. Negative control samples were withdrawn from the cultures before induction and further cultivated as described above. P2G3, P11G3 and P11F6 were expected as bands corresponding to ∼ 62 kDa on the SDS-PAGE gels presented in Figure 4.1 and Figure 4.2 (see 7.2, appendix B for an overview of the exact peptide chain lengths and MWs of each enzyme).

Expression of P11G3 (theoretical MW = 61.692 kDa) was observed when the *E. coli* culture was induced with IPTG (Figure 4.1, lane 1), but only marginally (if any) in the absence of the inducer and CuCl$_2$ (Figure 4.1, lane 3). The cell pellet of the expression induced culture also contained P11G3 (Figure 4.1, lane 2), indicating the formation of inclusion bodies or incomplete lysis.
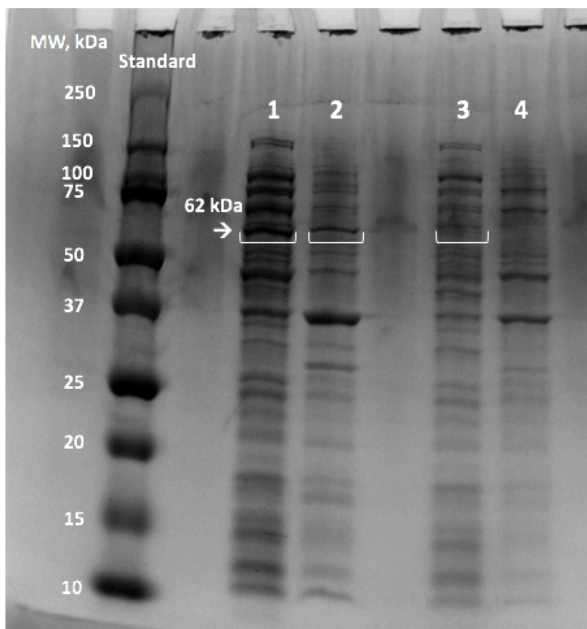
Figure 4.1. Expression of P11G3 in *E. coli*. Expression of the Psychrobacter laccase P11G3 (MW = 62 kDa) in *E. coli* was analyzed by SDS-PAGE. The SDS-PAGE gel shown displays the following samples: lane marked "standard": Precision Plus Protein™ Dual Color Standard from BioRad, lane 1): Cell extract containing P1G3 after sonication, lane 2): Cell pellet and insoluble proteins obtained after sonication of P1G3 *E. coli*, lane 3): Cell extract of P1G3 control sample (not induced with IPTG, and not supplemented with CuCl$_2$), lane 4): Cell pellet and insoluble proteins of P1G3 control sample (not induced with IPTG, and not supplemented with CuCl$_2$). All cultures were cultured according to section 3.2.5.1 and protein was extracted according to section 3.3.1.

Expression of P2G3 (theoretical MW = 61.714) and P11F6 (theoretical MW = 61.887) was observed when the two *E. coli* cultures each encoding either P2G3 or P11F6 were induced with IPTG (Figure 4.2, lane 1 and 5, respectively), but only marginally (if any) in the absence of the inducer and CuCl$_2$ (Figure 4.2, lane 3 and 4, and lane 7 and 8, respectively). P2G3 and P11F6 were also in larger amounts observed in the cell pellets (Figure 4.2, lane 2 and 6, respectively), indicating formation of inclusion bodies or incomplete lysis. The cell pellet containing the expressed enzyme P2G3 (Figure 4.2, lane 2) indicates particularly high levels of inclusion body formation.
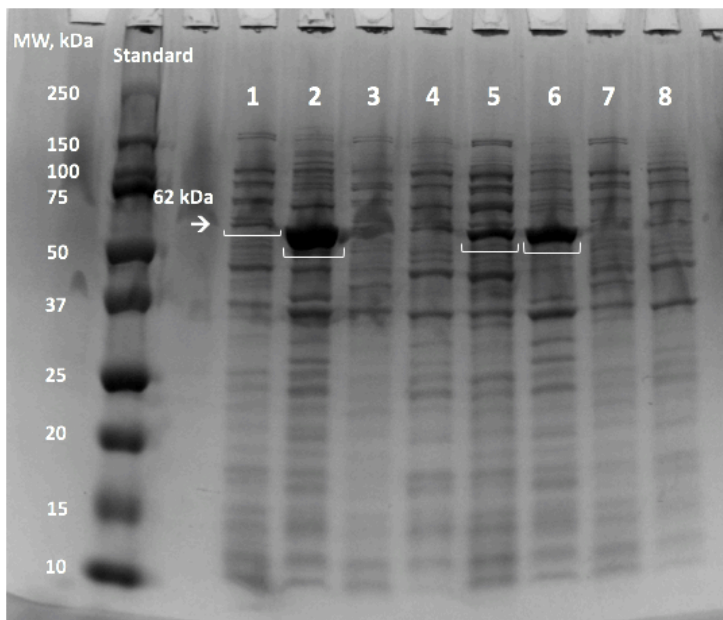
Figure 4.2. Expression of P2G3 and P11F6 in *E. coli*. Expression of the *Psychrobacter* laccases P2G3 (MW ~ 62 kDa) and P11F6 (MW ~ 62 kDa) in *E. coli* was analyzed by SDS-PAGE. The SDS-PAGE gel shown displays the following samples: lane marked as "standard": Precision Plus Protein™ Dual Color Standard from BioRad, lane 1): Cell extract containing P2G3 after sonication, lane 2): Cell pellet and insoluble proteins obtained after sonication of P2G3 *E. coli,* lane 3): Cell extract pf P2G3 control sample (not induced with IPTG, and not supplemented with CuCl2), lane 4): Cell pellet and insoluble proteins obtained after sonication of P2G3 control sample (not induced with IPTG, and not supplemented with CuCl2), lane 5) Cell extract containing P11F6 after sonication, lane 6): Cell pellet and insoluble proteins obtained after sonication of P11F6 *E. coli*, lane 7): Cell extract after sonication of P11F6 control sample (not induced with IPTG, and not supplemented with CuCl2), lane 8): Cell pellet and insoluble proteins obtained after sonication of P11F6 control sample (not induced with IPTG, and not supplemented with CuCl2). All cultures were cultured according to section 3.2.5.1*,* and protein was extracted according to section 3.3.1.

After verification of the expression of the three *Psychrobacter* laccases by SDS-PAGE in the initial protein expression experiment, the activity of P2G3, P11G3 and P11F6 in the soluble fraction of cell extracts were verified as specific activity by activity assay using the laccase substrate ABTS. The results are presented in Table 4.1.

Table 4.1. Specific activity of P2G3, P11G3 and P11F6 after the initial protein expression experiment. Activity assay with the substrate ABTS was performed for the protein extracts containing P2G3, P11G3, and P11F6. The specific activity with standard deviation for three replicates is listed.

Cell extract containing the enzyme	Average specific activity of three replicates, with standard deviation, with

	the substrate ABTS (U/mg) (Protein extract)
P2G3	0.27 ± 0.01
P11G3	2.34 ± 1.05
P11F6	2.77 ± 0.28

After verifying the expression and specific activity for the three *Psychrobacter* laccases, all enzymes were purified using HIS-Select® spin columns, as described in section 3.4.2.2, and analyzed by SDS-PAGE (Figure 4.3 and Figure 4.4). After purification P2G3, P11G3 and P11F6 underwent buffer exchange as described in section 3.4.3.2.

Purification of the enzyme P11G3 was achieved by obtaining an ∼ 95% pure enzyme solution compared to the protein extract (Figure 4.3, lane 1 and 2).
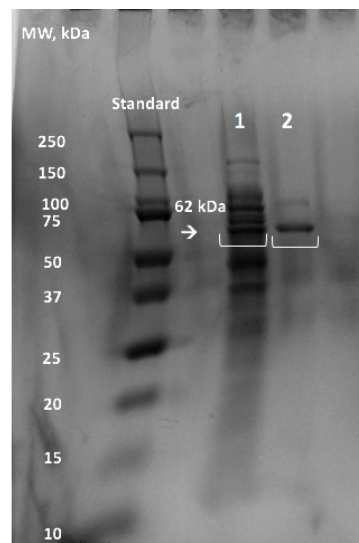

Figure 4.3. Purification of P11G3 expressed in *E. coli*. Purification of the laccase P11G3 (MW ∼ 62 kDa) with immobilized metal affinity chromatography (IMAC) was analyzed by SDS-PAGE. The SDS-PAGE gel shown displays the following samples: lane marked "standard": Precision Plus Protein™ Dual Color Standard from BioRad, lane 1): Cell extract of *E. coli* containing P11G3, lane 2) Enzyme solution containing purified P11G3 enzyme.

Also, purification of the enzyme P11F6 was successful, resulting in an ∼ 95% pure enzyme solution compared to the protein extract (Figure 4.4, lane 1 and 2). A similar result was also obtained for the enzyme P2G3 (Figure 4.4, lane 3 and 4).
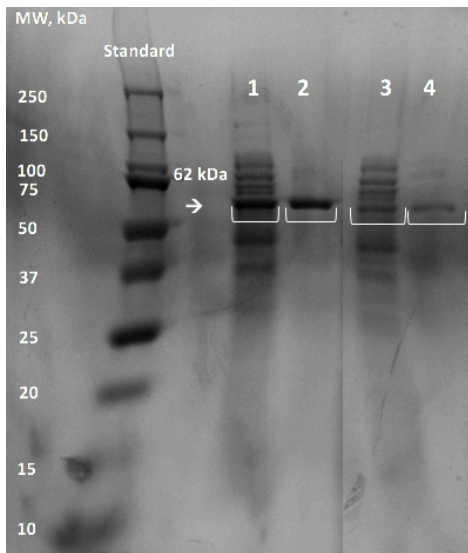
Figure 4.4. Purification of P11F6 and P2G3 expressed in *E. coli*. Purification of the two laccases P11F6 (MW ~ 62 kDa) and P2G3 (MW ~ 62 kDa) with immobilized metal affinity chromatography (IMAC) was analyzed by SDS-PAGE. The SDS-PAGE gel shown displays the following lanes: lane marked "standard": Precision Plus Protein™ Dual Color Standard from BioRad, lane 1): Cell extract of *E. coli* containing P11F6, lane 2) Enzyme solution containing purified P11F6, lane 3): Cell extract of *E. coli* containing P2G3, lane 4): Enzyme solution containing purified P2G3.

After purification, activity assays were performed for all three *Psychrobacter* laccases with the substrate ABTS. Activity assay after buffer exchange with the substrate ABTS was also run. None of the enzymes, P2G3, P11G3 and P11F6, was found to be active with ABTS after purification, or after buffer exchange.

4.1.2. The effect of inducer and cofactor on the expression of three *Psychrobacter* laccases

To further investigate systematically how the expression of laccases P2G3, P11G3 and P11F6 would be affected in the presence and absence of the inducer IPTG, in combination with the presence and absence of the co-factor Cu^{2+}, cell extracts (containing soluble proteins) and cell pellets (containing insoluble protein and cell debris) of respective expression cultures were analyzed by SDS-PAGE (Figure 4.5 and Figure 4.6). All cultures were cultivated according to section 3.2.5.1 and the protein was extracted according to section 3.3.1.

Expression of P2G3 (theoretical MW = 61.714) was observed when the *E. coli* culture was cultivated in the absence of $CuCl_2$ (Figure 4.5, lane 1). However, the enzyme was primarily

observed in the cell pellet, indicating formation of inclusion bodies or incomplete lysis (Figure 4.5, lane 2). Expression of P2G3 could hardly be observed in the absence of the inducer, indicating only little (if any) background expression of the enzyme (Figure 4.5 lane 3 and 4). Primarily soluble expression of P11G3 (theoretical MW = 61.692) was observed when the *E. coli* bacterial culture was cultivated in the absence of CuCl$_2$ (Figure 4.5, lane 5), with hardly any denatured enzyme observable in the cell pellet (Figure 4.5, lane 6). In absence of the inducer IPTG, no expression of P11G3 was observed in neither of the protein extract (Figure 4.5, lane 7) nor the cell pellet (Figure 4.5, lane 8), indicating tight promotor control.
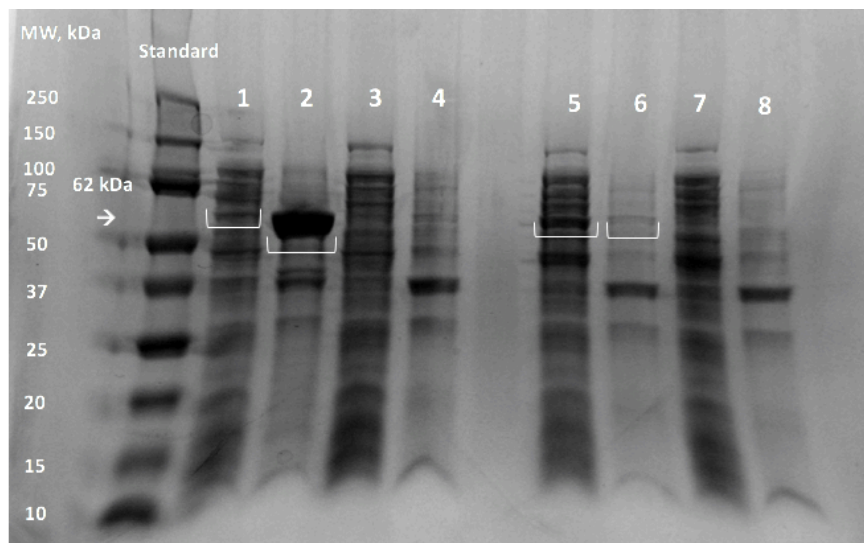

Figure 4.5. Expression of P2G3 and P11G3 in E. coli in the absence of either CuCl$_2$, or the inducer IPTG. Expression of the *Psychrobacter* laccases P2G3 (MW ~ 62 kDa) and P11G3 (MW ~ 62 kDa) in the absence of CuCl$_2$, and background expression in the absence of the inducer IPTG was analyzed by SDS-PAGE. The SDS-PAGE gel shown displays the following samples: lane marked "standard": Precision Plus Protein™ Dual Color Standard from BioRad, lane 1): Protein extract after sonication of P2G3 *E. coli* induced with IPTG and in absence of CuCl$_2$, lane 2): Cell pellet and insoluble proteins obtained after sonication of P2G3 *E. coli* induced with IPTG and in absence of CuCl$_2$, lane 3): Protein extract after sonication of P2G3 *E. coli* with CuCl$_2$ and in the absence of the inducer IPTG, lane 4): Cell pellet and insoluble proteins obtained after sonication of P2G3 *E. coli* with CuCl$_2$ and in the absence of the inducer IPTG, lane 5): Protein extract after sonication of P11G3 *E. coli* induced with ITPG and in absence of CuCl$_2$, lane 6): Cell pellet and insoluble proteins obtained after sonication of P11G3 *E. coli* induced with IPTG and in absence of CuCl$_2$, lane 7): Protein extract after sonication of P11G3 *E. coli* with CuCl$_2$ and in the absence of the inducer IPTG, lane 8): Cell pellet and insoluble proteins obtained after sonication of P11G3*E. coli* with CuCl$_2$ and in the absence of the inducer IPTG.

Soluble expression of P11F6 (theoretical MW =61.887) was observed when the *E. coli* culture was cultured, and expression induced in the absence of CuCl$_2$ (Figure 4.6, lane 1). Larger amounts of P11F6 could, however also be observed in the cell pellet, indicating the formation

of inclusion bodies or incomplete lysis. In the absence of the inducer and only supplementation with CuCl$_2$ expression of P11F6 could hardly be observed in neither soluble or insoluble fraction (Figure 4.6, lane 3 and 4).
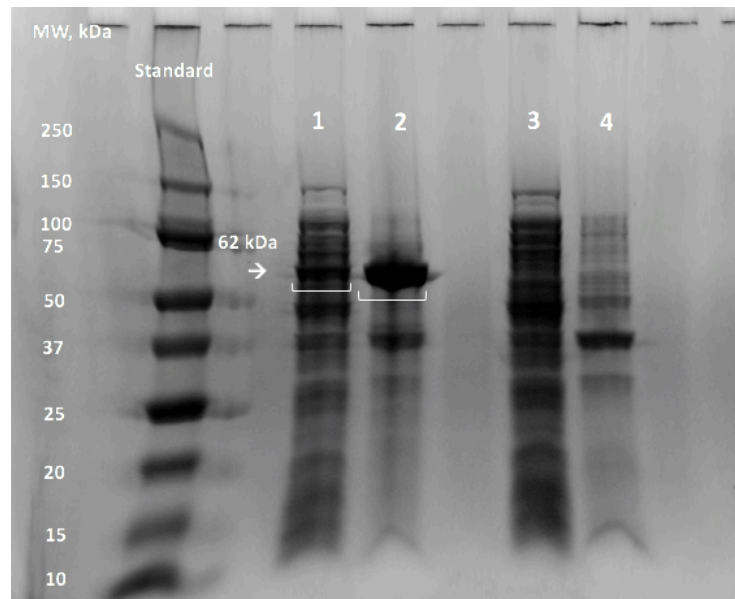

Figure 4.6. Expression of the laccase P11F6 in E. coli in the absence of either CuCl$_2$, and or the inducer IPTG. Expression of the *Psychrobacter* laccases P11F6 (MW ~ 62 kDa) in the absence of CuCl$_2$, and background expression in the absence of the inducer IPTG was analyzed by SDS-PAGE. The SDS-PAGE gel shown displays the following samples: lane marked "standard": Precision Plus Protein™ Dual Color Standard from BioRad, lane 1): Protein extract after sonication of P11F6 *E. coli* induced with ITPG and in absence of CuCl$_2$, lane 2): Cell pellet and insoluble proteins obtained after sonication of P11F6 *E. coli* induced with IPTG and in absence of CuCl$_2$, lane 3): Protein extract after sonication of P11F6 *E.* with CuCl$_2$ and in the absence of the inducer IPTG, lane 4): Cell pellet and insoluble proteins obtained after sonication of P11F6 *E. coli* with CuCl$_2$ and in the absence of the inducer IPTG

To investigate how the absence of either the inducer or the supplementation of CuCl$_2$ during cultivation would affect the activity of P2G3, P11G3 and P11F6, activity assays were performed. Activity was not observed for any of the enzymes in the absence of CuCl$_2$ indicating the importance of cofactor supplementation. The cell extracts of P2G3, P11G3 and P11F6 that had not been supplemented with CuCl$_2$, but induced with IPTG, were supplemented with additional CuCl$_2$ to investigate if it would allow the enzymes to gain activity towards ABTS. P11G3 and P11F6 gained activity after CuCl$_2$ soaking, but no activity was observed for P2G3 after respective treatment. The calculated specific activities are presented in Table 4.2. Activity could be observed for P11G3 and P11F6 in the absence of the inducer with supplementation of CuCl$_2$ during cultivation, but no activity was observed for P2G3.

Table 4.2. Overview of detected activities and, if positive, the average specific activity and standard deviation of three parallels with the substrate ABTS measured from the cell extract of the enzymes P11G3, P11F6 and P2G3 in the absence of inducer, supplemented with $CuCl_2$, and cell extract that had been induced with IPTG during cultivation and soaked with. Absence of IPTG or $CuCl_2$ is indicated with -, and presence of IPTG or $CuCl_2$ is indicated with +.

Enzyme	Specific activity (U/mg) and standard deviation of three parallels with the substrate ABTS
P11G3 cultured -IPTG, + $CuCl_2$	0.15 ± 0.009
P11G3 cultured + IPTG, - $CuCl_2$	No activity detected
P11G3 cultured + IPTG, - $CuCl_2$; soaked with $CuCl_2$	0.18 ± 0.01
P11F6 cultured - IPTG, + $CuCl_2$	0.03 ± 0.004
P11F6 cultures + IPTG, - $CuCl_2$	No activity detected
P11F6 cultured + IPTG, - $CuCl_2$; soaked with $CuCl_2$	0.25 ± 0.16
P2G3 cultured - IPTG, + $CuCl_2$	No activity detected
P2G3 cultured + IPTG, - $CuCl_2$	No activity detected
P2G3 cultured + IPTG, - $CuCl_2$; soaked with $CuCl_2$	No activity detected

4.1.3. Expression of laccases in the presence of $CuCl_2$

To investigate the effect of $CuCl_2$ supplementation during cultivation and/or after extraction, P2G3, P11G3 and P11F6 cell extracts (containing soluble proteins) and purified enzyme solutions (containing purified protein) were analyzed using SDS-PAGE (Figure 4.7 and Figure 4.8) and by calculating the specific activity of each enzyme running activity assays with the substrate ABTS (Table 4.4). All bacterial cultures were cultivated as described in section 3.2.5.1 and supplemented with $CuCl_2$ as described in Table 4.3.

Table 4.3: Different strategies of supplementing CuCl₂ to the bacterial cultures or protein extracts during cultivation and after protein extraction. All the cultures were cultivated as described in section 3.2.5.1 and supplemented with CuCl₂ as presented in this table.

Cultivation and soaking strategy	IPTG induction	CuCl₂ supplementation during cultivation	CuCl₂ soaking of cell extract
1	+	+	-
2	+	+	+
3	+	-	+

Expression of P11F6, P11G3, and P2G3 in *E. coli* under any CuCl₂ supplementation strategy (Table 4.3) was observed when *E. coli* cultures were induced with IPTG (Figure 4.7 and Figure 4.8), meaning that different strategies of CuCl₂ supplementation did not appear to affect the level of expression of the different *E. coli* cultures producing the same enzyme. SDS-PAGE band size of purified enzyme solutions of P11F6 (Figure 4.7, lane 2, 4 and 6) was observed to have approximately the same size. This was also observed for P11G3 (Figure 4.7, lane 8 and 10, and Figure 4.8, lane 2) and P2G3 (Figure 4.8, lane 4, 6 and 8). Purification of the cell extracts (see section 3.4.2.2) were successful, though some impurities did remain. Impurities could be observed after purification of P11F6 (Figure 4.7, lane 2, 4 and 6), P11G3 (Figure 4.7, lane 8 and 10, and Figure 4.8, lane 2) and P2G3 (Figure 4.8, lane 4, 6 and 8).
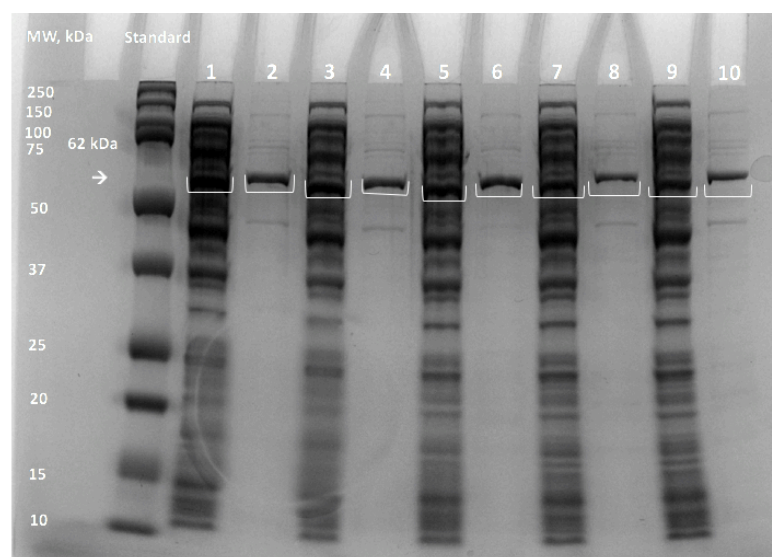

Figure 4.7. Expression and purification of P11F6 and P11G3 with different CuCl₂ supplementation strategy. Expression and purification of P11F6 and P1G3 were analyzed by SDS-PAGE. The different strategies refer to the strategies presented in Table 4.3. The SDS-PAGE gel shown displays the following samples: lane marked

"standard": Precision Plus Protein™ Dual Color Standard from BioRad, lane 1): Cell extract containing P11F6 supplemented with $CuCl_2$ as in strategy 3, lane 2) Purified enzyme solution containing P11F6 supplemented with $CuCl_2$ as in strategy 3, lane 3): Cell extract containing P11F6 supplemented with $CuCl_2$ as in strategy 2, lane 4): Purified enzyme solution containing P11F6 supplemented with $CuCl_2$ as in strategy 2, lane 5): Cell extract containing P11F6 supplemented with $CuCl_2$ as in strategy 1, lane 6): Purified enzyme solution containing P11F6 supplemented with $CuCl_2$ as in strategy 1, lane 7): Cell extract containing P11G3 supplemented with $CuCl_2$ as in strategy 3, lane 8): Purified enzyme solution containing P11G3 supplemented with $CuCl_2$ as in strategy 3, lane 9): Cell extract containing P11G3 supplemented with $CuCl_2$ as in strategy 2, lane 10): Purified enzyme solution containing P11G3 supplemented with $CuCl_2$ as in strategy 2.
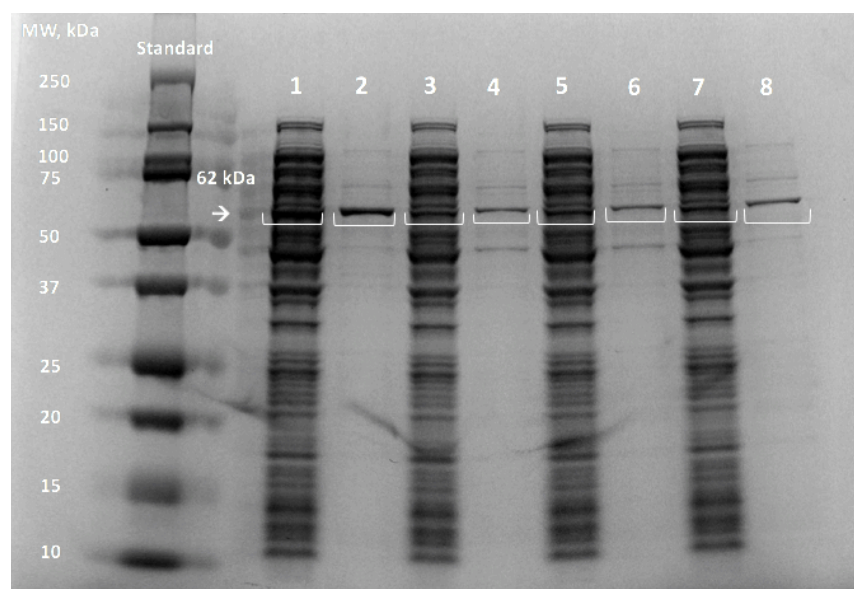

Figure 4.8. Expression and purification of P11G3 and P2G3 with different $CuCl_2$ variations. Expression and purification of P1G3 and P2G3 was analyzed by SDS-PAGE. The different strategies refer to the strategies presented in Table 4.3. The SDS-PAGE gel shown displays the following samples: lane marked "standard": Precision Plus Protein™ Dual Color Standard from BioRad, lane 1): Cell extract containing P11G3 supplemented with $CuCl_2$ as in strategy 1, lane 2): Purified enzyme solution containing P11G3 supplemented with $CuCl_2$ as in strategy 1, lane 3): Cell extract containing P2G3 supplemented with $CuCl_2$ as in strategy 3, lane 4): Purified enzyme solution containing P2G3 supplemented with $CuCl_2$ as in strategy 3, lane 5): Cell extract containing P2G3 supplemented with $CuCl_2$ as in strategy 2, lane 6): Purified enzyme solution containing P2G3 supplemented with $CuCl_2$ as in strategy 2, lane 7): Cell extract containing P2G3 supplemented with $CuCl_2$ as in strategy 1, lane 8): Purified enzyme solution containing P2G3 supplemented with $CuCl_2$ as in strategy 1.

After purification (see section 3.4.2.2) of the cell extracts containing laccases P2G3, P11G3 and P11F6 with different $CuCl_2$ supplementation strategies (Table 4.3), buffer exchange was performed, as described in section 3.4.3.2, for all the cell extracts to replace the elution buffer with 0.1 M sodium phosphate buffer pH 7.5. Imidazole in the elution buffer interferes with

measurement of protein concentration, which makes it difficult to calculate specific activity for the enzymes. Activity assay with the substrate ABTS was run for all samples after purification, and after buffer exchange. Again (as in 4.1.1), no activity could be observed for P2G3, P11G3 and P11F6 after purification, and after buffer exchange.

A second purification (see section 3.4.2.2) was performed for all the cell extracts of P2G3, P11G3 and P11F6, but this time supplementing the equilibration buffer, wash buffer, and elution buffer with 0.25 mM $CuCl_2$ prior to purification. Activity assays with the substrate ABTS were run for all purified samples after buffer exchange, now detecting activity for all P11F6 and P11G3 samples. P2G3, however, still, did not show activity towards ABTS, even though there was protein present in the enzyme solution (see 7.3, appendix C). The specific activities for all the enzymes before and after purification and buffer exchange are summarized in Table 4.4.

Table 4.4. Average specific activity and standard deviation of P2G3, P11G3 and P11F6 supplemented with $CuCl_2$ using different strategies before purification, and after purification and buffer exchange. Buffers used during purification were supplemented with 0.25 mM $CuCl_2$ prior to purification.

Enzyme and supplementation (Table 4.3)	$CuCl_2$ strategy	Average specific activity of three parallels and standard deviation before purification	Average specific activity of three parallels and standard deviation after purification and buffer exchange
P11F6, strategy 1		0.24 ± 0.04	0.14 ± 0.05
P11F6, strategy 2		1.28 ± 0.02	0.09 ± 0.03
P11F6, strategy 3		2.06 ± 0.13	0.34 ± 0.07
P11G3, strategy 1		No activity	0.03 ± 0.01
P11G3, strategy 2		0.84 ± 0.04	0.03 ± 0.01
P11G3, strategy 3		0.93 ± 0.06	0.47 ± 0.02
P2G3, strategy 1		No activity	No activity
P2G3, strategy 2		0.26 ± 0.02	No activity
P2G3, strategy 3		0.93 ± 0.55	No activity

4.1.4. Enzymatic activity after storage

After coincidentally observing that the specific activity for P11F6, P11G3 and P2G3 (from section 4.1.3) had increased after five days of storage in an ice box placed in a 4 °C storage room (see Table 4. 5), new cultivations (see section 3.2.5.1) to produce all three *Psychrobacter* enzymes were performed.

Table 4. 5. Specific activity with standard deviation of three parallels for P11F6, P11G3 and P2G3 with different CuCl$_2$ supplementation strategies according to Table 4.3 determined directly after extraction and after five days of storage in an ice box placed at a 4 °C storage room.

Enzyme and CuCl$_2$ supplementation strategy (Table 4.3)	Average specific activity of three parallels and standard deviation before purification measured 28.11.18	Average specific activity of three parallels and standard deviation before purification measured 03.12.18
P11F6, strategy 1	0.24 ± 0.04	0.70 ± 0.01
P11F6, strategy 2	1.28 ± 0.02	19.5 ± 1.17
P11F6, strategy 3	2.06 ± 0.14	19.35 ± 2.05
P11G3, strategy 1	No activity	0.42 ± 0.05
P11G3, strategy 2	0.84 ± 0.05	3.02 ± 0.16
P11G3, strategy 3	0.93 ± 0.06	3.15 ± 0.40
P2G3, strategy 1	No activity	0.31 ± 0.31
P2G3, strategy 2	0.26 ± 0.02	1.46 ± 0.11
P2G3, strategy 3	0.94 ± 0.56	1.56 ± 0.10

The specific activity was analyzed by activity assays (see section 3.6), with ABTS as substrate, on cell extracts and not on purified samples due to previous difficulties with the purification method (see section 3.4.2.2 and 3.4.3.2) resulting in substantial loss of activity (see Table 4.4). Two bacteria cultures each were cultivated for P11F6, P11G3 and P2G3 supplemented with two different concentrations of CuCl$_2$, i.e. 0.25 mM and 1 mM. CuCl$_2$ was supplemented both during cultivation and to the cell extracts obtained after sonication.

Unfortunately possibly due to instrument issues, the activity assay experiments with the enzymes P11G3 and P2G3 gave irregular curves (Figure 4.9) and low absorption changes

(Figure 4.10), that was considered not significant, for nearly all activity measurements and could not be used for calculating enzyme activity. The results for P11G3 and P2G3 were therefore excluded from further analysis. The specific activity for P11F6 supplemented with 0.25 mM $CuCl_2$ was observed to be increasing over the eight-day period (Figure 4.12). When supplemented with 1 mM $CuCl_2$ the activity of P11F6 decreased after one day of storage followed by a steady activity between 2 and 3 U/mg for the remaining days (Figure 4.13). The specific activity was calculated, as described in section 3.13, from activity assay results displaying assay-curves as showed in Figure 4.11 by measuring the change in absorption using a linear part of the graph at the beginning of the measurements.
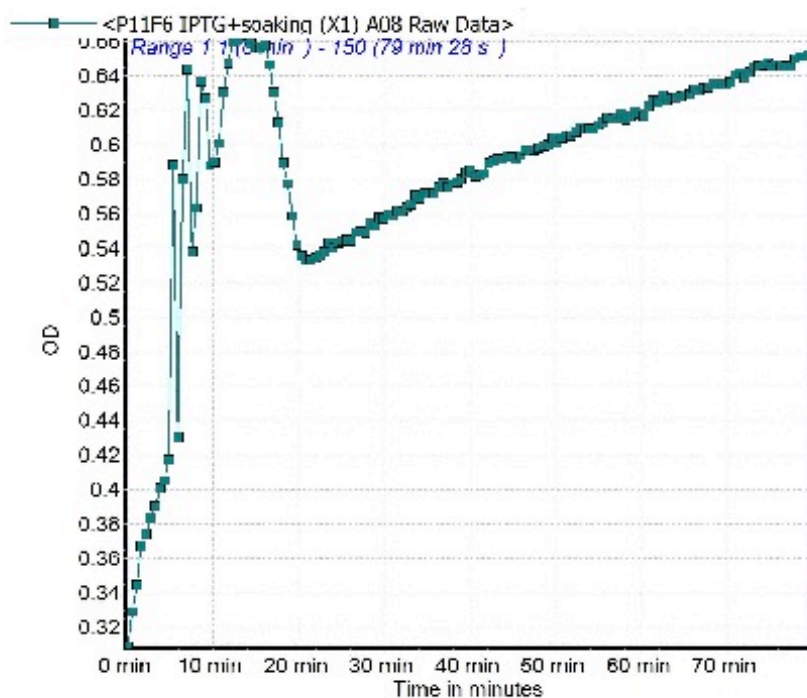

Figure 4.9. Irregular activity assay curve. Absorption values resulting in an irregular assay curve makes it difficult to impossible to calculate the specific activity of the enzyme. Activity assays resulting in irregular assay curves have not been used to calculate enzyme activities.
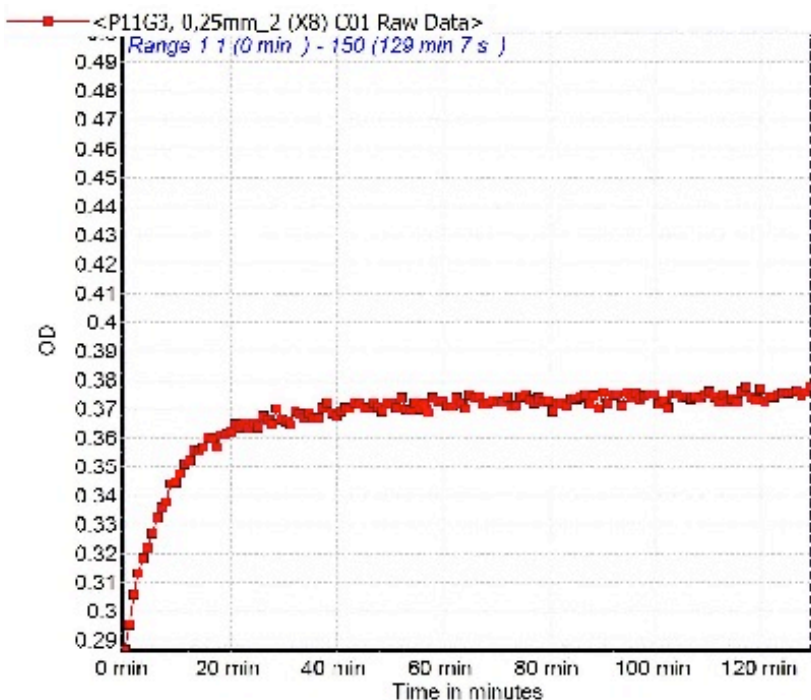
Figure 4.10. Activity assay for P11G3. The change in absorption was observed to be very low for this activity assay. When the absorption change is very low, the activity is considered to be not significant, and therefore excluded from the results.
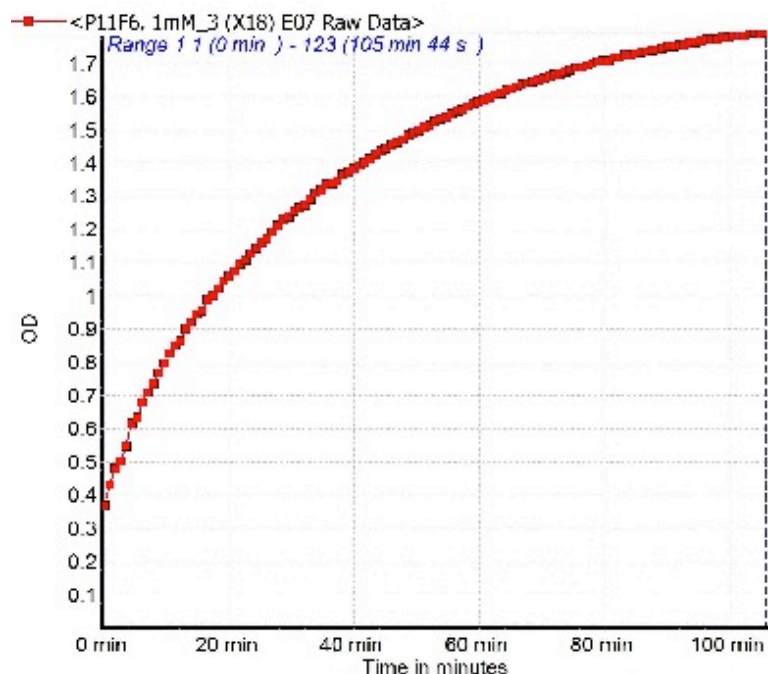

Figure 4.11. Activity assay curve used to calculate specific activity. Activity assay curves that show a somewhat linear initial increase can be used to calculate enzyme activity. In this assay curve the initial, linear part of the curve (approximately up to 10 min) was used to calculate enzyme activity.
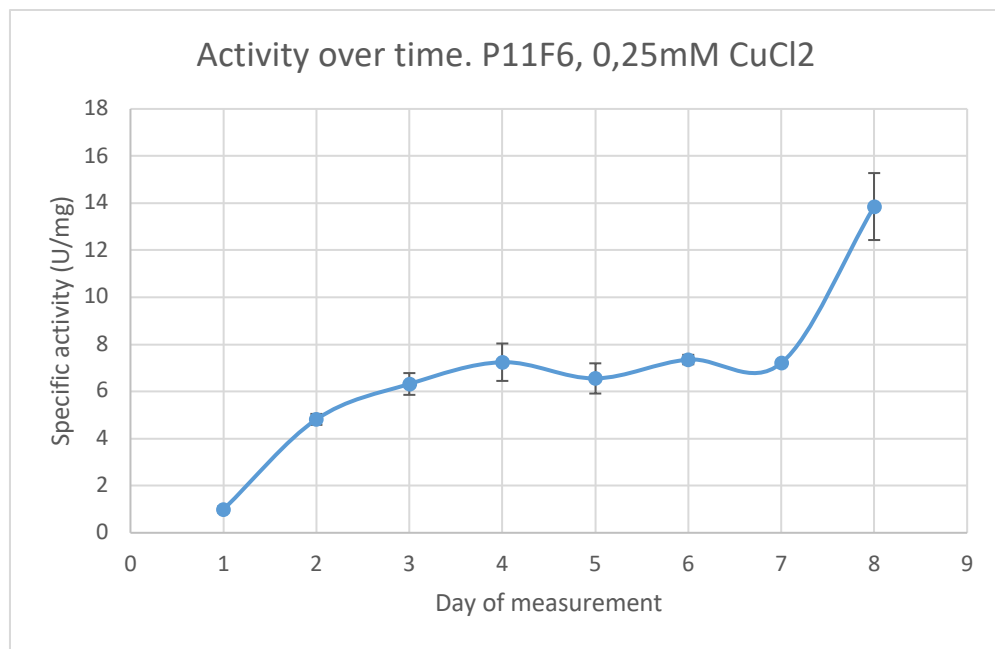
Figure 4.12. Specific activity changes of P11F6 over eight days. The specific activity for P11F6 supplemented with 0.25 mM CuCl$_2$ during cultivation, and of the cell extract after sonication, was measured once a day in a period of eight days to see how storage in an ice box placed at a 4 °C storage room would affect the activity. The specific activity of P11F6 increased over the eight-day period.
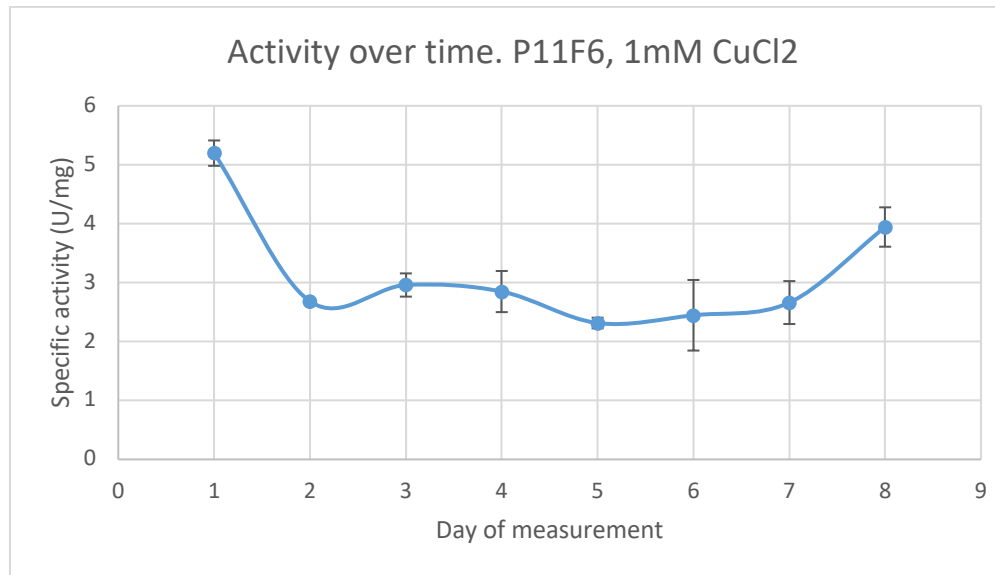

Figure 4.13. Specific activity changes of P11F6 over eight days. The specific activity for P11F6 supplemented with 1 mM CuCl$_2$ during cultivation, and of the cell extract after sonication, was measured once a day in a period of eight days to see how storage in an ice box placed at a 4 °C storage room would affect the activity. After one day of storage the specific activity decreased before remaining a steady activity between 2 and 4 U/mg for the remaining days.

After extensive work with the *Psychrobacter* laccases P11F6, P11G3 and P2G3, purified active enzyme solutions were finally achieved, and the methods used for expression, protein extraction and activity assays were well incorporated. The enzymes were, however, found to be very challenging to work with due to difficulties with purification, and the stability of the enzymatic activity upon purification and storage. Parallel with working with the *Psychrobacter* enzymes, activity for the new laccases from *Actinobacteria* was observed. The newly discovered laccases from *Actinobacteria* were of higher priority, and the work with the *Psychrobacter* laccases was discontinued.

4.2. Selection of laccase candidates from *Actinobacteria* for extensive characterization

In order to identify new laccases for the OXYMOD project, a selection of seven laccase candidates from newly sequenced genomes from *Actinobacteria* was defined as described in section 3.12. These laccase candidates are presented in Figure 4.14 in a phylogenetic tree to illustrate their kinship to *B. subtilis* cotA and the three *Psychrobacter* laccases subject to investigations in part 4.1. The candidates subject to extensive characterization are marked with a red star in Figure 4.14. The phylogenetic tree was created and kindly provided by Giang-Son Nguyen (SINTEF) by using the online multiple sequence alignment service called MUSCLE (Multiple Sequence Comparison by Log-Expectation).
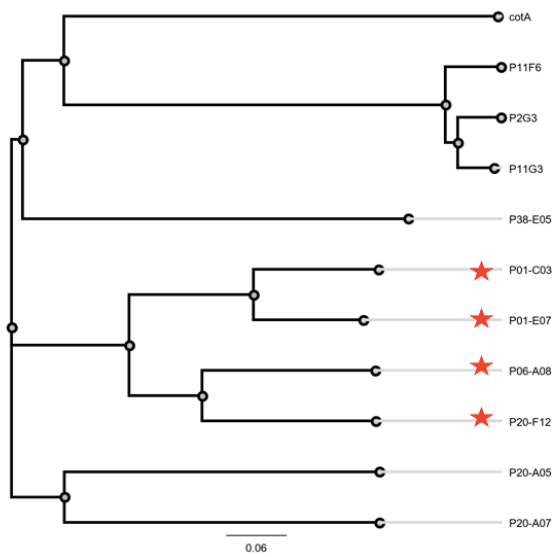

Figure 4.14. Phylogenetic tree representing all laccase enzymes used in this study. The kinship between all the laccases analyzed in this study are presented. The four laccases marked with a red star represents the laccases from *Actinobacteria* that underwent extensive characterization.

4.3. Characterization of newly sequenced *Actinobacteria* laccases P01-C03, P01-E07, P06-A08 and P20-F12

Seven *Actinobacteria* laccase candidates (Table 4.6) were cloned and expressed in *E. coli* as described in section 3.2.5.1 to determine whether putative activity towards ABTS could be observed. All the enzyme.encoding genes were synthesized at GenScript and cloned in the pET-21a(+) expression plasmids, containing the gene *ampR* providing ampicillin resistance, in three variants; with target gene-fused C-terminal His-tag, N-terminal His-tag, and without His-tag (theoretical MWs for all variants are presented in Table 4.6 .

Table 4.6. List of seven Actinobacteria laccase candidates synthesized and cloned by GenScript and the theoretical MWs for enzyme variants with N-terminal His-tag, C-terminal His-tag and without His-tag.

Laccase	Theoretical molecular weight (kDa)	Theoretical molecular weight with N-terminal His-tag (kDa)	Theoretical molecular weight with C-terminal His-tag (kDa)
P01-C03	40.471	41.217	41.114
P01-E07	37.538	38.098	38.181
P06-A08	39.385	40.028	40.028
P20-A05	78.919	79.562	79.562
P20-A07	77.974	78.720	78.617
P20-F12	37.978	38.537	38.620
P38-E05	71.630	72.190	72.273

To investigate expression of all *Actinobacteria* laccase candidates in *E. coli*, cell extracts (containing soluble proteins) and IMAC purified enzyme solutions were analyzed by SDS-PAGE (Figure 4.15, Figure 4.16 and Figure 4.17). Expression of P01-C03 with N-terminal His-tag, C-terminal His-tag and no His-tag was investigated first. Soluble expression of N-terminal and C-terminal His-Tagged P01-C03 was observed, and the protein could be purified by IMAC (Figure 4.15, lane 1-4). Expression of P01-C03 without His-tag was also observed (Figure 4.15, lane 5).
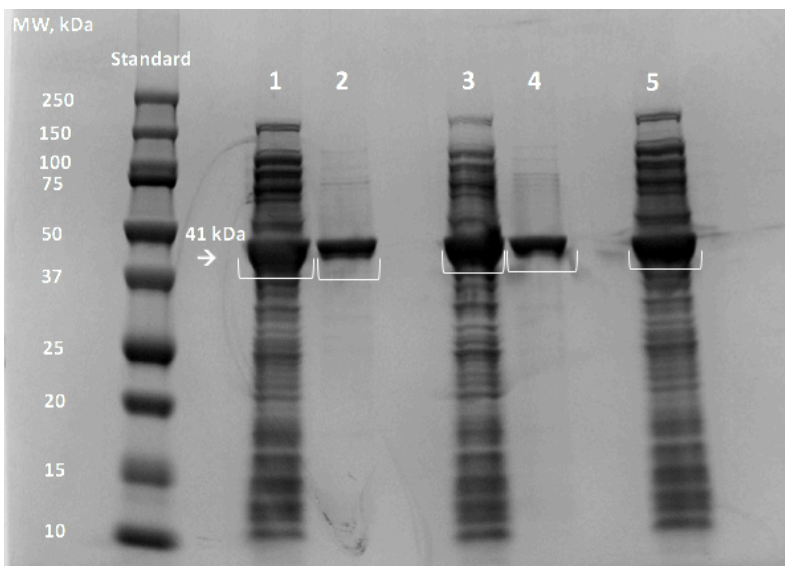
Figure 4.15. Expression of P01-C03. Expression of the *Actinobacteria* laccase N-terminal His-tag P01-C03, C-terminal His-tag P01-C03, and P01-C03 with no His-tag in *E. coli* was analyzed by SDS-PAGE. The SDS-PAGE gel shown displays the following samples: lane marked "standard": Precision Plus Protein™ Dual Color Standard from BioRad, lane 1): Cell extract containing the enzyme P01-C03 with N-terminal His-tag, lane 2) Purified enzyme solution containing the enzyme P01-C03 with N-terminal His-tag, lane 3): Cell extract containing the enzyme P01-C03 with C-terminal His-tag, lane 4): Purified enzyme solution containing the enzyme P01-C03 with N-terminal His-tag, lane 5): Cell extract containing the enzyme P01-C03 with no His-tag. All bacteria cultures were cultivated as described in section 3.2.5.1 and purified as described in section 3.4.2.2. All cell extracts were obtained by sonication as described in section 3.3.1.

Expression of the other six laccase variants P01-E07, P06-A08, P20-A05, P20-A07, P20-F12 and P38-E05 was done similarly, though only using the variant for containing N-terminal His-tag. Only marginal expression of P01-E07 (MW = 38 kDa) was observed as a faint band on the SDS-PAGE gel after purification of the cell extract containing the enzyme (Figure 4.16, lane 2). Expression of P06-A08 (MW= 40 kDa) was clearly observed as broad distinct bands at ∼ 40 kDa both in the cell extract and after purification (Figure 4.16, lane 3 and 4). Expression of P20-A05 (MW = 79) could not be observed as a clear band after the attempt to purify the enzyme from the cell extract (Figure 4.16, lane 5 and 6).
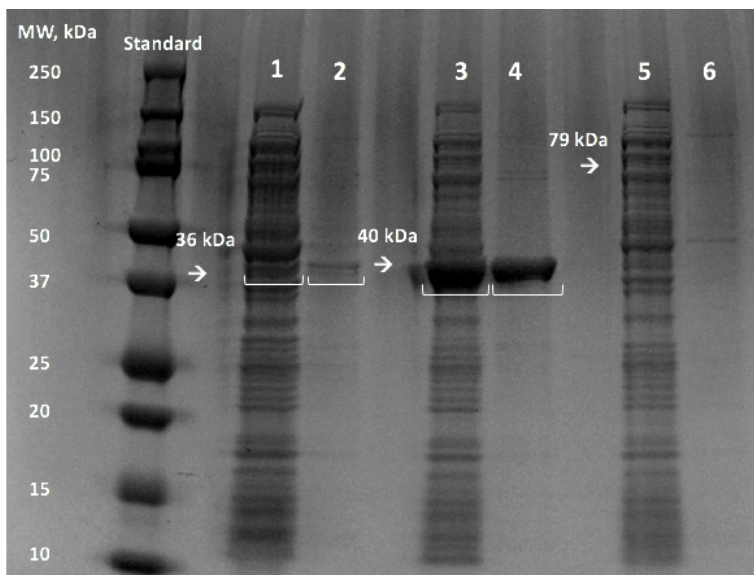
Figure 4.16. Expression of P01-E07, P06-A08 and P20-A05. Expression of the *Actinobacteria* laccase candidates P01-E07, P06-A08 and P20-A05 (all with N-terminal His-tag) was analyzed by SDS-PAGE. The SDS-PAGE gel shown displays the following samples: lane marked "standard": Precision Plus Protein™ Dual Color Standard from BioRad, lane 1): Cell extract containing the enzyme P01-E07, lane 2) Purified enzyme solution containing P01-E07, lane 3): Cell extract containing the enzyme P06-A08, lane 4): Purified enzyme solution containing P06-A08, lane 5): Cell extract that should contain the enzyme P20-A05, lane 6): Purified enzyme solution that should contain P20-A05. All bacteria cultures were cultivated as described in section 3.2.5.1 and purified as described in section 3.4.2.2. All cell extracts were obtained by sonication as described in section 3.3.1.

P20-A07 should appear as a band at 78 kDa, and P38-E05 should appear as a band at 72 kDa, but clear, high-level expression could not be observed for any of these two enzymes including after attempting to purify them from the cell extracts (Figure 4.17, lane 2 and 6, respectively). Observation of P20-A07 and P38-E05 in the cell extract is uncertain, due high levels of unspecific proteins in the sample (Figure 4.17, lane 1 and 3 respectively). Expression of P20-F12 (MW = 38.5 kDa) was clearly observed both before and after purification (Figure 4.17, lane 3 and 4).
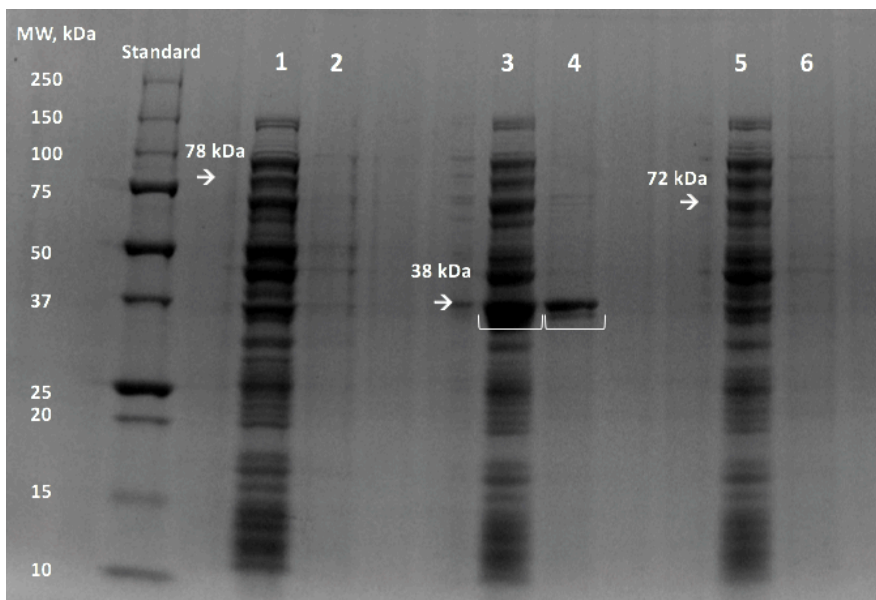
Figure 4.17. Expression of P20-A07, P20-F12 and P38-E05. Expression of the *Actinobacteria* laccases P20-A07, P20-F12 and P38-E05 (all with N-terminal His-tag) was analyzed by SDS-PAGE. The SDS-PAGE gel shown displays the following samples: lane marked "standard": Precision Plus Protein™ Dual Color Standard from BioRad, lane 1): Cell extract that should contain the enzyme P20-A07, lane 2): Purified enzyme solution that should contain P20-A07, lane 3): Cell extract containing the enzyme P20-F12, lane 4): Purified enzyme solution containing P20-F12, lane 5): Cell extract that should contain the enzyme P38-E05, lane 6): Purified enzyme solution that should contain P38-E05. All bacteria cultures were cultivated as described in section 3.2.5.1 and purified as described in section 3.4.2.2. All cell extracts were obtained by sonication as described in section 3.3.1.

The crude extracts and purification fractions of all seven *Actinobacteria* laccase candidates were tested for laccase activity using ABTS as substrate according to section 3.6. Laccase activity could be detected in all cell extracts and purified enzyme samples of the enzymes P01-C03, P01-E07, P06-A08 and P20-F12, while no ABTS converting activity could be detected for the enzyme candidates P20-A05, P20-A07 and P38-E05 (data not shown) which corresponds well with the observable protein bands after SDS-PAGE. Based on this result, the readily producible four *Actinobacteria* laccases P01-C03, P01-E07, P06-A08 and P20-F12 were selected for a more extensive characterization.

4.3.1.   Large-scale shake flask scale cultivation

To perform a more extensive characterization of the four *Actinabacteria* laccases P01-C03, P01-E07, P06-A08 and P20-F12, *E. coli* bacterial cultures were grown in larger shake-flask batches as described in section 3.2.5.2 in order to obtain sufficient quantities of each enzyme.

For each enzyme, two bacterial cultures were grown with the intention of generating two cell extracts each, one to be processed with sonication (see section 3.3.1) and with BugBuster™ Protein Extraction Reagent (see section 3.3.2) to compare the two methods. The main difference between the two methods is that sonication lyses bacterial cells with the use of soundwaves, while the BugBuster™ Protein Extraction Reagent gently disrupts the bacteria cell wall, resulting in the liberation of soluble proteins. Sonication has previously been shown not to be an optimal method for cell lysis, in particular with larger samples. Foaming, insufficient cooling, and lack of reproducibility are problems that have occurred with this extraction method in the current study. The same problems occurred again when processing the large-scale cultivations to produce the four selected *Actinobacteria* laccases. Therefore, only cell extracts generated with the BugBuster™ Protein Extraction Reagent were used for the extensive characterization of these enzymes.

His-tag purification using His-select spin columns (see section 3.4.2.2) can only purify 600 µL of sample each time, making it time-consuming and unsuitable as a purification method for larger volumes. His-tag purification using Ni-NTA resin and gravity-flow columns (see section 3.4.2.1) was therefore used instead. Buffer exchange was previously been done with Amicon® Ultra-0.5 Centrifugal filter devices (see section 3.4.3.2), but this method can only handle 500 µL of sample each time, making this method also unsuitable for larger volumes. As an alternative, PD-10 Desalting columns for gravity flow were used for buffer exchange (see section 3.4.3.1).

To verify expression and purification of P01-C03, P01-E07, P06-A08 and P20-F12, cell extracts (containing soluble proteins) and IMAC purified protein samples were analyzed by SDS-PAGE (Figure 4.18). IMAC purified protein samples were subjected to buffer exchange and were also analyzed by SDS-PAGE (Figure 4.19). To monitor any changes in protein concentration, Qubit assays were performed on the cell extracts, purified enzyme solutions, and purified enzyme solutions after buffer exchange. The results are presented in Table 4.7.

Expression of P01-C03 (MW = 41 kDa) was observed in the cell extract obtained from the bacterial culture of *E. coli* (Figure 4.18, lane 1), and the enzyme was also observed after purification of the cell extract (Figure 4.18, lane 2). Purification of P01-C03 resulted in highly impure samples, which could be a result of insufficient washing. Purification with Ni-NTA resin gave impure samples, compared to purification using HIS-select spin columns for all the

enzymes. The purified enzyme solution containing P01-C03 had a substantial decrease in protein concentration after buffer exchange (Figure 4.19 and Table 4.7). When measuring protein concentration before purification, the BugBuster reagent was considered and also measured in the Qubit assay. The BugBuster measurement was deducted from the measurement of the protein samples. The same was done for the samples after purification, considering the elution buffer. The sodium phosphate buffer that was exchanged with the elution buffer did not have an effect on the protein concentration.

Expression of P01-E07 (MW = 38 kDa), P06-A08 (MW = 40 kDa), and P20-F12 (MW = 38 kDa) was also observed in the cell extract obtained from the bacterial culture of *E. coli* (Figure 4.18, lane 3, 5 and 7, respectively). Purification of P01-E07, P06-A08 and P20-F12 also resulted in highly impure samples (Figure 4.18, lane 4, 6 and 8, respectively), and the protein concentration had decreased substantially after buffer exchange of the purified protein samples (Table 4.7), which could also be confirmed by the SDS-PAGE (Figure 4.19, lane 4, 6 and 8, respectively).

Table 4.7: Average protein concentration (mg/mL) and standard deviation of three replicates measured for all four *Actinobacteria* laccases before and after purification and after buffer exchange. The concentration has decreased substantially after purification, except for P06-A08. The protein concentration was further reduced after buffer exchange due to the removal of imidazole and other unspecific proteins that has an impact on the concentration.

| Laccase	Protein concentration before purification (mg/mL)	Protein concentration after purification (mg/mL)	Protein concentration after buffer exchange (mg/mL)
P01-C03	4.52 ± 0.17	0.646 ± 0.01	0.124 ± 0.002
P01-E07	5.39 ± 0.50	0.346 ± 0.002	0.137 ± 0.006
P06-A08	5.12 ± 0.41	3.745 ± 0.11	0.465 ± 0.001
P20-F12	5.53 ± 0.01	0.607 ± 0.02	0.482 ± 0.042
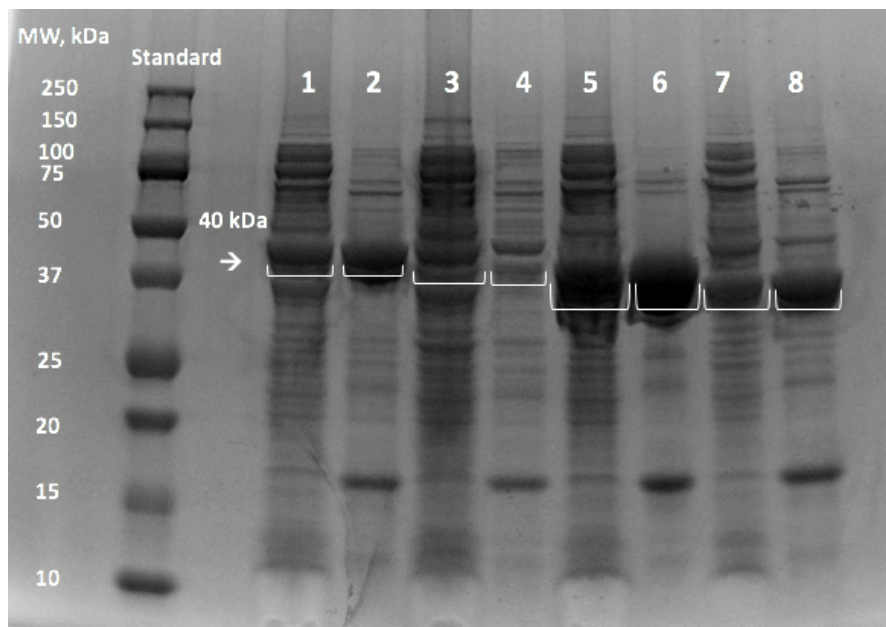
Figure 4.18. Expression of P01-C03, P01-E07, P06-A08 and P20-F12 in E. coli and purification of the enzymes from cell extracts. Expression and purification of the four *Actinobacteria* laccases were analyzed by SDS-PAGE. The SDS-PAGE gel shown displays the following samples: lane marked "standard": ": Precision Plus Protein™ Dual Color Standard from BioRad, lane 1): Cell extract containing P01-C03, lane 2): Purified enzyme solution containing P01-C03, lane 3): Cell extract containing P01-E07, 4): Purified enzyme solution containing P01-E07, lane 5): Cell extract containing P06-A08, lane 6): Purified enzyme solution containing P06-A08, lane 7): Cell extract containing P20-F12, lane 8): Purified enzyme solution containing P20-F12. Bacterial cultures were cultivated as described in section 3.2.5.2. All cell extracts were obtained using the BugBuster™ Protein Extraction Reagent as described in section 3.3.2, and the cell extracts were purified using Ni-NTA resin and gravity-flow columns as described in section 3.4.2.1.
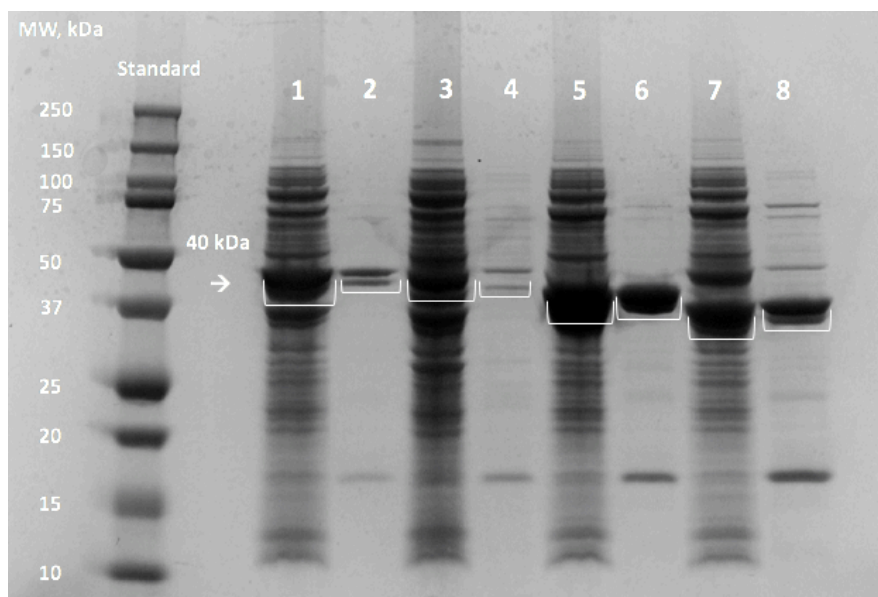

Figure 4.19. Cell extracts of P01-C03, P01-E07, P06-A08 and P20-F12 expressed in *E. coli* and buffer exchange of purified enzyme solutions obtained from the cell extract. Cell extracts and buffer exchange after

purification of the four *Actinobacteria* laccases was analyzed by SDS-PAGE. The SDS-PAGE gel shown displays the following samples: lane marked "standard": Precision Plus Protein™ Dual Color Standard from BioRad, lane 1): Cell extract containing P01-C03, lane 2): Purified enzyme solution after buffer exchange containing P01-C03, lane 3): Cell extract containing P01-E07, lane 4): Purified enzyme solution after buffer exchange containing P01-E07, lane 5): Cell extract containing P06-A08, lane 6): Purified enzyme solution after buffer exchange containing P06-A08, lane 7): Cell extract containing P20-F12, lane 8): Purified enzyme solution after buffer exchange containing P20-F12. Bacterial cultures were cultivated as described in section 3.2.5.2, and buffer exchange was performed on purified enzyme solutions as described in section 3.4.3.1.

For verification of enzymatic activity after purification and buffer exchange, activity assays for the four *Actinobacteria* laccases were performed using ABTS as substrate (see section 3.6). The specific activities for P01-C03, P01-E07, P06-A08 and P20-F12 before purification (cell extract containing soluble proteins), after IMAC purification, and after buffer exchange of the purified samples, is presented in Table 4.8. The specific activity for P01-C03, P01-E07, P06-A08 and P20-F12 increases after purification. The enzymatic activity will in theory remain after removal of other insoluble proteins, and the protein concentration will subsequently decrease. Both factors contribute to the increase in specific activity. A minor decrease in specific activity after buffer exchange was observed for P01-C03 and P01-E07, and a minor increase in specific activity was observed for P06-A08 and P20-F12.

Table 4.8 Average specific activity and standard deviation of three parallels for the newly discovered *Actinobacteria* laccases with ABTS as substrate before and after purification of the cell extract, and after buffer exchange.

Laccase	Specific activity before purification (U/mg)	Specific activity after purification (U/mg)	Specific activity after buffer exchange (U/mg)
P01-C03	$0{,}074 \pm 0{,}002$	$0{,}52 \pm 0{,}028$	$0{,}43 \pm 0{,}002$
P01-E07	$0{,}12 \pm 0{,}010$	$0{,}54 \pm 0{,}017$	$0{,}50 \pm 0{,}017$
P06-A08	$0{,}01 \pm 0{,}001$	$0{,}009 \pm 0{,}0007$	$0{,}07 \pm 0{,}001$
P20-F12	$0{,}025 \pm 0{,}00079$	$0{,}18 \pm 0{,}0048$	$0{,}27 \pm 0{,}016$

4.3.2. Temperature stability

The four laccase candidates have their origin from marine *Actinobacteria* isolates from sediment and sponge samples collected at locations in the Trondheim fjord, where temperatures can be as low as 4 ℃, assuming that the laccases are cold-active enzymes. Based on this, the temperature stability was characterized by incubating 100 µL of P01-C03 (protein concentration = 0.124 mg/mL), P01-E07 (protein concentration = 0.137 mg/mL), P06-A08 (protein concentration = 0.465 mg/mL) and P20-F12 (protein concentration = 0.452 mg/mL) as described in section 3.6.1, analyzing enzyme solution samples obtained after buffer exchange.

Though it appears counterintuitive with respect to the enzymes' origin, the results of this analysis revealed that all four enzymes were indicated to be highly thermostable (see Figure 4.20). Activity still was detected for all four enzymes after being incubated 30 min at 90 ℃, and three of the four enzymes were still active after being incubated at 99 ℃. P01-E07 had lost activity after incubation at 99 ℃. P06-A08 was observed to be highly stable, keeping more or less the same specific activity at all temperatures.
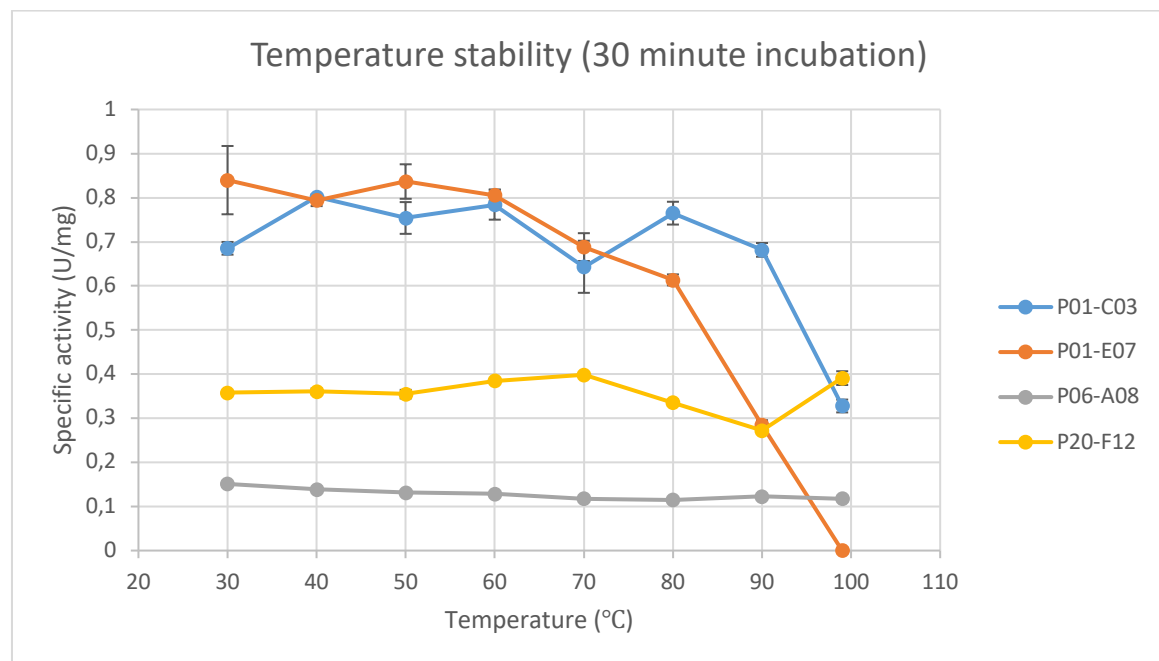

Figure 4.20. Temperature stability of P01-C03, P01-E07, P06-A08 and P20-F12. Temperature stability of the four *Actinobacteria* laccases was analyzed by incubation at 30 ℃, 40 ℃, 50 ℃, 60 ℃, 70 ℃, 80 ℃, 90 ℃ and 99 ℃ for 30 minutes and then analyzing the specific activity by activity assay with ABTS after each incubation at room temperature.

After observing thermostability of P01-C03, P01-E07, P06-A08 and P20-F12, further analysis was done to investigate how longer incubation periods at high temperatures would affect the

enzymatic activity. The four laccases were incubated at 80 °C, 90 °C, and 99 °C for 30 minutes (see results above), 1 hour, 1.5 hours and 2 hours (Figure 4.21, Figure 4.22, Figure 4.23, and Figure 4.24).

P01-C03 retained activity at 80 °C and 90 °C for the entire time period, while at 99 °C all activity was lost after 2 hours incubation (Figure 4.21). Surprisingly, the activity of P01-C03 increased approximately two-fold increase after incubation for 30 minutes at 80 °C and 90 °C followed by a decrease in activity at longer incubation periods.
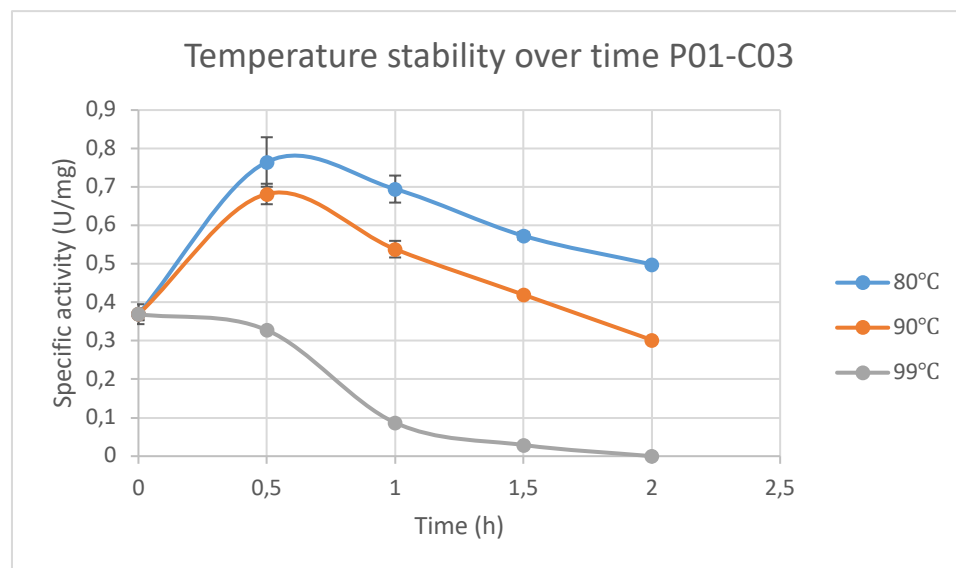

Figure 4.21. Temperature stability of P01-C03. P01-C03 was incubated at 80 °C, 90 °C and 99 °C for 30 minutes, 1 hour, 1.5 hours and 2 hours. The specific activity was calculated after each incubation as described in section 3.6 with 5 mM ABTS. The initial protein concentration of the samples used in each incubation was 0.124 mg/mL, taking 100 μL from the original purified enzyme solution.

P01-E07 can be considered the least thermostable enzyme among the four *Actinobacteria* laccases with complete loss of activity already after 30 min incubation at 99 °C (Figure 4.22). The activity determined for incubations at 90 °C decreased over time with nearly completely loss of activity after incubation for 2 hours. P01-E07 did retain activity for all incubation periods at 80 °C with a similar curve profile as obtained for P01-C03 (see Figure 4.21).
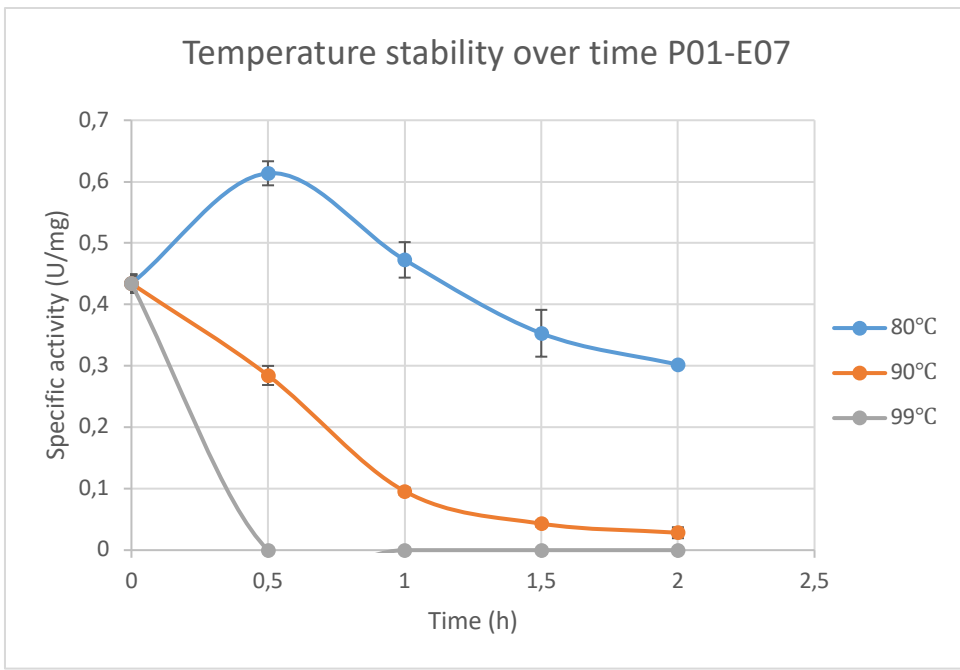
Figure 4.22. Temperature stability of P01-E07. P01-E07 was incubated at 80 °C, 90 °C and 99 °C for 30 minutes, 1 hour, 1.5 hours and 2 hours. The specific activity was analyzed after each incubation as described in section 3.6 with 5 mM ABTS. The initial protein concentration of the samples used in each incubation was 0.137 mg/mL, taking 100 μL from the original purified enzyme solution.

Both P06-A08 and P20-F12 were observed to be the most thermostable enzymes of the four *Actinobacteria* laccases (Figure 4.23 and Figure 4.24). The specific activity for both P06-A08 and P20-F12 at all incubation temperatures and incubation periods were higher than the initial activity before incubation, except for the P06-A08 sample incubated at 99 °C for 2 hours (Figure 4.23). P20-F12 was observed to increase in activity at all incubation periods at 90 °C (Figure 4.24).
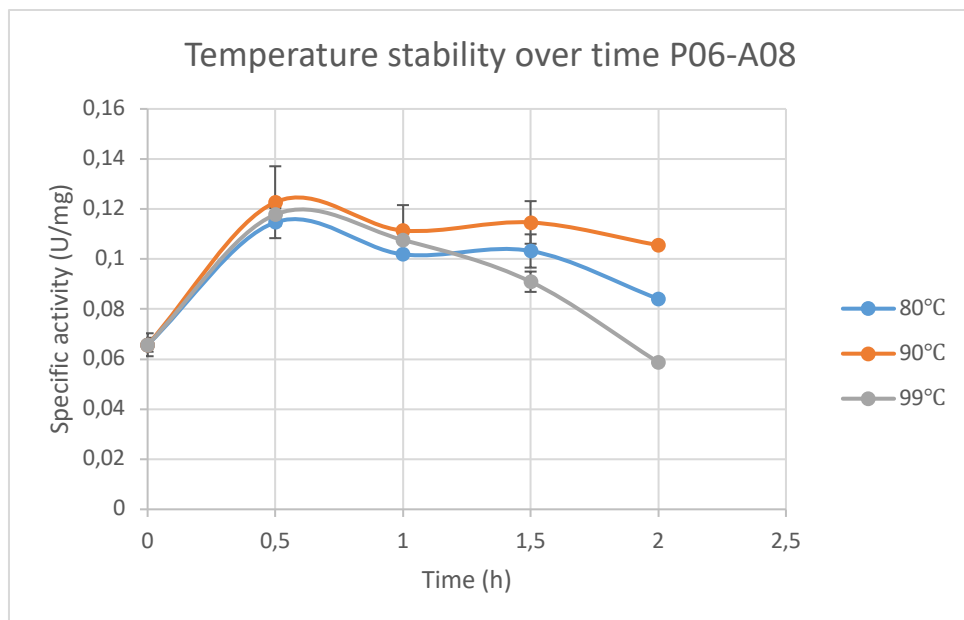
Figure 4.23. Temperature stability of P06-A08. P06-A08 was incubated at 80 ℃, 90 ℃ and 99 ℃ for 30 minutes, 1 hour, 1.5 hours and 2 hours. The specific activity was analyzed after each incubation as described in section 3.6 with 5 mM ABTS. The initial protein concentration of the samples used in each incubation was, 0.465 mg/mL taking 100 μL from the original purified enzyme solution.
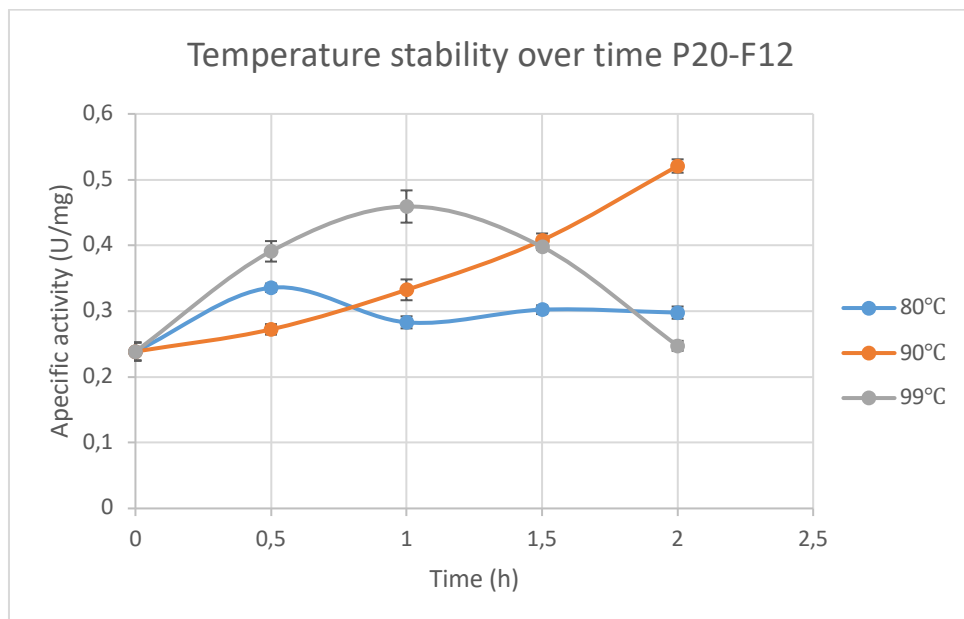
**Figure 4.24. Temperature stability of P20-F12**. P20-F12 was incubated at 80 ℃, 90 ℃ and 99 ℃ for 30 minutes, 1 hour, 1.5 hours and 2 hours. The specific activity was analyzed after each incubation as described in section 3.6 with 5 mM ABTS. The initial protein concentration of the samples used in each incubation was 0.452 mg/mL taking 100 μL from the original purified enzyme solution

4.3.3. pH activity spectrum

The performance of P01-C03, P01-E07, P06-A08 and P20-F12 at different pH was analyzed as described in section 3.6.2, monitoring the specific activity of all four enzymes between pH 3 and 8.6. All four *Actinobacteria* laccases displayed pH optima at low pH values (Figure 4.25). P20-F12 and P06-A08 were observed to have very narrow pH optimum between pH 3.8 and 4.2, P01-E07 was observed to have a pH optimum at pH 4.6, and P01-C03 was observed to have a pH optimum at pH 4.2.
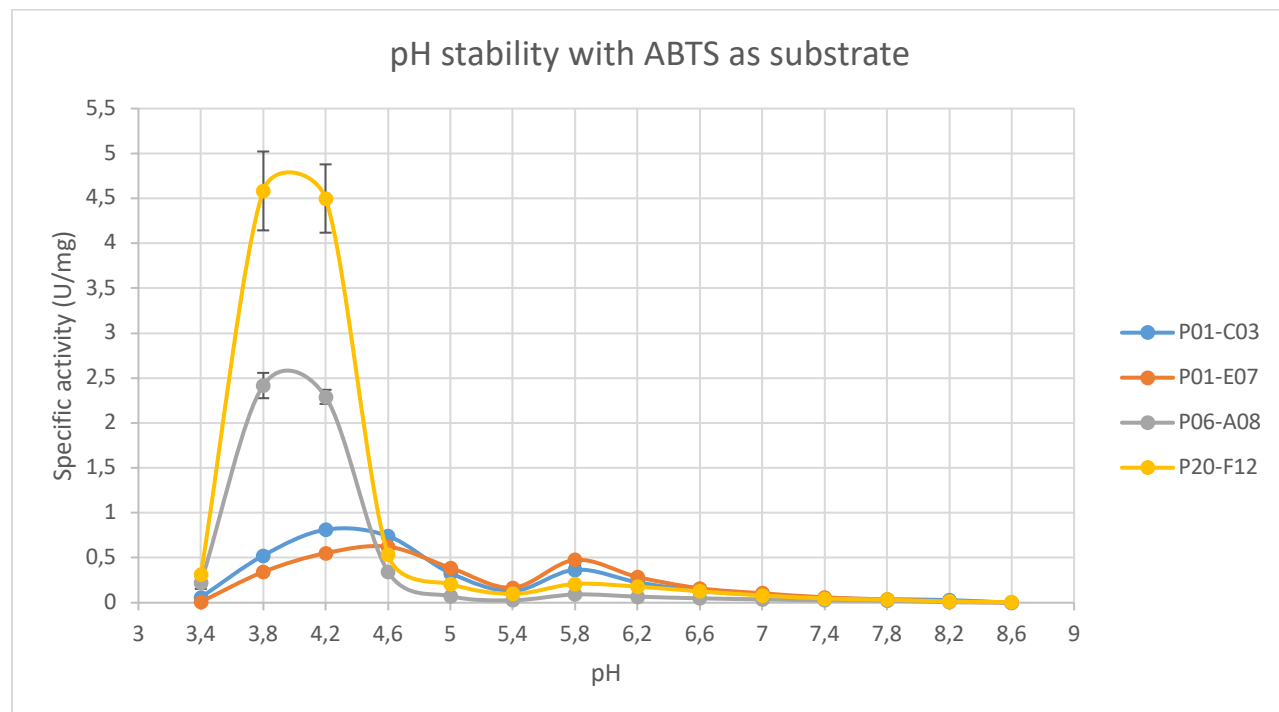

Figure 4.25. pH stability of P01-C03, P01-E07, P06-A08 and P20-F12. The pH stability of the *Actinobacteria* laccases was analyzed as described in section 3.6.2.

4.3.4. Substrate screening

In order for laccases to overcome their restriction to oxidize phenolic substrates not able to enter the active site, mediators can be used to widen their substrate specificity (see section 1.5). Bacterial laccases from natural isolates have not been shown to degrade lignin directly, so the use of mediators for depolymerization of lignin could be key in enabling laccase enzymes to be used as lignin degraders. Based on this, a set of small phenolic substances was screened for their potential as mediators with the new *Actinobacteria* laccases included in this study (Figure 4.26). The substrate list generated was based on previous substrate screenings with CotA (see

7.1, appendix A) and other potential lignin degrading enzymes discovered in the of ERA-IB project OXYPOL, that was coordinated by SINTEF.
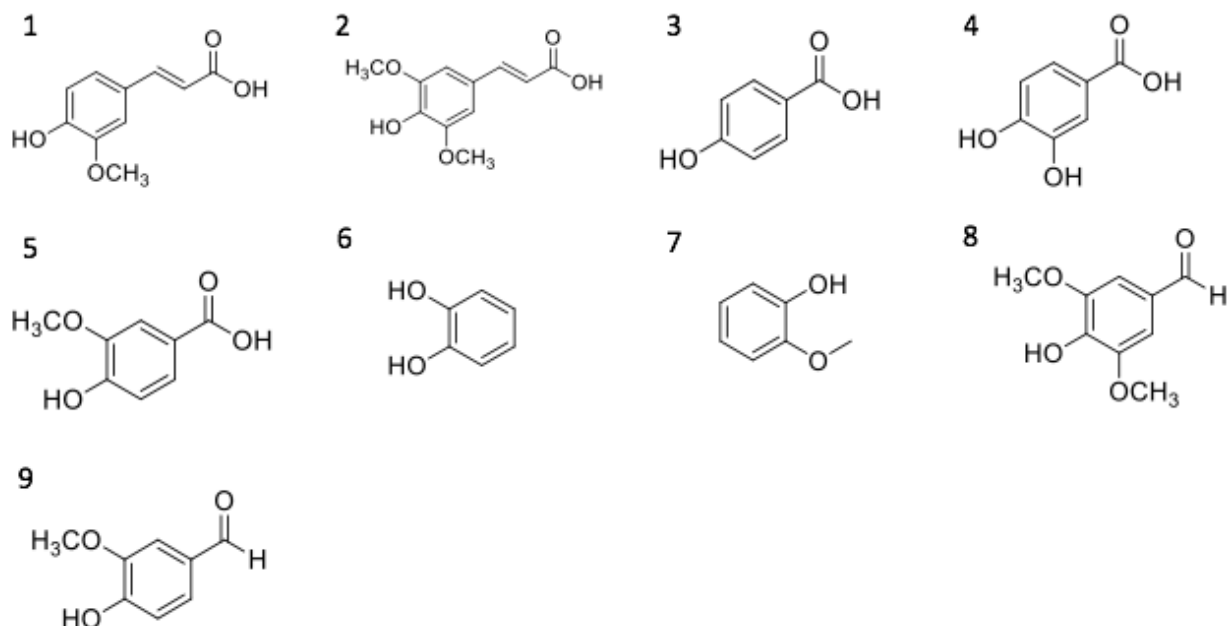

Figure 4.26. Small phenolic substances for substrate screening. 1): Ferulic acid, 2): Sinapic acid, 3): 4-hydrobenzoic acid, 4): 3,4-dihydrobenzoic acid, 5): Vanillic acid, 6): Catechol, 7): Guaiacol, 8): Syringealdehyde, 9): Vanillin. Substrate screening was performed as described in section 3.6.3.

Absorption changes during an activity assay need to be monitored at specific wavelengths depending on the substrate. Absorption scans were performed to identify the wavelength with the highest absorption for each substrate shown in Figure 4.26 (results not shown). The substrate screening was performed as described in section 3.6.3.

All assays were initially performed in 0.1 M acetate buffer pH 4.2 because all enzymes displayed high enzymatic activity towards ABTS at this pH value. No activity was observed for any of the enzymes with any of the substrate, and it was decided to do a new substrate screening, performing all the assays in 0.1 M sodium phosphate buffer pH 7.5. Under these conditions, P20-F12 clearly displayed activity towards sinapic acid, catechol, ferulic acid and 3,4-dihydrobenzoic acid. The specific activities of the enzyme towards the substrates are presented in

Table 4.*9*. P01-C03, P01-E07 and P06-A08 did not display activity towards any of the substrates.

Table 4.9. Specific activity of P20-F12 with sinapic acid, catechol, ferulic acid and 3,4-dihydroxybenzoic acid

Substrate	Molar absorption coefficient	P20-F12 Specific activity (U/mg)
Sinapic acid (0.5 mM)	2 160	16,0 $\pm$ 1.48
Catechol (0.5 mM)	22 600	0,07 $\pm$ 0.006
Ferulic acid (0.05 mM)	18 600	0,05 $\pm$ 0.0002
3,4-dihydrobenzoic acid (0.5 mM)	Not available	Not determined

The specific activity for P20-F12 with sinapic acid was calculated by using the initial part of the assay curve presented in Figure 4.27, that represents the fastest substrate conversion by the enzyme. When less substrate is available the substrate conversion rate will automatically decrease, so it is more expedient to analyze the initial turnover.

The specific activity for 3,4-dihydroxybenzoic could not be quantified due to missing information about the molar absorption coefficient of this substrate.
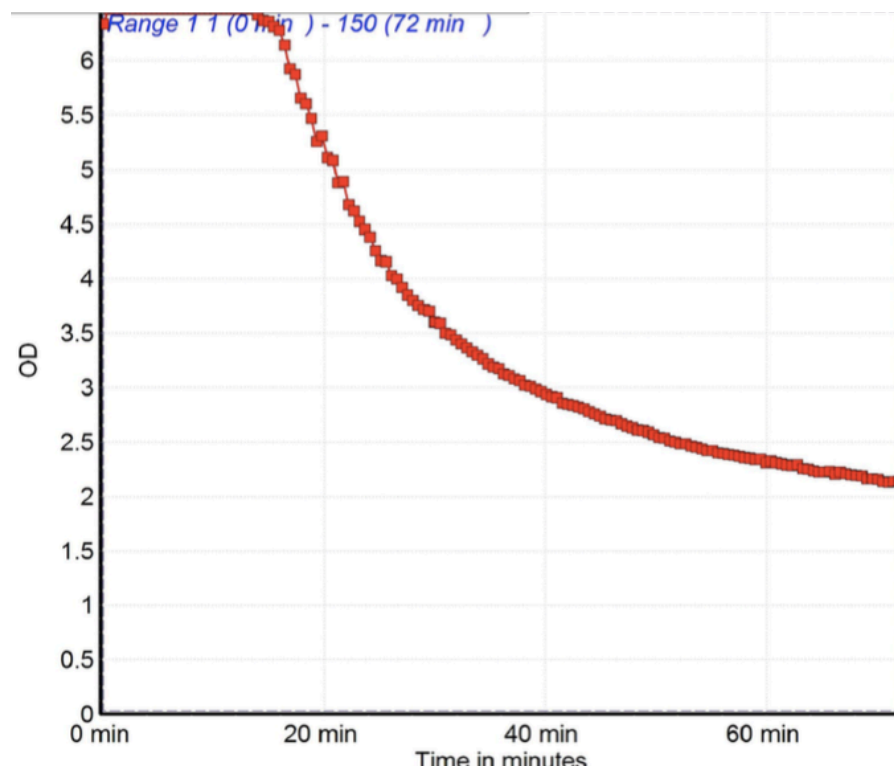
Figure 4.27. Activity assay curve for P20-F12 with sinapic acid as substrate. The fastest conversion, approximately between 18 and 26 minutes, was used to calculate the specific activity

4.3.5.   Lignin assay

Lignin has an undefined structure due to the variation in composition and linkage of the three monolignol building blocks depending on source and species of lignocellulosic biomass (see section 1.3). Consequentially, no molar absorption coefficient can be defined for lignin, and the specific activity for potential lignin degrading enzymes is therefore difficult to determine. The potential lignin degrading trait of P20-F12 in a laccase-mediator system was analyzed by activity assay with the substrates ABTS, sinapic acid, catechol, and ferulic acid as potential mediators.

Horse-radish peroxidase (HRP) has previously been shown to degrade lignin (Dordick, Marletta, and Klibanov 1986) and was therefore used as a reference in the lignin degradation assay. The three-domain laccase CotA (produced by SINTEF in the frame of ERA-IB OXYPOL) was also used as a reference during the lignin assays, representing a well-characterized laccase. In this lignin assay Kraft Lignin from Sigma-Aldrich was used, and in order to monitor depolymerization of lignin, the absorption wavelength for lignin was set to 465 nm (Rahmanpour and Bugg 2015). After each degradation experiment, a UV/visible absorbance spectrum scan was performed in addition in order to see at which wavelength absorbance wavelength changes could be observed.

Peroxidase enzymes catalyze the H_2O_2 dependent oxidation of their substrate (Spiker, Crawford, and Thiel 1992), making addition of H_2O_2 to the activity assay crucial for the enzymes oxidizing abilities. The oxidation of lignin was monitored at 465 nm during the assay (Figure 4.28), and a UV/visible absorbance spectrum was run to compare the absorbance wavelengths with and without the addition of H_2O_2 (Figure 4.29). HRP together with lignin (Figure 4.29, red line) showed no significant absorption change at 465 nm, but when H_2O_2 is added to the assay sample, (Figure 4.29, green graph) an increase in absorption at 465 nm was observed, indicating oxidation of lignin. Increasing absorption values during the lignin assay (Figure 4.28) indicate the degradation of lignin. The slow decrease in absorption observed after ~ 15 minutes may be explained by potential repolymerization of lignin.
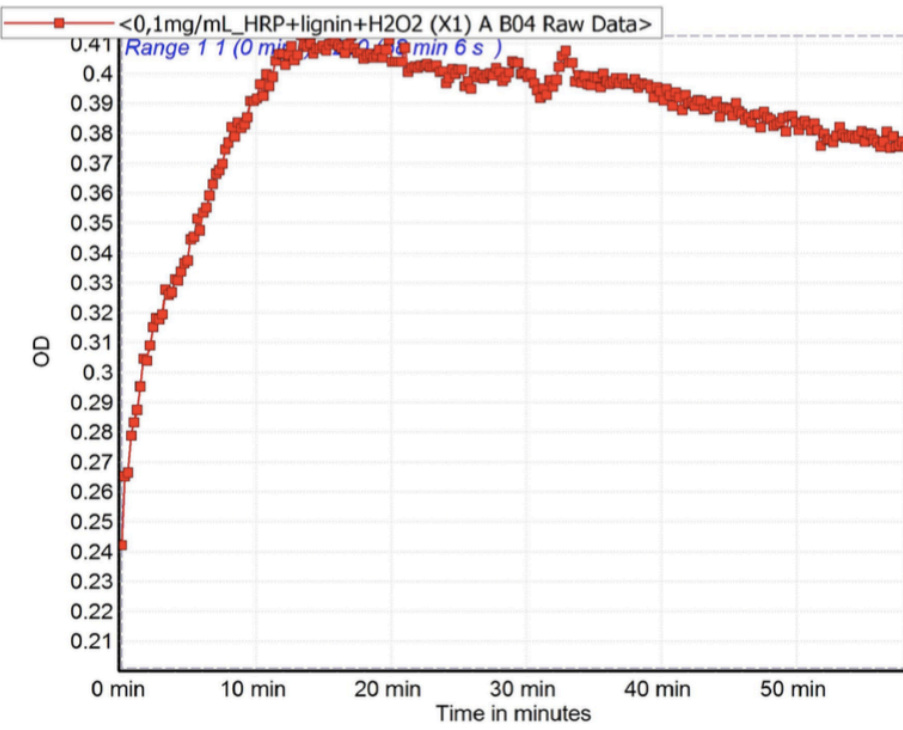
Figure 4.28. Activity assay curve showing lignin degradation by HRP. The degradation of lignin by HRP was monitored at 465 nm, and the change in absorption during the assay is presented.
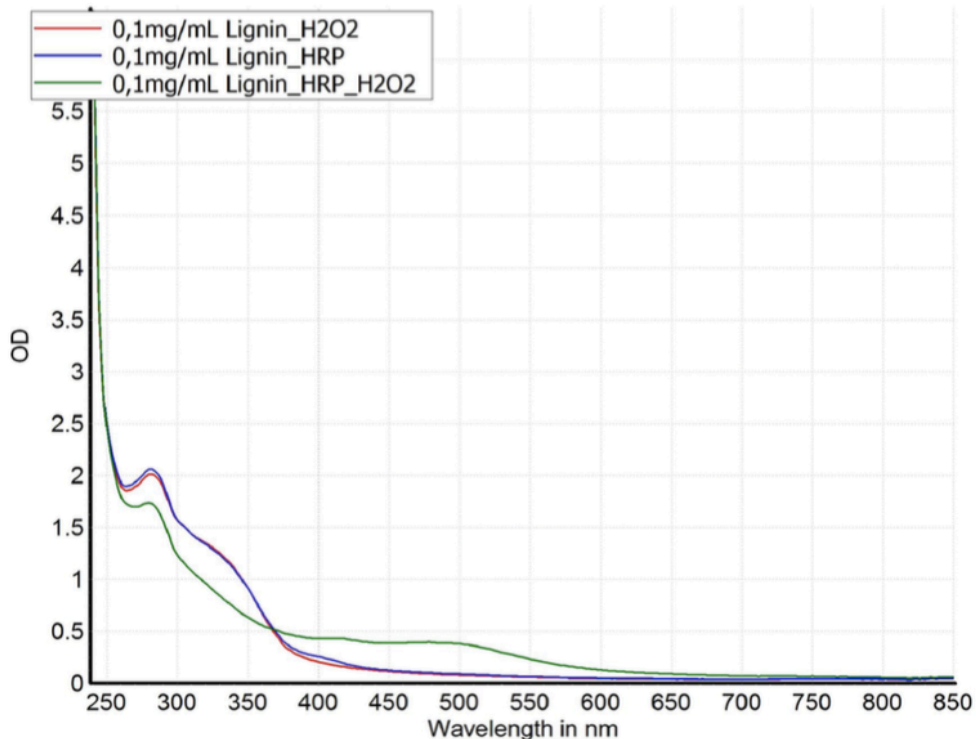

Figure 4.29. UV/visible absorbance spectrum after activity assay with horse-radish peroxidase and lignin. The following graphs in this figure represents: Green): Lignin, HRP, and H_2O_2, blue): Lignin and HRP, red): Lignin and H_2O_2.

92

ABTS was investigated as a potential mediator for the laccase CotA in the lignin degradation assay involving ABTS, CotA and lignin (Figure 4.30, b). The change in absorption was monitored at 420 nm (ABTS) and 465 nm (lignin). The absorption change observed at 465 nm in Figure 4.30 b) seems to indicate depolymerization of lignin, but in a control reaction in the absence of lignin (Figure 4.30 a), absorption change at 465 nm was also observed. This points to interference of the ABTS absorption spectrum with lignin degradation measurement at 465 nm signal, which makes it difficult to determine whether lignin has actually been degraded or not.
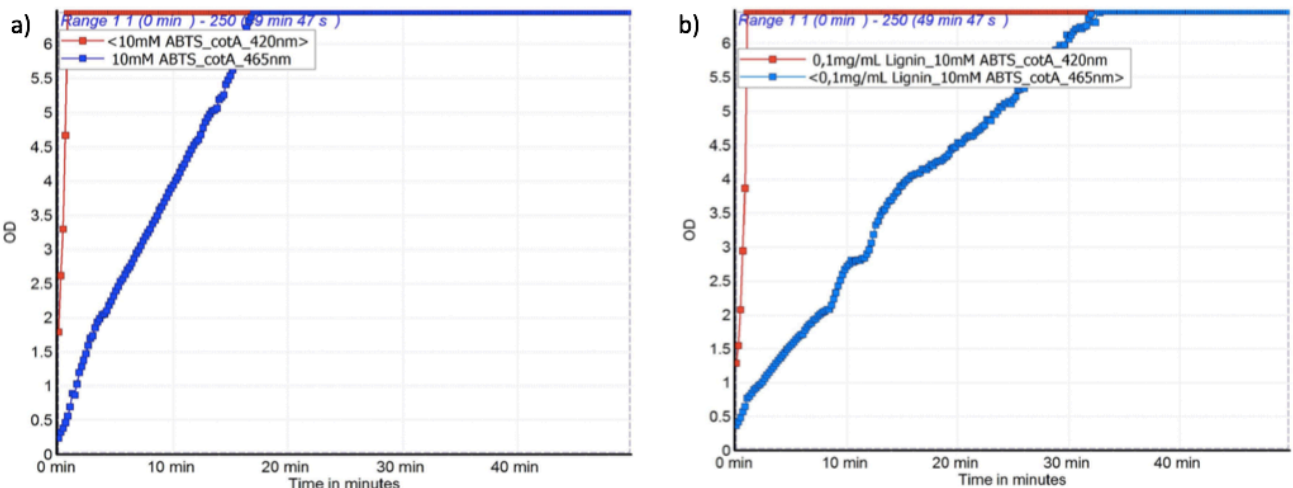

Figure 4.30. Activity assay curves of CotA with ABTS and CotA with ABTS and lignin. Activity assays were run for a) CotA with ABTS and b) CotA with ABTS and lignin to investigate whether the signal of ABTS would affect absorption at both 420 nm and 465 nm.

The interference of ABTS on the absorption signal at 465 nm can be observed in the UV/visible absorption scan of the two assays (Figure 4.31 a and b), with low absorption values at $OD_{465} \sim$ 0.1 in a) and 0.05 in b) that taking the dilution into account corresponds to $OD_{465} \sim 10$ in a) and b). UV/visible absorption scans for Kraft lignin, and Kraft lignin with CotA (Figure 4.32) also have absorption signals at 465 nm with absorption values at $OD_{465} \sim 0.05$. The similar absorption value for the activity assay in Figure 4.30 and the UV/visible scan in Figure 4.31 and Figure 4.32 makes it difficult to distinguish between the presence or absence of Kraft lignin, and if a depolymerization has occurred or not.
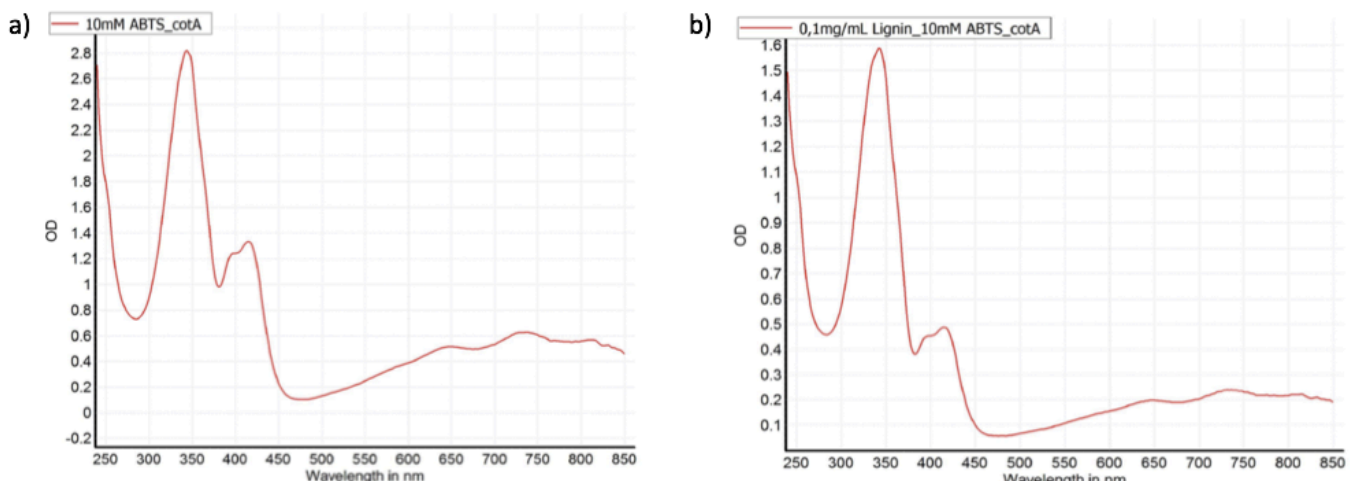
Figure 4.31. UV/ visible absorbance spectrum of CotA with ABTS and CotA with ABTS and lignin after an activity assay. a) CotA 10 mM ABTS diluted 100x. Absorption at 465 nm displays an OD_{465} at $\sim$ 0.1, b) CotA with 10 mM ABTS and 0.1 mg/mL Kraft lignin diluted 200x. Absorption at 465 nm displays an OD_{465} of $\sim$ 0.05.
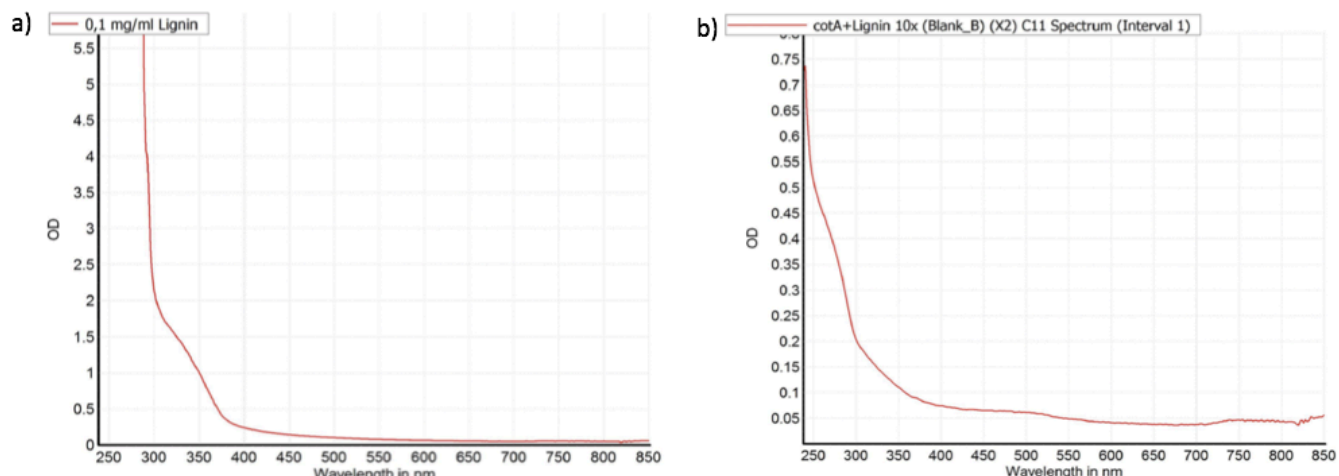
Figure 4.32. UV/visible absorption scan of Kraft lignin (a), and Kraft lignin with CotA (b). Absorption for Kraft lignin (a) at 465 nm displays an $OD_{465} \sim$ 0.05, and absorption for Kraft lignin with CotA (b) also displays an $OD_{465} \sim$ 0.05.

A similar lignin assay with P20-F12 and ABTS as mediator was also performed. Similar results like the results observed for CotA were observed for P20-F12 (results not shown). Based on that it can be concluded that measuring lignin degradation by absorbance at 465 nm is not feasible when ABTS is used as a mediator.

The oxidation of ABTS by P20-F12 and CotA was compared by generating UV/visible absorption spectra after comparable activity assays (Figure 4.33), illustrating that CotA has a higher catalytic activity to ABTS than P20-F12. Oxidized ABTS appears at 420 nm, and the

absorption of oxidized ABTS present after the activity assay is higher for CotA (Figure 4.33 a), red graph) compared to P20-F12 (Figure 4.33 a), blue graph). The absorption peak at ∼ 320 nm represents ABTS in its unoxidized form (Figure 4.33 b)) and is observed to be more than twice as high for P20-F12 compared to CotA, indicating that CotA has oxidized more ABTS than P20-F12 during the course of the experiment.
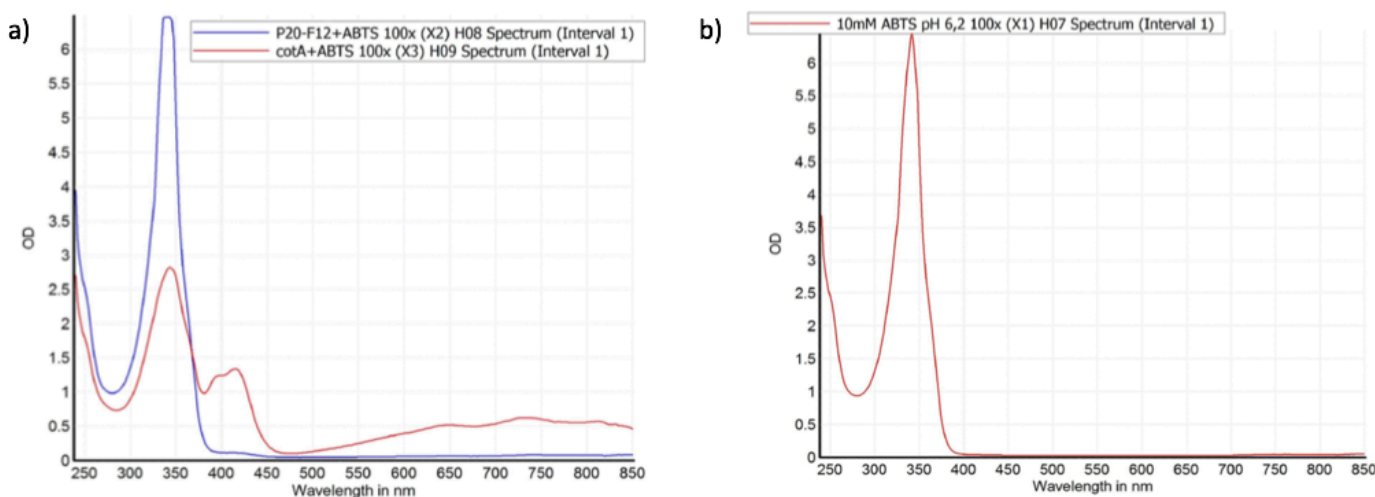

Figure 4.33. UV/visible absorbance spectrum of ABTS. Absorption of oxidized ABTS can be observed at 420 nm. The figure displays the following UV/visible absorption spectra: a) Blue line representing ABTS oxidation with P20-F12, red line representing ABTS oxidation with cotA, b) Non-oxidized ABTS.

From the substrate screening (see section 4.3.4), P20-F12 was observed to have highest specific activity with sinapic acid, and it was therefore decided to investigate its potential as a mediator for lignin degradation. A UV/visible substrate spectrum was generated after performing a lignin assay with sinapic acid as the mediator for both P20-F12 and CotA (Figure 4.34) to analyze absorption values at 465 nm. A control reaction with sinapic acid and lignin was also analyzed (Figure 4.34). An absorption peak at 465 nm was observed for the control sample, but higher absorption peaks were observed for both P20-F12 and CotA, indicating degradation of lignin. The degradation of lignin was disproved after running a UV/visible absorption scan in the absence of lignin for P20-F12 and CotA with sinapic acid (Figure 4.35) where absorption peaks at 465 nm can be observed. In resemblance with ABTS, sinapic acid also interferes with the absorption at 465 nm, subsequently making it difficult to determine whether lignin has been degraded or not.
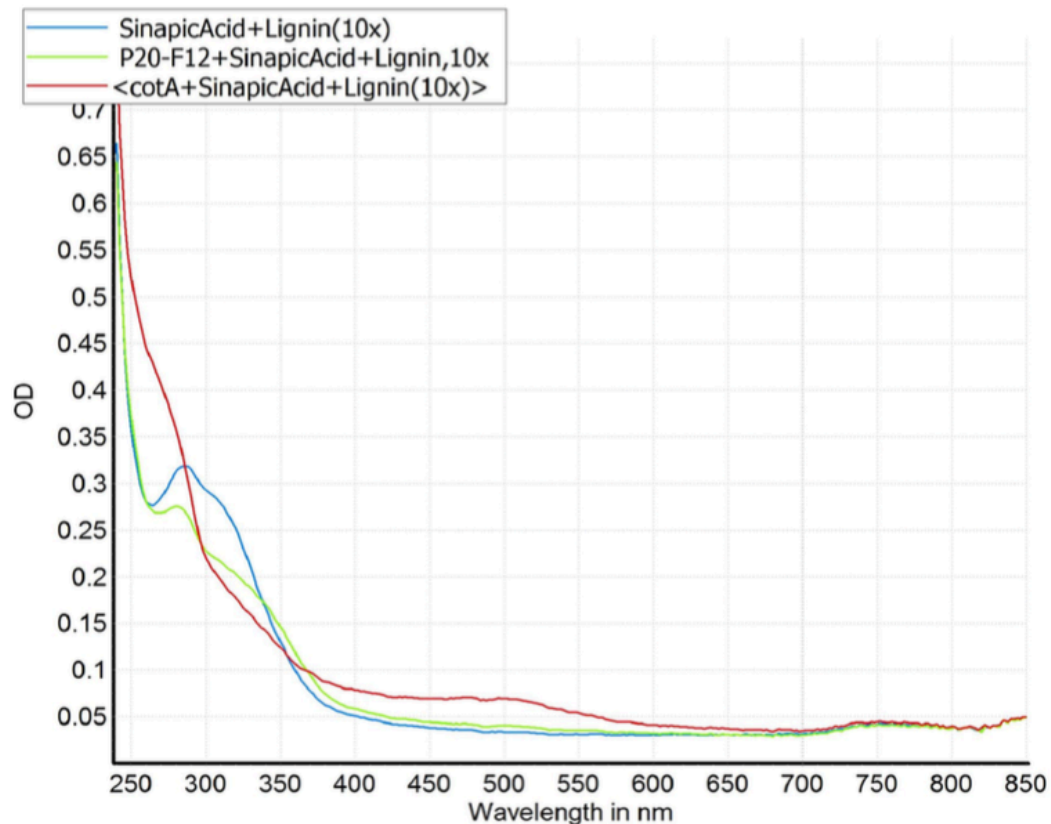
Figure 4.34. UV/visible absorption spectrum after activity assay with P20-F12, sinapic acid and lignin, and CotA with sinapic acid and lignin. The red graph represents CotA with sinapic acid, and lignin. The green graph represents P20-F12 with sinapic acid and lignin. The blue graph represents sinapic acid with lignin without enzyme. Reduction of the absorption peak at 290 nm represents the oxidation of sinapic acid.
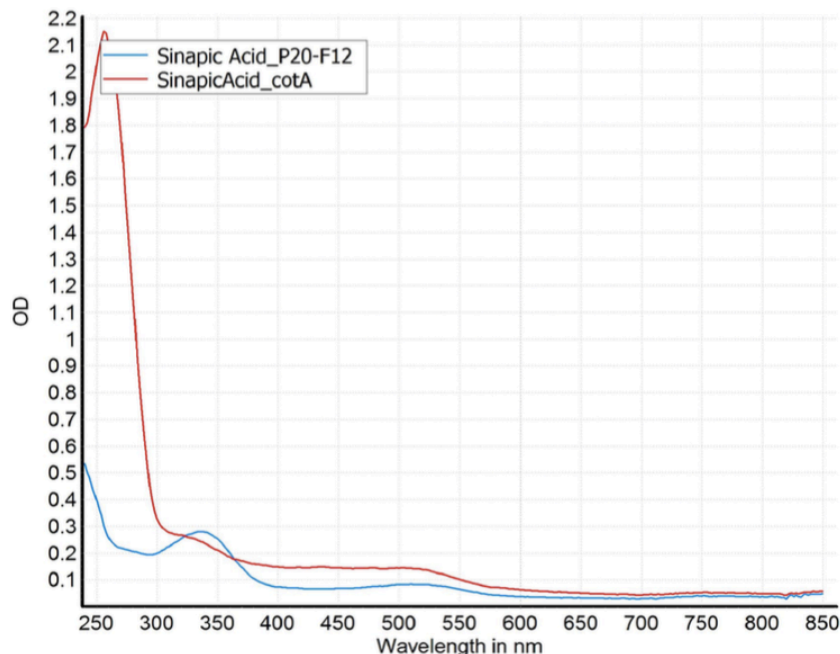

Figure 4.35. UV/ visible absorption spectrum after activity assay of CotA and P20-F12 with sinapic acid as substrate.

Ferulic acid and catechol were also potential mediators. However, no changes in absorption were observed during the assay with lignin, and therefore no further effort were made regarding these two phenolic substances.

4.3.6. Determination of the kinetic parameters K_m, V_{max}, k_{cat} and k_{cat}/K_m of the four *Actinobacteria* laccases P01-C03, P01-E07, P06-A08 and P20-F12

In order to explore and describe the enzymatic activity of the four *Actinobacteria* laccases towards ABTS in more depth it was decided to calculate K_m, V_{max}, k_{cat} and k_{cat}/K_m for P01-C03, P01-E07, P06-A08 and P20-F12. K_m and k_{cat} for each enzyme were determined as described in section 3.7. Michaelis-Menten kinetics hyperbola curves for P01-C03, P01-E07, P06-A08, and P20-F12 (Figure 4.36, Figure 4.37, Figure 4.38, and Figure 4.39) were generated as described in section 3.7. The formation of oxidized ABTS in µM/min was calculated by using the Lambert-Beer law (see section 1.6.1) where

$$A = \varepsilon * d * C$$

Reorganization of the equation to calculate ABTS in µM/min gives

$$C = \frac{\Delta E / d}{\varepsilon}$$

where $A = \Delta E / d$

Observation of the hyperbola curves generated for P01-C03 (Figure 4.36), P01-E07 (Figure 4.37), P06-A08 (Figure 4.38) and P20-F12 (Figure 4.39) suggests that all enzymes follow Michaelis-Menten kinetics. For P06-A08 (Figure 4.38) observations suggest that V_{max} have not been reached, indicating that V_{max} occurs at higher ABTS concentrations than those tested here. The program therefore has to extrapolate in order to calculate the V_{max}, which in turn results in high standard deviation (Table 4. *10*). A similar observation was made for P20-F12 (Figure 4.39).
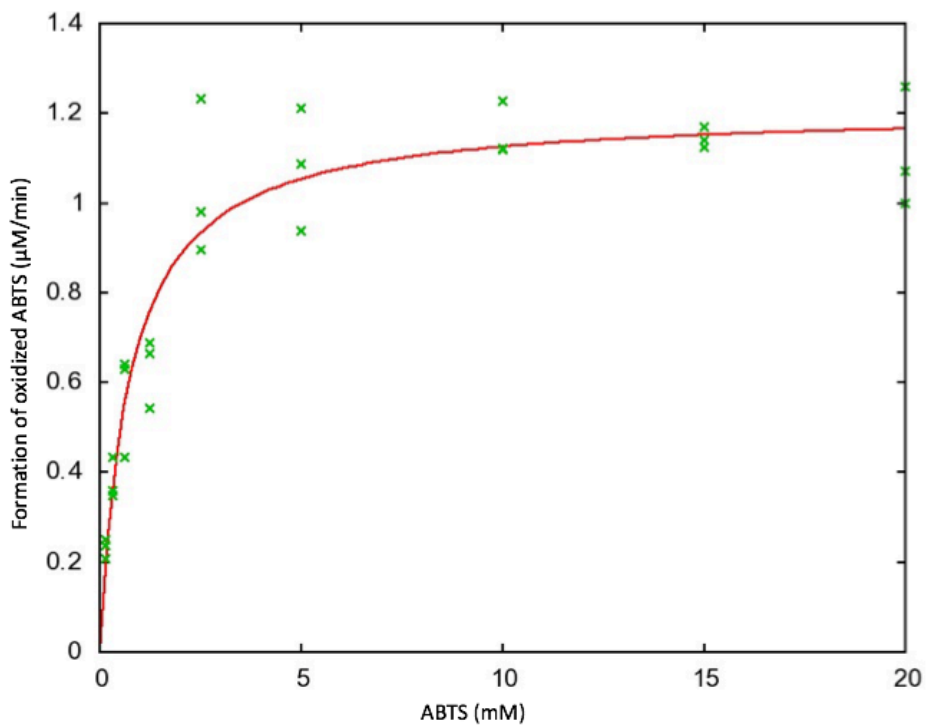
Figure 4.36. Michaelis-Menten kinetics for P01-C03 with ABTS. Activity assay for P01-C03 (protein concentration = 0.104 mg/mL) with different ABTS concentrations diluted in acetate buffer, pH 4.2, was performed as described in section 3.7 to investigate if the enzyme follows Michaelis-Menten kinetics. Each measurement was done in triplicate.
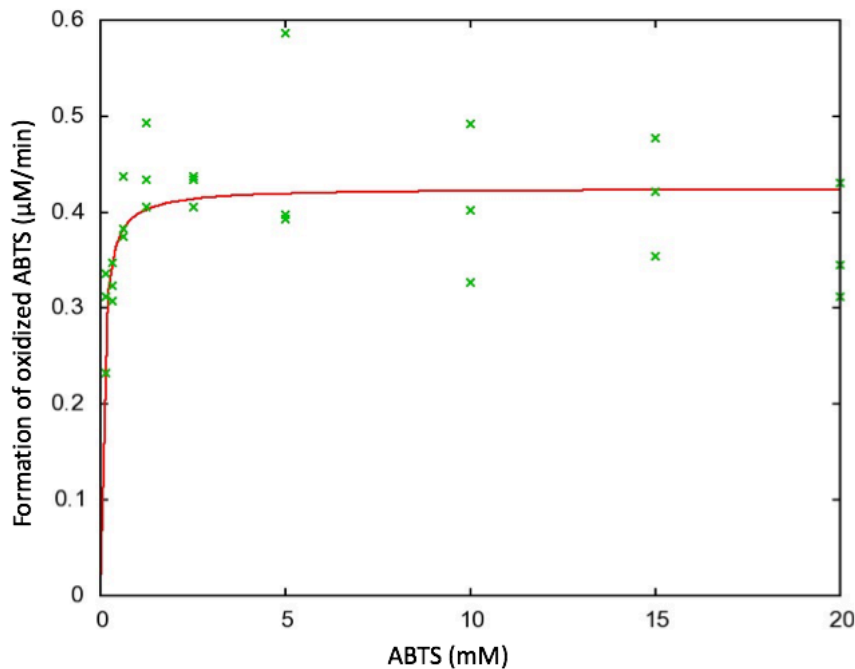
Figure 4.37. Michaelis-Menten kinetics for P01-E07 with ABTS. Activity assay for P01-E07 (protein concentration = 0.106 mg/mL) with different ABTS concentrations diluted in acetate buffer, pH 4.2, was performed as described in section 3.7 to investigate if the enzyme follows Michaelis-Menten kinetics. Each measurement was done in triplicate.
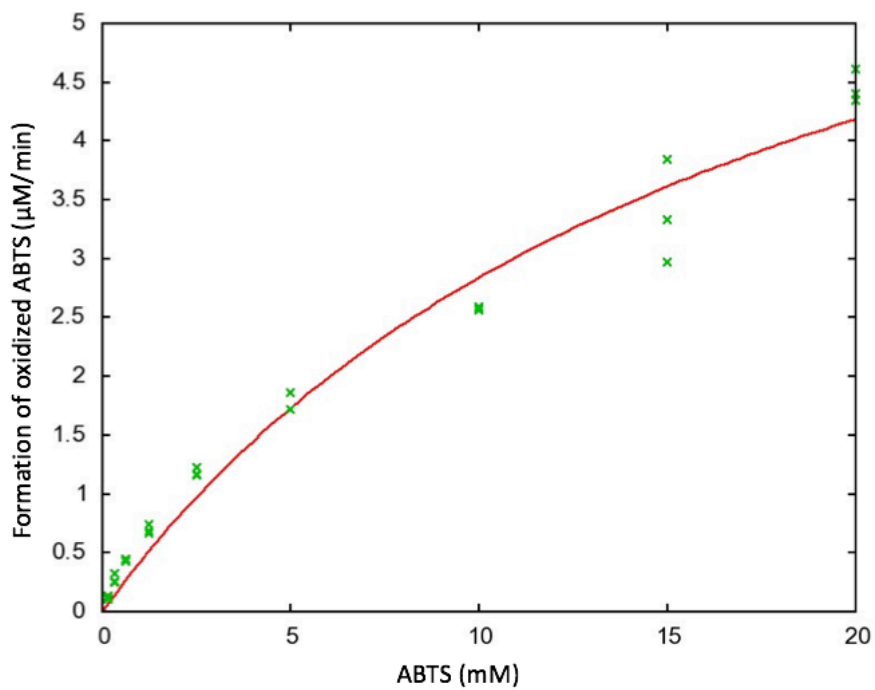
Figure 4.38. Michaelis-Menten kinetics for P06-A08 with the substrate ABTS. Activity assay for P06-A08 (protein concentration = 0.41 mg/mL) with different ABTS concentrations diluted in acetate buffer, pH 4.2, was performed as described in section 3.7 to investigate if the enzyme follows Michaelis-Menten kinetics. Each measurement was done in triplicate.
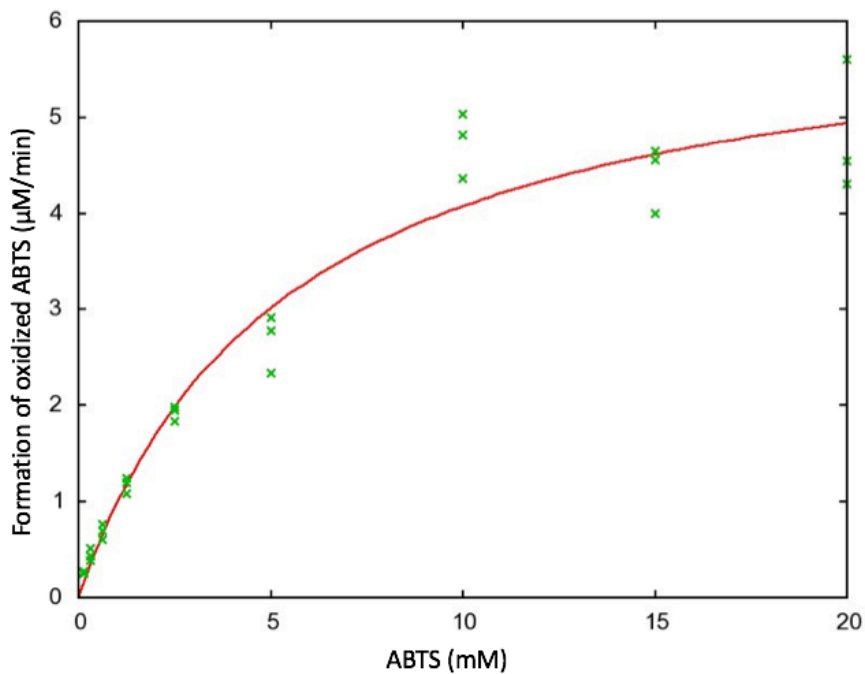

Figure 4.39. Michaelis-Menten kinetics for P20-F12 with ABTS. Activity assay for P20-F12 (protein concentration = 0.331 mg/mL) with different ABTS concentrations diluted in acetate buffer, pH 4.2, was performed as described in section 3.7 to investigate if the enzyme follows Michaelis-Menten kinetics. Each measurement was done in triplicate.

The kinetic parameters for P01-C03, P01-E07, P06-A08 and P20-F12 using ABTS as substrate at pH 4.2 are presented in Table 4. *10*. The parameter K_m represents the substrate concentration of ABTS when the reaction velocity is ½ V_{max}, and the high K_m seen for P06-A08 indicates that the enzyme has low substrate affinity. The same can be stated for P20-F12. A low K_m is displayed for both P01-C03 and P01-E07, indicating higher substrate affinity than the other two enzymes, and that the enzymes achieves maximal catalytic effect (V_{max}) at a low substrate concentration. The four *Actinobacteria* laccases all have low k_{cat} values, which measures the number of catalytic cycles that the active site undergoes per unit time (here, per second). The catalytic effect (k_{cat}/K_m) accounts for both catalysis and specific substrate binding, and is relatively low for all the enzymes, indicating that the enzymes are not highly efficient in oxidizing ABTS.

Table 4. 10: Kinetic parameters of the four new Actinobacteria laccases. Activity assays were performed in room temperature (25 °C) with ABTS diluted in acetate buffer pH 4.2. The formation of oxidized ABTS was calculated with a molar absorption coefficient of 36 000 M^{-1} cm^{-1} (Reiss et al. 2013) and the values for K_m, V_{max} and k_{cat} were determined as described in section 3.7.

Laccase	K_m (mM)	V_{max} (µM/min)	k_{cat} (s^{-1})	k_{cat}/K_m
P01-C03	0.735 ± 0.107	1.208 ± 0.0387	0.309	0.42
P01-E07	0.068 ± 0.024	0.425 ± 0.0153	0.101	1.485
P06-A08	18.103 ± 3.88	7.97 ± 0.969	0.518	0.028
P20-F12	5.427 ± 0.893	6.283 ± 0.378	0.488	0.0899

P20-F12 was also analyzed with respect to its activity towards sinapic acid and to see if the enzyme followed Michaels-Menten kinetics also with this substrate. The following sinapic acid concentrations were used: 0.5 mM, 0.25 mM, 0.125 mM, 0.0625 mM and 0.03125 mM dissolved in sodium phosphate buffer pH 7.5. Observations of the graph generated for P20-F12 with sinapic acid (Figure 4.40) indicates that it does not follow a hyperbolic shape within the substrate concentration range applied. If Michaelis-Menten kinetics apply for P20-F12, V_{max} will be reached at much higher concentrations than 0.5 mM. Extrapolation based in the concentrations measured gives K_m and V_{max} values with very high standard deviation (Table 4.11). Concentrations higher than 0.5 mM did not show any change in absorption during the activity assay. It was determined that the enzyme did have activity towards sinapic acid at higher concentrations due to a distinct color change that was observed after the assay (see 7.4, appendix D).
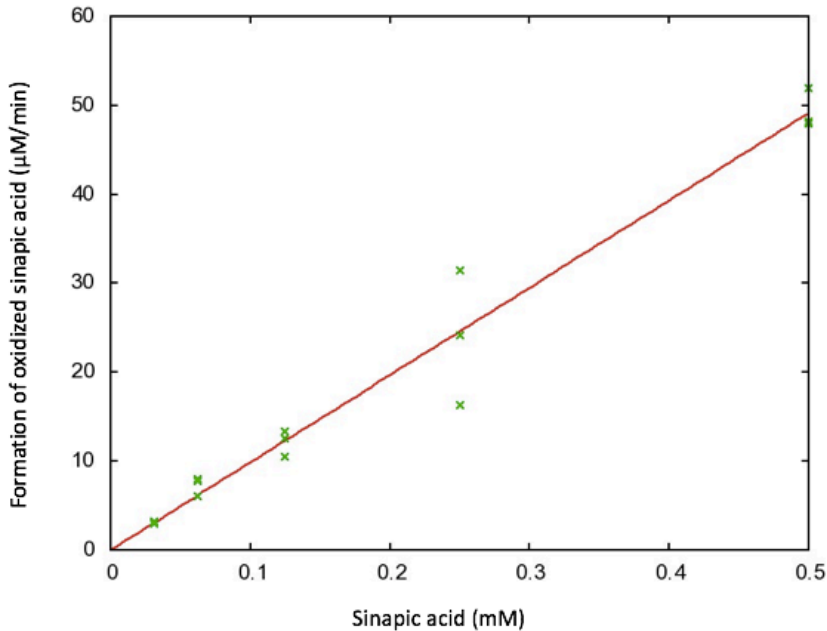
Figure 4.40. Michaelis-Menten kinetics for P20-F12 with sinapic acid. Activity assay for P20-F12 (protein concentration = 0.331 mg/mL) with different concentrations of sinapic acid diluted in sodium phosphate buffer, pH 7.5, was performed to investigate if the enzyme follows Michaelis-Menten kinetics. Each measurement was done in triplicate. V_{max} and k_{cat} was generated as described in section 3.7.

Table 4.11. Kinetic parameters for P20-F12 with sinapic acid. Activity assays were performed in room temperature (25 °C) with sinapic acid diluted in sodium phosphate buffer pH 7.5. The formation of oxidized sinapic acid was calculated with a molar absorption coefficient of 2160 M^{-1} cm^{-1} (Cai and Arntfield 2001) and the values for K_m, V_{max}, and k_{cat} was determined as described in section 3.7

Laccase	K_m (mM)	V_{max} (μM/min)	K_{cat} (s^{-1})	k_{cat}/K_m
P20-F12	2066.7 $\pm$ 1.108e+06	202995 $\pm$ 6.352e-06	15758	7.62

4.4. Protein engineering of cotA from *B. subtilis*

In order to obtain insight into protein engineering and to obtain an even deeper understanding of the function and mechanism of laccases, it was decided to attempt changing the substrate

specificity of the laccase CotA of *B. subtilis* by engineering the active site of the enzyme. The background for the engineering approach lies in work performed by SINTEF and partners at Aberystwyth University (Wales) in the frame of ERA-IB project OXYPOL. In this separate project, analysis of Kraft lignin provided by a commercial partner in OXYPOL showed that vanillin, syringaldehyde, acetovanillone, and acetosyringone are the most abundant monomers directly derivable from this feedstock (unpublished data). Previous studies (Reiss et al. 2013) revealed that CotA does not display activity towards vanillin, which itself has valuable applications in the food and fragrance industry, but also has the potential to function as low-cost mediator for lignin depolymerization. This is the motivational background for protein engineering of CotA to achieve the ability to oxidize vanillin. In the OXYPOL project, suggestions were made for mutations of CotA to optimize the binding site for vanillin utilization (unpublished results from the OXYPOL project). Because there are no available structures of CotA with vanillin, more than 2000 models of CotA variants were generated based on the structure of CotA bound to sinapic acid, which possesses structural similarities with vanillin (Figure 4.26). From this analysis, the following mutations were suggested in a first approach to try to achieve vanillin conversion by CotA variants: P226M, L386A, A471P, A376S and G377V. Primers used for site-directed mutagenesis were provided by Eurofins Genomics (see section 2.4).

4.4.1. Site-directed mutagenesis

Site-directed mutagenesis to generate specific amino acid mutations in the genetic sequence of CotA was performed as described in section 3.9. The mutations that were introduced and how these affected the enzymatic activity of CotA towards ABTS is presented in

Table 4.*12*. The single mutation leading to the amino acid changes P226M and L386A allowed CotA to retain activity towards ABTS, but the double mutation leading to P226M and L386A resulted in loss of activity towards ABTS (results not shown). The triple mutation combining P226M, L386A and A471P were introduced in the *cotA* gene and respective gene variants cloned in *E. coli*. However, no enzyme productions and activity assays were performed with these due to the loss in activity with the double mutation (P226M and L386A).

Table 4.12. Amino acid mutations performed and if cotA displayed activity towards ABTS with the respective mutations

Amino acid mutations	Enzymatic activity with ABTS
P226M (single mutation)	Yes
L386A (single mutation)	Yes
P226M and L386A (double mutation)	No
P226M, L386A and A471P (triple mutation)	Not available

The variants of CotA containing the different mutations were also verified by sequencing at Eurofins Genomics.

Enzymes with the P226M and L386A single mutation and double mutation were investigated to see if they displayed activity towards vanillin. No activity could be observed. Based on this, the last two mutations (A376S and G377V) were not completed and the study was concluded

5. Discussion and future perspectives

The scientific study represented by this master´s degree project is an integrated part of the OXYMOD project of the Centre for Digital Life Norway (DLN; see section 1.7). The main objective of this study was to express and characterize a selection of newly discovered *Actinobacteria* laccases and evaluate their potential as lignin degraders in a laccase-mediator system. Prior to the extensive characterization of the selected *Actinobactera* laccases, three *Psychrobacter* laccases were expressed inhouse to obtain practical knowledge on the expression and characterization of bacterial laccases in *E. coli* while simultaneously investigating the effect of $CuCl_2$ supplementation on the activity of these enzymes. The last part of this study involved protein engineering of Cota from *B. subtilis* with the aim to make CotA active against vanillin.

5.1. Expression of three *Psychrobacter* laccases P2G3, P11G3, and P11F6

One part of the project was dedicated to investigating how addition of free copper to *E. coli* expressing laccases would influence the activity of the enzymes purified from these cultures. Addition of copper seemed to influence the purified proteins. In the absence of $CuCl_2$, P2G3, P11G3 and P11F6 did not display activity towards ABTS, indicating the importance of cofactor supplementation during cultivation or directly to the cell extract. All the three *Psychrobacter* laccases are MCOs, which are dependent on Cu^{2+} ions in order to oxidize their substrate. The enzymes do, however, appear to demand additional supplementation of $CuCl_2$ in order to retain their activity after purification (section 3.4.2.2) and buffer exchange (section 3.4.3.2), unlike the *Actinobacteria* laccases that showed activity without additional $CuCl_2$ after application of the same purification and buffer exchange methods. Previous studies have determined the three *Psychrobacter* laccases to be three-domain laccases, unlike the *Actinobacteria* laccases that are predicted to be two-domain laccases, with trimers as their active form. Analysis of the three-dimensional structure of a previously described three-domain and a two-domain laccase indicated that the T1 copper in the three-domain laccase could be, to some extent, exposed to the solvent while the T2/T3 coppers are shielded from the enzyme's surroundings (Figure 5.1 a), while all copper atoms in the two-domain laccase were more or less shielded from the surroundings (Figure 5.1 b). During purification and buffer exchange, the T1 copper in the

Psychrobacter laccase could have been lost during the wash step due to its exposure to the solvent, resulting in the loss of enzymatic activity.
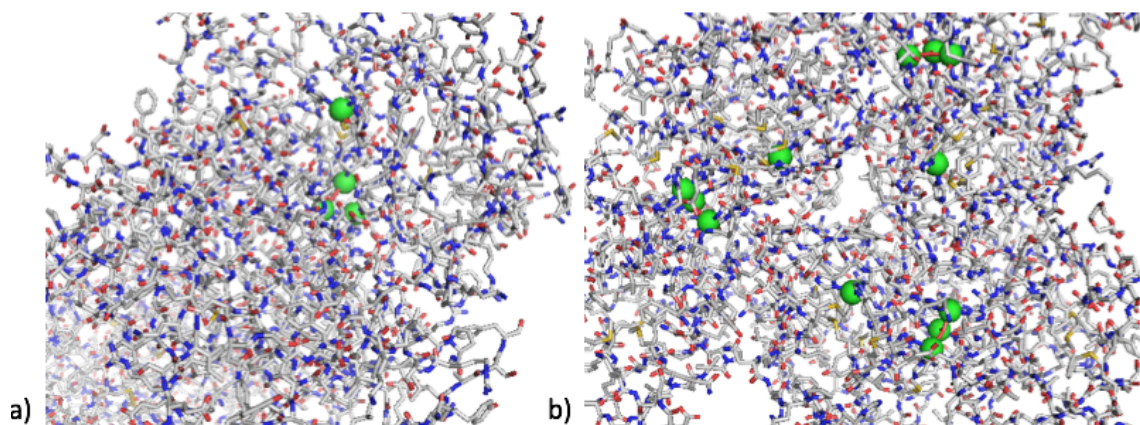

Figure 5.1. Three-dimensional structure illustrating the placement of copper ions. The placement of copper ions in a) three-domain laccase and b) two-domain laccase, indicate the close to the surface location of the T1 copper in the three-somain enzyme. The 3D structures were downloaded from RCSB PDS (PDB ID 4Q89 for the three-domain laccase and 4GXF for the two-domain laccase) and altered using PyMol.

Another explanation could be in a potentially negative effect of performing the purification and buffer exchange at room temperature. The *Psychrobacter* laccases may not be able to retain activity when treated at room temperature for extended periods of time. That would, however, not explain why the enzyme showed activity after purification and buffer exchange when using buffers supplemented with 0.25 mM $CuCl_2$, rendering this potential explanation less likely.

After investigating how the presence of $CuCl_2$ supplementation with different strategies (Table 4.3) would affect the enzymatic activity with ABTS, it was observed that both P11F6 and P11G3 achieved the highest specific activity with strategy 3 (induction with IPTG and $CuCl_2$ supplementation (soaking) of the cell extract). Induction with IPTG during cultivation in the absence of $CuCl_2$ could allow the enzyme to fold without having to take the copper into consideration, making the folding procedure to occur without interruptions. Incomplete copper incorporation is often observed in both three-domain and two-domain laccases, but how copper is incorporated is still poorly understood (Gabdulkhakov et al. 2018). Adding copper to already folded enzymes could therefore result in more efficient implementation of all the copper atoms, which could reduce the number of potential incomplete copper incorporations. The results showed that by excluding copper from the cultivation and supplementing it directly to the cell extract, the laccases displayed the highest specific activity, indicating that copper incorporation

to already folded enzymes is possible, and potentially the method of choice for these particular set of enzymes. The stability of the *Psychrobacter* laccases could also have been affected by the concentration of $CuCl_2$. Different cultivation batches expressed different levels of laccases, and 0.25 mM $CuCl_2$ could be a limiting factor. Determining the optimum $CuCl_2$ concentration for P2G3, P11G3 and P11F6 could contribute to minimizing losses due to instability, if this is a limiting factor.

During this study, the *Psychrobacter* laccases were cultivated several times resulting in different enzyme batches. In the second batch (section 4.1.2), P2G3 did not display activity towards ABTS, while P11G3 and P11F6 did. In the third batch (section 4.1.3), P2G3 and P11G3 did not show activity towards ABTS when induced with IPTG and supplemented with $CuCl_2$ during cultivation, while in the first batch (4.1.1), P2G3 and P11G3 displayed activity after being cultivated under the same conditions. This variation in enzymatic activity of P2G3, P11G3 and P11F6 from batch to batch have not been described elsewhere, and would be interesting to analyze more in depth, to determine if this instability lies in the intrinsic properties of the enzyme or is caused by the cultivation method. A potential solution could be to alter the temperature during cultivation, and express the proteins at even lower temperatures than those applied, which is common for psychrophilic enzymes and handling of cells that are optimized for protein production at low temperatures, such as ArcticExpress competent cells (Prete et al. 2015). It should also be noted that the significant amounts of P2G3, P11G3 and P11F6 were observed in the cell pellet, indicating the formation of inclusion bodies. The formation of inclusion bodies is very common when proteins are overexpressed and may occur when protein folding does not occur fast enough in relation to protein synthesis. It has been shown that aggregation increases as the protein concentration increases, however little is known about their structure of inclusion bodies and their formation mechanism (Fink 1998).

5.2. Expression and characterization of the *Actinobacteria* laccases P01-C03, P01-E07, P06-A08 and P20-F12

Laccases originating from bacterial sources exhibit higher thermal and pH stability compared to fungal laccases, potentially making them more applicable in industrial applications (Moghadam et al. 2016). The high thermal stability observed for the four *Actinobacteria* laccases is a trait that increases their potential as lignin degraders in potential future industrial application.

106

The four *Actinobacteria* laccases were found to be highly thermostable, retaining activity after incubation at 90 °C. P06-A08 and P20-F12 were observed to retain activity after incubation at 99 °C up to two hours, indicating highly thermostable properties. However, longer incubation periods are needed to determine the nature of their thermostability, in particular if the observed thermostability is due to the enzyme retaining their folded structure at high temperature (and thus being active at high temperature) or spontaneous refolding after heating and before/during assaying. Incubation at temperatures lower then 30 °C would also be interesting to analyze to observe whether the laccases also display activity at lower temperatures and their eventual level of activity under such conditions. An important requirement for an enzyme to be applicable in many industrial processes is high stability, and in particular thermotolerance or thermostability. Thermostable enzymes offer biotechnological advantages over commonly studied mesophilic enzymes, as they usually also have other desirable traits such as higher resistance to chemical denaturants, high alkalinity or extreme acidity. Also, the possibility to apply heat-treatment for cheap enzyme purification is a desired feature provided by thermostability, as well as the possibility to store the enzyme at ambient temperature without loss of function. Enzyme reactions at higher temperatures are also faster and less susceptible to microbial contamination (Hildén, Hakala, and Lundell 2009).

P01-C03, P01-E07, P06-A08 and P20-F12 were all observed to display the highest specific activity at pH values between 3.8 and 4.6 with ABTS, but marginal activity was observed at neutral and basic pH values (Figure 4.25). It should be noted that ABTS is not a natural substrate for laccase, but nevertheless is the most used model substrate for characterization of these enzymes (Chaurasia, Yadav, and Yadava 2013). One potential problem with using model substrates is that catalytic characterization could be misleading and not reveal the true nature of the laccase enzymatic activity. P20-F12, however, did display activity towards four phenolic substrates during substrate screening at neutral pH, indicating that the pH optimum could vary between different substrates. Initial substrate screening was performed at pH 4.2, based on pH stability analysis observations indicating that all enzymes displayed high levels of activity with ABTS at this pH, which resulted in no observed activity towards any of the substrates. It was, therefore, decided to run another substrate screening using assay solutions with substrates diluted in sodium phosphate buffer pH 7.5, due to speculations that the low pH could have resulted in deprotonation of the OH groups in the substrates, leaving the enzyme with nothing to oxidize. Amines and phenols are natural substrates of laccases (Jones and Solomon 2015),

thus sinapic acid, catechol, ferulic acid and 3,4-dihydrobenzoic acid were suggested to be substrates more in resemblance to the natural substrates for the four *Actinobacteria* laccases, unlike ABTS which is not a natural substrate. It would therefore be expedient to investigate temperature stability, pH stability, and kinetic parameters using phenolic substrates. P01-C03, P01-E07 and P06-A08 did not display activity towards any of the substrates during the substrate screening which could be due to the neutral pH, but it is possible that they display activity towards phenolic substrates at other pH values, which should be investigated further.

Kinetic parameters were calculated for all four *Actinobacteria* laccases with ABTS as the substrate. P06-A08 displayed the highest K_m and k_{cat} values, i.e. 18.1 mM and 0.52 s^{-1}, respectively, but was found to be the least efficient of the four laccases with the lowest k_{cat}/K_m = 0.03 (Table 4. 10). P01-E07 was observed to have the lowest K_m = 0.07 mM and k_{cat} = 0.1 s^{-1}, but the laccase was found to be the most efficient of the four laccases with the highest k_{cat}/K_m = 1.5 (Table 4.10), which could be a result of the enzymes high affinity for the substrate. P20-F12 was observed to have the second highest K_m and k_{cat} values where K_m = 5.4 mM and k_{cat} = 0.49, and the second lowest k_{cat}/K_m = 0.09, while P01-C03 were observed to have the second lowest K_m, k_{cat} and k_{cat}/K_m value. The relatively high variation in kinetic parameters between the four laccases could be explained by observing their low sequence similarity to each other (see appendix E and F). This is something that can be further investigated in more dept, but an overall observation clearly indicates low sequence similarities which might suggest that P01-C03, P01-E07, P06-A08 and P20-F12 have different properties concerning their natural roles in *Actinobacteria*, for instance with respect to substrate specificity.

In previous studies, a small laccase (SLAC) from *Streptomyces coelicolor* showed similar characteristics to the four *Actinobacteria* laccases (Fernandes et al. 2014). The small laccase also exhibits a pH optimum at low pH, 4.0, with ABTS, but was found to have a k_{cat} = 4 s^{-1} and a K_m = 0.4 mM, which gives a k_{cat}/K_m = 10, indicating that the SLAC from *S. coelicolor* has a higher efficiency towards ABTS compared to the four *Actinobacteria* laccases. It should be noted that P01-C03, P01-E07 and P06-A08 were found to have the highest sequence similarity with the SLAC from *S. coelicolor* with 80%, 70% and 54% sequence identity, respectively (see 7.7, appendix G). However, their enzymatic efficiencies towards ABTS were much lower compared to the SLAC from *S. coelicolor*. P20-F12 has have high sequence similarity with the SLAC SsI1 from *Streptomyces sviecus* which also has been shown in previous studies (Fernandes et al. 2014) to have a pH optimum of 4.0 with ABTS, low K_m = 0.36 mM and a high

$k_{cat} = 7.38$ s^{-1}. The catalytic efficiency of SsI1 is thus $k_{cat}/K_m = 20.5$, more than 200-fold higher than the catalytic efficiency of P20-F12.

The *Actinobacteria* laccases described in this study may have resemblance with *S. coelicolor* and *S. sviecus*, but they do not display the same level of catalytic efficiency towards ABTS, indicating that they are, at least as non-optimized versions, simply poor laccases for lignin degradation in a laccase-mediator system, at least using ABTS as a mediator.

ABTS and sinapic acid were considered to be potential mediators for the degradation of lignin with P20-F12. However, both substrates were observed to interfere with the 465 nm signal used to detect the oxidation of lignin, making it difficult to decide if lignin has been oxidized or not. Alternative approaches need to be considered to determine the oxidation of lignin not based on the change in absorption, e.g. by using mass spectrometry to detect and monitor occurrence of any low molecular products as a result of potential lignin breakdown.

However, the detection of lignin oxidation by spectroscopic methods could still be applicable for LMS with mediators that does not interfere with e.g. the suggested 465 nm signal upon lignin oxidation.

5.3. Protein engineering of CotA from *B. subtilis*

Vanillin is one of the most abundant monomers in Kraft lignin (unpublished data) and has the potential to function as a low-cost mediator in a laccase-mediator system for the degradation of lignin. This was the motivational background for protein engineering of CotA in order to optimize its binding site for vanillin utilization. Specific amino acids mutations (Table 4.12) were designed by an external partner in the ERA-IB project OXYPOL.

The single amino acid exchanges of P226M and L386A both resulted in CotA variants retaining activity towards ABTS, but a double mutation combining these exchanges in one variant resulted in loss of activity towards ABTS, indicating that proline 226 and leucine 386 in combination play important roles in the enzymes active site. Figure 5.2 displays the two amino acids P226 and L386 in CotA of *B. subtilis*. The two amino acids are observed to be situated

near the T1 copper site, where substrate oxidation occurs, indicating that P226 and L386 could play a direct role in oxidation of laccase substrates.
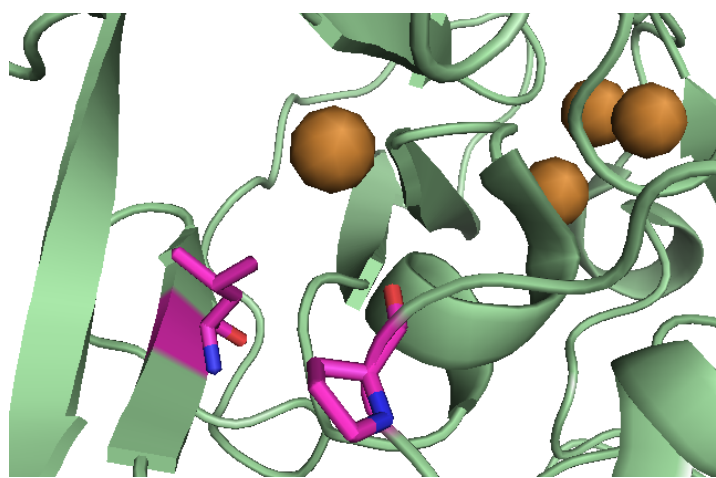

Figure 5.2. Amino acid P226 and L386 in cotA from B. subtilis

The suggested amino acid changes in combination were detrimental for the enzymatic activity of CotA. The enzyme lost activity towards ABTS, and neither of the three constructs tested obtain enzymatic activity towards vanillin. However, it would still be interesting to determine the kinetic parameters K_m and k_{cat} for CotA variants with the two single mutations, P226M and L386A, in comparison to the wild type in order to evaluate further engineering steps towards the ultimate goal to obtain a highly active CotA that can use vanillin as substrate in a bacterial LMS for efficient lignin depolymerization.

5.4. Spectrophotometric analysis of enzymatic activity

In this study the enzymatic activity of all laccases that have been described was determined by a spectrophotometric approach using a FLUOstar omega microplate reader that detects change in absorption over time. The FLUOstar Omega instrument has been a large and vital part to during this study, which is why the method is extensively discussed.

In section 4.1.4 and Figure 4.9 a reoccurring issue with this method can be observed, where irregular absorption curves have occurred when measuring activity assays of cell extracts. Optimally, pure protein samples should be used, as other proteins in the cell extract could have an effect on the absorption changes that are measured. The same problem did not occur when purified protein samples were used in the assay.

110

To determine the enzymes activity based on change in absorption over time, the molar absorption coefficient of the substrate was used. The molar absorption coefficient of each substrate is determined under specific conditions of pH and temperature. If the conditions of the enzymatic assay are not equal to the conditions used to determine the molar absorption coefficient, the results that are obtained could be misleading and would most likely differ from the results that would have been achieved under identical conditions. This influencing factor could affect the determination of the enzymatic activity by either over-or under-estimating its catalytic abilities towards the substrate in question.

Determination of the change in absorption over a given period of time was done by selecting a linear part of the assay curve by eye measurement, and calculate the absorption change per minute. This could possibly not be the optimal approach, as the true linearity of the assay curve was not determined. To verify that the linear selection was truly linear, the extraction was plotted against the number of measurements that was done during that period of time. This example is an extraction that was used to calculate the specific activity of P20-F12 with 20 mM ABTS at pH 4.2. During a ten-minute time period a total of 77 measurements had been done, while approximately 30 measurements during the same period of time was displayed in the graph. This additional data was collected from the program used to process the absorption data (not shown). Figure 5.3 confirms that the linear extraction of the assay curve is indeed more or less linear, concluding that eye measurement of the linearity in the assay graph is sufficient.
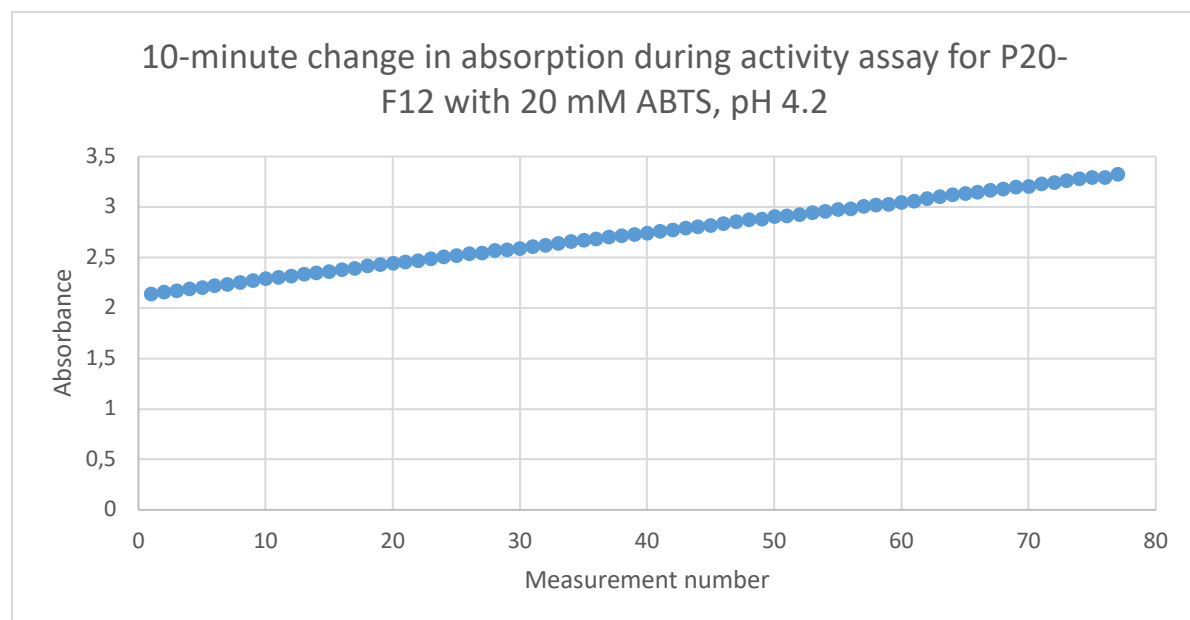

Figure 5.3. Linear extraction of an assay curve generated by an activity assay with P20-F12 and ABTS at pH 4.2. The graph is a result of 77 absorption measurements done during a 10-minute time period in the activity

assay. This extraction is an example of a linear part of the assay graph used in determination of the enzyme's activity, to verify that the line is more or less linear, although it is based on eye-measurement.

Another drawback with this method was the absorption detection limit of the instrument. It appeared that the FLUOstar Omega could not detect absorbance higher than OD = 6.5. This was clearly illustrated when activity assay with P20-F12 and sinapic acid at various concentrations was performed (see section 4.3.6). Concentrations exceeding 0.5 mM sinapic acid were too concentrated for the instrument to detect a change in absorption. It was clearly observed that a reaction had occurred based on the distinct color change in the 96-well microtiter plate (7.4, appendix D), while it could not be observed from the absorption measurements in the FLUOstar Omega, where all measurements showed OD = 6.5 throughout the entire assay period (data not shown).

The critical assessment of the FLUOstar Omega does not mean that this method is unsuitable for determination of enzyme activity. When the molar absorption coefficient of the substrate is known, simple calculations to determine the enzymatic activity can be done (see section 4.3.6). If the molar absorption coefficient is not known for the substrate, standard curve assay could be preferred.

5.5. Concluding remarks

The present study has demonstrated the potential use of the underexplored group of redox-enzymes for lignin degradation in a laccase-mediator system. Characterization of four newly discovered *Actinobacteria* laccases were observed to have a high thermotolerance, a trait that is desired in industrial applications. Further research regarding the four laccases P01-C03, P01-E07, P06-A08 and P20-F12 could include in-depth characterization of their thermostability over longer periods of time, screening for other phenolic substrates that could be used in a laccase-mediator system, as well as protein engineering to optimize the binding site.

Site-directed mutation in efforts to make CotA active towards vanillin was not successful. The two first mutations that were suggested, resulted in loss of activity towards ABTS, and activity with vanillin was not achieved. Further research could include the comparison of how the two single mutations (P226M and L386A) affected the catalytic site, as well as protein engineering to obtain catalytic activity towards vanillin.

The four *Psychrobacte* enzymes would also need to be characterized in-depth to determine their true catalytic nature in terms of thermostability, pH optimum, substrate screening, and production.

6. References

Alcalde, Miguel. 2007. "Laccases: Biological Functions, Molecular Structure and Industrial Applications." In *Industrial Enzymes: Structure, Function and Applications*, 461–76. https://doi.org/10.1007/1-4020-5377-0_26.

Amezcua-Allieri, Myriam Adela, and Jorge Aburto. 2017. "Conversion of Lignin to Heat and Power, Chemicals or Fuels into the Transition Energy Strategy." *Lignin - Trends and Applications*, December. https://doi.org/10.5772/intechopen.71211.

Anwar, Zahid, Muhammad Gulfraz, and Muhammad Irshad. 2014. "Agro-Industrial Lignocellulosic Biomass a Key to Unlock the Future Bio-Energy: A Brief Review." *Journal of Radiation Research and Applied Sciences* 7 (2): 163–73. https://doi.org/10.1016/j.jrras.2014.02.003.

Asina, Fnu, Ivana Brzonova, Keith Voeller, Evguenii Kozliak, Alena Kubátová, Bin Yao, and Yun Ji. 2016. "Biodegradation of Lignin by Fungi, Bacteria and Laccases." *Bioresource Technology* 220 (November): 414–24. https://doi.org/10.1016/j.biortech.2016.08.016.

Bachman, Julia. 2013. "Site-Directed Mutagenesis." *Methods in Enzymology* 529: 241–48. https://doi.org/10.1016/B978-0-12-418687-3.00019-7.

Bajpai, Pratima. 2016. *Pretreatment of Lignocellulosic Biomass for Biofuel Production*. SpringerBriefs in Molecular Science. Singapore: Springer Singapore. https://doi.org/10.1007/978-981-10-0687-6.

Baltierra-Trejo, Eduardo, Liliana Márquez-Benavides, and Juan Manuel Sánchez-Yáñez. 2015. "Inconsistencies and Ambiguities in Calculating Enzyme Activity: The Case of Laccase." *Journal of Microbiological Methods* 119 (Supplement C): 126–31. https://doi.org/10.1016/j.mimet.2015.10.007.

Baneyx, François. 1999. "Recombinant Protein Expression in Escherichia Coli." *Current Opinion in Biotechnology* 10 (5): 411–21. https://doi.org/10.1016/S0958-1669(99)00003-8.

Barka, Essaid Ait, Parul Vatsa, Lisa Sanchez, Nathalie Gaveau-Vaillant, Cedric Jacquard, Hans-Peter Klenk, Christophe Clément, Yder Ouhdouch, and Gilles P. van Wezel. 2016. "Taxonomy, Physiology, and Natural Products of Actinobacteria." *Microbiol. Mol. Biol. Rev.* 80 (1): 1–43. https://doi.org/10.1128/MMBR.00019-15.

Bowman, John P. 2006. "The Genus Psychrobacter." In *The Prokaryotes*, edited by Martin Dworkin, Stanley Falkow, Eugene Rosenberg, Karl-Heinz Schleifer, and Erko Stackebrandt, 920–30. Springer New York. https://doi.org/10.1007/0-387-30746-X_35.

Bozal, Núria, M. Jesús Montes, Encarna Tudela, and Jesús Guinea. 2003. "Characterization of Several Psychrobacter Strains Isolated from Antarctic Environments and Description of Psychrobacter Luti Sp. Nov. and Psychrobacter Fozii Sp. Nov." *International Journal of Systematic and Evolutionary Microbiology* 53 (4): 1093–1100. https://doi.org/10.1099/ijs.0.02457-0.

Brunelle, Julie L., and Rachel Green. 2014. "Chapter Twelve - One-Dimensional SDS-Polyacrylamide Gel Electrophoresis (1D SDS-PAGE)." In *Methods in Enzymology*, edited by Jon Lorsch, 541:151–59. Laboratory Methods in Enzymology: Protein Part C. Academic Press. https://doi.org/10.1016/B978-0-12-420119-4.00012-4.

Bugg, Timothy DH, Mark Ahmad, Elizabeth M Hardiman, and Rahul Singh. 2011. "The Emerging Role for Bacteria in Lignin Degradation and Bio-Product Formation."

Current Opinion in Biotechnology, Energy biotechnology – Environmental biotechnology, 22 (3): 394–400. https://doi.org/10.1016/j.copbio.2010.10.009.

Cai, R., and S. D. Arntfield. 2001. "A Rapid High-Performance Liquid Chromatographic Method for the Determination of Sinapine and Sinapic Acid in Canola Seed and Meal." *Journal of the American Oil Chemists' Society* 78 (9): 903–10. https://doi.org/10.1007/s11746-001-0362-4.

Calvo-Flores, Francisco García, and José A. Dobado. 2010. "Lignin as Renewable Raw Material." *ChemSusChem* 3 (11): 1227–35. https://doi.org/10.1002/cssc.201000157.

Cavicchioli, R., T. Charlton, H. Ertan, S. Mohd Omar, K. S. Siddiqui, and T. J. Williams. 2011. "Biotechnological Uses of Enzymes from Psychrophiles." *Microbial Biotechnology* 4 (4): 449–60. https://doi.org/10.1111/j.1751-7915.2011.00258.x.

Chaurasia, Pankaj Kumar, Rama Shanker Singh Yadav, and Sudha Yadava. 2013. "A Review on Mechanism of Laccase Action," 6.

Chen, Inês, and David Dubnau. 2004. "DNA Uptake during Bacterial Transformation." *Nature Reviews Microbiology* 2 (3): 241–49. https://doi.org/10.1038/nrmicro844.

Chio, Chonlong, Mohini Sain, and Wensheng Qin. 2019. "Lignin Utilization: A Review of Lignin Depolymerization from Various Aspects." *Renewable and Sustainable Energy Reviews* 107 (June): 232–49. https://doi.org/10.1016/j.rser.2019.03.008.

Christopher, Lew Paul, Bin Yao, and Yun Ji. 2014. "Lignin Biodegradation with Laccase-Mediator Systems." *Frontiers in Energy Research* 2. https://doi.org/10.3389/fenrg.2014.00012.

Chudobova, Dagmar, Simona Dostalova, Iva Blazkova, Petr Michalek, Branislav Ruttkay-Nedecky, Matej Sklenar, Lukas Nejdl, et al. 2014. "Effect of Ampicillin, Streptomycin, Penicillin and Tetracycline on Metal Resistant and Non-Resistant Staphylococcus Aureus." *International Journal of Environmental Research and Public Health* 11 (3): 3233–55. https://doi.org/10.3390/ijerph110303233.

Claus, Harald. 2004. "Laccases: Structure, Reactions, Distribution." *Micron*, XIIIth International Conference on Invertebrate Dioxygen Binding Proteins, 35 (1): 93–96. https://doi.org/10.1016/j.micron.2003.10.029.

Dordick, Jonathan S., Michael A. Marletta, and Alexander M. Klibanov. 1986. "Peroxidases Depolymerize Lignin in Organic Media but Not in Water." *Proceedings of the National Academy of Sciences* 83 (17): 6255–57. https://doi.org/10.1073/pnas.83.17.6255.

Dowd, E. 1965. "A Comparison of Estimates of Michaelis-Menten Kinetic Constants from Various Linear Transformations," 7.

Dubé, Etienne, François Shareck, Yves Hurtubise, Claude Daneault, and Marc Beauregard. 2008. "Homologous Cloning, Expression, and Characterisation of a Laccase from Streptomyces Coelicolor and Enzymatic Decolourisation of an Indigo Dye." *Applied Microbiology and Biotechnology* 79 (4): 597–603. https://doi.org/10.1007/s00253-008-1475-5.

Durão, Paulo, Zhenjia Chen, André T. Fernandes, Peter Hildebrandt, Daniel H. Murgida, Smilja Todorovic, Manuela M. Pereira, Eduardo P. Melo, and Lígia O. Martins. 2008. "Copper Incorporation into Recombinant CotA Laccase from Bacillus Subtilis: Characterization of Fully Copper Loaded Enzymes." *JBIC Journal of Biological Inorganic Chemistry* 13 (2): 183–93. https://doi.org/10.1007/s00775-007-0312-0.

Dusselier, Michiel, Mark Mascal, and Bert Sels. 2014. *Top Chemical Opportunities from Carbohydrate Biomass: A Chemist's View of the Biorefinery*. Vol. 353. https://doi.org/10.1007/128_2014_544.

Engelking, Larry R. 2015. "Chapter 6 - Enzyme Kinetics." In *Textbook of Veterinary Physiological Chemistry (Third Edition)*, edited by Larry R. Engelking, 32–38. Boston: Academic Press. https://doi.org/10.1016/B978-0-12-391909-0.50006-2.

Fang, Zhen, and Richard L. Smith, eds. 2016. *Production of Biofuels and Chemicals from Lignin*. Biofuels and Biorefineries. Singapore: Springer Singapore. http://link.springer.com/10.1007/978-981-10-1965-4.

Fernandes, Tatiana Alves Rigamonte, Wendel Batista da Silveira, Flávia Maria Lopes Passos, and Tiago Domingues Zucchi. 2014. "Laccases from <I>Actinobacteria</I>—What We Have and What to Expect." *Advances in Microbiology* 04 (06): 285–96. https://doi.org/10.4236/aim.2014.46035.

Fink, Anthony L. 1998. "Protein Aggregation: Folding Aggregates, Inclusion Bodies and Amyloid." *Folding and Design* 3 (1): R9–23. https://doi.org/10.1016/S1359-0278(98)00002-9.

FitzPatrick, Michael, Pascale Champagne, Michael F. Cunningham, and Ralph A. Whitney. 2010. "A Biorefinery Processing Perspective: Treatment of Lignocellulosic Materials for the Production of Value-Added Products." *Bioresource Technology* 101 (23): 8915–22. https://doi.org/10.1016/j.biortech.2010.06.125.

Fong, D. H., D. L. Burk, and A. M. Berghuis. 2005. "Aminoglycoside Kinases and Antibiotic Resistance." In *Inhibitors of Protein Kinases and Protein Phosphates*, edited by Lorenzo A. Pinna and Patricia T.W. Cohen, 157–88. Handbook of Experimental Pharmacology. Berlin, Heidelberg: Springer Berlin Heidelberg. https://doi.org/10.1007/3-540-26670-4_7.

Forge, Andrew, and Jochen Schacht. 2000. "Aminoglycoside Antibiotics." *Audiology and Neurotology* 5 (1): 3–22. https://doi.org/10.1159/000013861.

Foustoukos, Dionysis. 2014. "Specific Activity." In *Encyclopedia of Astrobiology*, edited by Ricardo Amils, Muriel Gargaud, José Cernicharo Quintanilla, Henderson James Cleaves, William M. Irvine, Daniele Pinti, and Michel Viso, 1–1. Berlin, Heidelberg: Springer Berlin Heidelberg. https://doi.org/10.1007/978-3-642-27833-4_1481-2.

Gabdulkhakov, A. G., O. S. Kostareva, I. A. Kolyadenko, A. O. Mikhaylina, L. I. Trubitsina, and S. V. Tishchenko. 2018. "Incorporation of Copper Ions into T2/T3 Centers of Two-Domain Laccases." *Molecular Biology* 52 (1): 23–29. https://doi.org/10.1134/S0026893318010041.

Galaev, I. Yu., A. Kumar, R. Agarwal, M. N. Gupta, and B. Mattiasson. 1997. "Imidazole—a New Ligand for Metal Affinity Precipitation." *Applied Biochemistry and Biotechnology* 68 (1): 121–33. https://doi.org/10.1007/BF02785985.

Gianfreda, Liliana, Feng Xu, and Jean-Marc Bollag. 1999. "Laccases: A Useful Group of Oxidoreductive Enzymes." *Bioremediation Journal* 3 (1): 1–26. https://doi.org/10.1080/10889869991219163.

Hämäläinen, Veera, Toni Grönroos, Anu Suonpää, Matti Wilhem Heikkilä, Bastiaan Romein, Petri Ihalainen, Sara Malandra, and Klara R. Birikh. 2018. "Enzymatic Processes to Unlock the Lignin Value." *Frontiers in Bioengineering and Biotechnology* 6 (March). https://doi.org/10.3389/fbioe.2018.00020.

Hasunuma, Tomohisa, Fumiyoshi Okazaki, Naoko Okai, Kiyotaka Y. Hara, Jun Ishii, and Akihiko Kondo. 2013. "A Review of Enzymes and Microbes for Lignocellulosic Biorefinery and the Possibility of Their Application to Consolidated Bioprocessing Technology." *Bioresource Technology*, Biorefineries, 135 (May): 513–22. https://doi.org/10.1016/j.biortech.2012.10.047.

Hildén, Kristiina, Terhi K. Hakala, and Taina Lundell. 2009. "Thermotolerant and Thermostable Laccases." *Biotechnology Letters* 31 (8): 1117. https://doi.org/10.1007/s10529-009-9998-0.

Hullo, M. F., I. Moszer, A. Danchin, and I. Martin-Verstraete. 2001. "CotA of Bacillus Subtilis Is a Copper-Dependent Laccase." *Journal of Bacteriology* 183 (18): 5426–30.

Iimura, Yosuke, Tomonori Sonoki, and Hiroshi Habe. 2018. "Heterologous Expression of Trametes Versicolor Laccase in Saccharomyces Cerevisiae." *Protein Expression and Purification* 141 (January): 39–43. https://doi.org/10.1016/j.pep.2017.09.004.

Isikgor, Furkan H., and C. Remzi Becer. 2015. "Lignocellulosic Biomass: A Sustainable Platform for the Production of Bio-Based Chemicals and Polymers." *Polymer Chemistry* 6 (25): 4497–4559. https://doi.org/10.1039/C5PY00263J.

Jambovane, Sachin, Evert C. Duin, Se-Kwon Kim, and Jong Wook Hong. 2009. "Determination of Kinetic Parameters, Km and Kcat, with a Single Experiment on a Chip." *Analytical Chemistry* 81 (9): 3239–45. https://doi.org/10.1021/ac8020938.

Janusz, Grzegorz, Anna Pawlik, Justyna Sulej, Urszula Świderska-Burek, Anna Jarosz-Wilkołazka, and Andrzej Paszczyński. 2017. "Lignin Degradation: Microorganisms, Enzymes Involved, Genomes Analysis and Evolution." *FEMS Microbiology Reviews* 41 (6): 941–62. https://doi.org/10.1093/femsre/fux049.

Jones, Stephen M., and Edward I. Solomon. 2015. "Electron Transfer and Reaction Mechanism of Laccases." *Cellular and Molecular Life Sciences* 72 (5): 869–83. https://doi.org/10.1007/s00018-014-1826-6.

Jørgensen, Henning, Jan Bach Kristensen, and Claus Felby. 2007. "Enzymatic Conversion of Lignocellulose into Fermentable Sugars: Challenges and Opportunities." *Biofuels, Bioproducts and Biorefining* 1 (2): 119–34. https://doi.org/10.1002/bbb.4.

Kang, Aram, and Taek Soon Lee. 2015. "Converting Sugars to Biofuels: Ethanol and Beyond." *Bioengineering* 2 (4): 184–203. https://doi.org/10.3390/bioengineering2040184.

Komori, Hirofumi, and Yoshiki Higuchi. 2015. "Structural Insights into the O2 Reduction Mechanism of Multicopper Oxidase." *Journal of Biochemistry* 158 (4): 293–98. https://doi.org/10.1093/jb/mvv079.

Ledent, Philippe, Colette Duez, Marc Vanhove, Annabelle Lejeune, Eveline Fonzé, Paulette Charlier, Fouzia Rhazi-Filali, et al. 1997. "Unexpected Influence of a C-Terminal-Fused His-Tag on the Processing of an Enzyme and on the Kinetic and Folding Parameters." *FEBS Letters* 413 (2): 194–96. https://doi.org/10.1016/S0014-5793(97)00908-3.

Longe, Lionel F., Julien Couvreur, Mathilde Leriche Grandchamp, Gil Garnier, Florent Allais, and Kei Saito. 2018. "Importance of Mediators for Lignin Degradation by Fungal Laccase." *ACS Sustainable Chemistry & Engineering* 6 (8): 10097–107. https://doi.org/10.1021/acssuschemeng.8b01426.

Lu, Fachuang, and John Ralph. 2010. "Chapter 6 - Lignin." In *Cereal Straw as a Resource for Sustainable Biomaterials and Biofuels*, edited by Run-Cang Sun, 169–207. Amsterdam: Elsevier. https://doi.org/10.1016/B978-0-444-53234-3.00006-7.

Luo, Lin, Ester van der Voet, and Gjalt Huppes. 2010. "Biorefining of Lignocellulosic Feedstock – Technical, Economic and Environmental Considerations." *Bioresource Technology*, Special Issue on Lignocellulosic Bioethanol: Current Status and Perspectives, 101 (13): 5023–32. https://doi.org/10.1016/j.biortech.2009.12.109.

Machczynski, Michael C., Erik Vijgenboom, Bart Samyn, and Gerard W. Canters. 2004. "Characterization of SLAC: A Small Laccase from Streptomyces Coelicolor with Unprecedented Activity." *Protein Science* 13 (9): 2388–97. https://doi.org/10.1110/ps.04759104.

Mayer, Helmut. 1999. "Air Pollution in Cities." *Atmospheric Environment* 33 (24): 4029–37. https://doi.org/10.1016/S1352-2310(99)00144-2.

"Michaelis-Menten Kinetics and Briggs-Haldane Kinetics." n.d. Accessed May 9, 2019. https://depts.washington.edu/wmatkins/kinetics/michaelis-menten.html.

Miller, Richard G., and Steven R. Sorrell. 2014. "The Future of Oil Supply." *Philosophical Transactions. Series A, Mathematical, Physical, and Engineering Sciences* 372 (2006). https://doi.org/10.1098/rsta.2013.0179.

Moghadam, Morteza Shojaei, Andreas Albersmeier, Anika Winkler, Lorenzo Cimmino, Kjersti Rise, Martin Frank Hohmann-Marriott, Jörn Kalinowski, Christian Rückert, Alexander Wentzel, and Rahmi Lale. 2016. "Isolation and Genome Sequencing of Four Arctic Marine Psychrobacter Strains Exhibiting Multicopper Oxidase Activity." *BMC Genomics* 17: 117. https://doi.org/10.1186/s12864-016-2445-4.

Morozova, O. V., G. P. Shumakovich, S. V. Shleev, and Ya I. Yaropolov. 2007. "Laccase-Mediator Systems and Their Applications: A Review." *Applied Biochemistry and Microbiology* 43 (5): 523–35. https://doi.org/10.1134/S0003683807050055.

Munk, Line, Anna K. Sitarz, Dayanand C. Kalyani, J. Dalgaard Mikkelsen, and Anne S. Meyer. 2015. "Can Laccases Catalyze Bond Cleavage in Lignin?" *Biotechnology Advances* 33 (1): 13–24. https://doi.org/10.1016/j.biotechadv.2014.12.008.

Nataro, James P., and James B. Kaper. 1998. "Diarrheagenic Escherichia Coli." *Clinical Microbiology Reviews* 11 (1): 142–201. https://doi.org/10.1128/CMR.11.1.142.

"Oil and Natural Gas Depletion and Our Future." 2007. Resilience. July 20, 2007. https://www.resilience.org/stories/2007-07-21/oil-and-natural-gas-depletion-and-our-future/.

Oreskes, Naomi. 2004. "The Scientific Consensus on Climate Change." *Science* 306 (5702): 1686–1686. https://doi.org/10.1126/science.1103618.

Parthasarathi, R., Raymond A. Romero, Antonio Redondo, and S. Gnanakaran. 2011. "Theoretical Study of the Remarkably Diverse Linkages in Lignin." *The Journal of Physical Chemistry Letters* 2 (20): 2660–66. https://doi.org/10.1021/jz201201q.

Phillips, Allen T., and Mark W. Signs. 2005. "Desalting, Concentration, and Buffer Exchange by Dialysis and Ultrafiltration." *Current Protocols in Protein Science* Chapter 4 (January): Unit4.4. https://doi.org/10.1002/0471140864.ps0404s38.

Pollegioni, Loredano, Fabio Tonin, and Elena Rosini. 2015. "Lignin-Degrading Enzymes." *FEBS Journal* 282 (7): 1190–1213. https://doi.org/10.1111/febs.13224.

Prete, Sonia Del, Daniela Vullo, Viviana De Luca, Zeid AlOthman, Sameh M. Osman, Claudiu T. Supuran, and Clemente Capasso. 2015. "Biochemical Characterization of Recombinant β-Carbonic Anhydrase (PgiCAb) Identified in the Genome of the Oral Pathogenic Bacterium Porphyromonas Gingivalis." *Journal of Enzyme Inhibition and Medicinal Chemistry* 30 (3): 366–70. https://doi.org/10.3109/14756366.2014.931383.

Rahmanpour, Rahman, and Timothy D.H. Bugg. 2015. "Characterisation of Dyp-Type Peroxidases from Pseudomonas Fluorescens Pf-5: Oxidation of Mn(II) and Polymeric Lignin by Dyp1B." *Archives of Biochemistry and Biophysics* 574 (May): 93–98. https://doi.org/10.1016/j.abb.2014.12.022.

Reiss, Renate, Julian Ihssen, Michael Richter, Eric Eichhorn, Boris Schilling, and Linda Thöny-Meyer. 2013. "Laccase versus Laccase-Like Multi-Copper Oxidase: A Comparative Study of Similar Enzymes with Diverse Substrate Spectra." Edited by Claudio M. Soares. *PLoS ONE* 8 (6): e65633. https://doi.org/10.1371/journal.pone.0065633.

Scheich, Christoph, Volker Sievert, and Konrad Büssow. 2003. "An Automated Method for High-Throughput Protein Purification Applied to a Comparison of His-Tag and GST-Tag Affinity Chromatography." *BMC Biotechnology* 3 (1): 12. https://doi.org/10.1186/1472-6750-3-12.

Shafiee, Shahriar, and Erkan Topal. 2009. "When Will Fossil Fuel Reserves Be Diminished?" *Energy Policy* 37 (1): 181–89. https://doi.org/10.1016/j.enpol.2008.08.016.

Shraddha, Ravi Shekher, Simran Sehgal, Mohit Kamthania, and Ajay Kumar. 2011. "Laccase: Microbial Sources, Production, Purification, and Potential Biotechnological Applications." *Enzyme Research* 2011 (June). https://doi.org/10.4061/2011/217861.

Sigoillot, Jean-Claude, Jean-Guy Berrin, Mathieu Bey, Laurence Lesage-Meessen, Anthony Levasseur, Anne Lomascolo, Eric Record, and Eva Uzan-Boukhris. 2012. "Chapter 8 - Fungal Strategies for Lignin Degradation." In *Advances in Botanical Research*, edited by Lise Jouanin and Catherine Lapierre, 61:263–308. Lignins. Academic Press. https://doi.org/10.1016/B978-0-12-416023-1.00008-2.

Silva, E. A. Borges da, M. Zabkova, J. D. Araújo, C. A. Cateto, M. F. Barreiro, M. N. Belgacem, and A. E. Rodrigues. 2009. "An Integrated Process to Produce Vanillin and Lignin-Based Polyurethanes from Kraft Lignin." *Chemical Engineering Research and Design*, Special Issue on Biorefinery Integration, 87 (9): 1276–92. https://doi.org/10.1016/j.cherd.2009.05.008.

Skálová, Tereza, Jan Dohnálek, Lars Henrik Østergaard, Peter Rahbek Østergaard, Petr Kolenko, Jarmila Dušková, Andrea Štěpánková, and Jindřich Hašek. 2009. "The Structure of the Small Laccase from Streptomyces Coelicolor Reveals a Link between Laccases and Nitrite Reductases." *Journal of Molecular Biology* 385 (4): 1165–78. https://doi.org/10.1016/j.jmb.2008.11.024.

Solís-Oba, Myrna, Victor Manuel Ugalde-Saldívar, Ignacio González, and Gustavo Viniegra-González. 2005. "An Electrochemical–Spectrophotometrical Study of the Oxidized Forms of the Mediator 2,2′-Azino-Bis-(3-Ethylbenzothiazoline-6-Sulfonic Acid) Produced by Immobilized Laccase." *Journal of Electroanalytical Chemistry* 579 (1): 59–66. https://doi.org/10.1016/j.jelechem.2005.01.025.

Sondhi, Sonica, Prince Sharma, Shilpa Saini, Neena Puri, and Naveen Gupta. 2014. "Purification and Characterization of an Extracellular, Thermo-Alkali-Stable, Metal Tolerant Laccase from Bacillus Tequilensis SN4." *PloS One* 9 (May): e96951. https://doi.org/10.1371/journal.pone.0096951.

Spiker, Jennifer K., Don L. Crawford, and Elizabeth C. Thiel. 1992. "Oxidation of Phenolic and Non-Phenolic Substrates by the Lignin Peroxidase of Streptomyces Viridosporus T7A." *Applied Microbiology and Biotechnology* 37 (4): 518–23. https://doi.org/10.1007/BF00180980.

Stoll, Vincent S., and John S. Blanchard. 1990. "[4] Buffers: Principles and Practice." In *Methods in Enzymology*, edited by Murray P. Deutscher, 182:24–38. Guide to Protein Purification. Academic Press. https://doi.org/10.1016/0076-6879(90)82006-N.

Terrón, M.C., M. López-Fernández, J.M. Carbajo, H. Junca, A. Téllez, S. Yagüe, A. Arana-Cuenca, T. González, and A.E. González. 2004. "Tannic Acid Interferes with the Commonly Used Laccase-Detection Assay Based on ABTS as the Substrate." *Biochimie* 86 (8): 519–22. https://doi.org/10.1016/j.biochi.2004.07.013.

Torre, Mª Jesús de la, Ana Moral, Mª Dolores Hernández, Elena Cabeza, and Antonio Tijero. 2013. "Organosolv Lignin for Biofuel." *Industrial Crops and Products* 45 (February): 58–63. https://doi.org/10.1016/j.indcrop.2012.12.002.

Vashchenko, Ganna, and Ross T. A. MacGillivray. 2013. "Multi-Copper Oxidases and Human Iron Metabolism." *Nutrients* 5 (7): 2289–2313. https://doi.org/10.3390/nu5072289.

Ventura, Marco, Carlos Canchaya, Andreas Tauch, Govind Chandra, Gerald F. Fitzgerald, Keith F. Chater, and Douwe van Sinderen. 2007. "Genomics of Actinobacteria: Tracing the Evolutionary History of an Ancient Phylum." *Microbiol. Mol. Biol. Rev.* 71 (3): 495–548. https://doi.org/10.1128/MMBR.00005-07.

Vollum, R. L., D. G. Jamison, and C. S. Cummins, eds. 1970. "Chapter IV - The Cultivation of Bacteria." In *Fairbrother's Textbook of Bacteriology (Tenth Edition)*, 32–41. Butterworth-Heinemann. https://doi.org/10.1016/B978-0-433-10100-0.50008-X.

Wang, Chunlei, Daizong Cui, Lei Lu, Ning Zhang, Hongyi Yang, Min Zhao, and Shaojun Dai. 2016. "Cloning and Characterization of CotA Laccase from Bacillus Subtilis WD23 Decoloring Dyes." *Annals of Microbiology* 66 (1): 461–67. https://doi.org/10.1007/s13213-015-1128-8.

Xanthos, Dirk, and Tony R. Walker. 2017. "International Policies to Reduce Plastic Marine Pollution from Single-Use Plastics (Plastic Bags and Microbeads): A Review." *Marine Pollution Bulletin* 118 (1): 17–26. https://doi.org/10.1016/j.marpolbul.2017.02.048.

Yang, Sheng, Jia-Long Wen, Tong-Qi Yuan, and Run-Cang Sun. 2014. "Characterization and Phenolation of Biorefinery Technical Lignins for Lignin–Phenol–Formaldehyde Resin Adhesive Synthesis." *RSC Adv.* 4 (101): 57996–4. https://doi.org/10.1039/C4RA09595B.

Zeng, Ximin, and Jun Lin. 2013. "Beta-Lactamase Induction and Cell Wall Metabolism in Gram-Negative Bacteria." *Frontiers in Microbiology* 4 (May). https://doi.org/10.3389/fmicb.2013.00128.

Zhang, Zhanrong, Jinliang Song, and Buxing Han. 2016. "Catalytic Transformation of Lignocellulose into Chemicals and Fuel Products in Ionic Liquids." *Chemical Reviews*, November. https://doi.org/10.1021/acs.chemrev.6b00457.

7. Appendices

7.1. Appendix A

Table 7.1. Overview of small phenolic substances for laccase substrate screening. The observed activity of P01-C03, P01-E07, P06-A08 and P20-F12 towards the phenolic substances used for substrate screening is presented (+ = activity observed, - = no activity observed). The observed activity of CotA with the same substrates (previous work by SINTEF in ERA-IB OXYPOL) is also presented. The wavelengths used for absorption during activity assay with the respective substrates is indicated.

Substrate	P01-C03	P01-E07	P06-A08	P20-F12	cotA (previous work)
Ferulic acid (322 nm)	-	-	-	+ 0.05U/mg	+
Sinapic acid (330 nm)	-	-	-	+ 2.41 U/mg 16.07 U/mg	+
4-Hydroxybenzoic acid (254 nm)	-	-	-	-	-
3,4-Dihydroxybenzoic acid (258 nm)	-	-	-	+ (Not quantifiable)	+
Vanillic acid (262 nm)	-	-	-	-	+
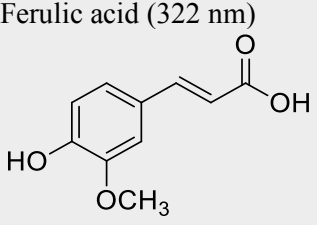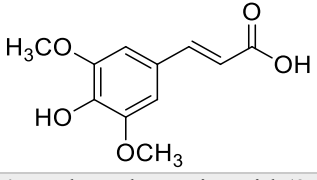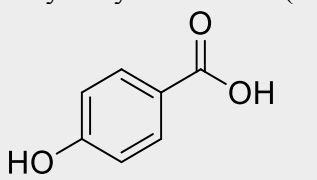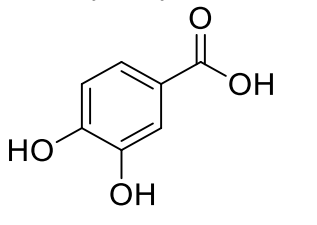
121
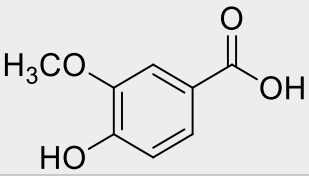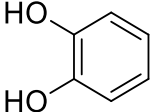
Compound					
Catechol (276 nm)	-	-	-	+	+
				0.07U/mg	
Guaiacol (278 nm)	-	-	-	-	+
Syringealdehyde (308 nm)	-	-	-	-	+
Vanillin (280 nm)	-	-	-	-	-
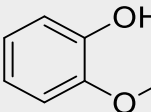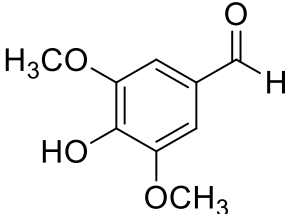
7.2. Appendix B

Table 7.2. Length (amino acids) and MW (kDa) of the three Psychrobacter enzymes P2G3, P11G3 and P11F6

Enzyme	Length (amino acids)	MW (kDa)
P2G3	545	61.714
P11G3	547	61.692
P11F6	549	61.887

7.3. Appendix C

Table 7.3. Average protein concentration (mg/mL) of three biological replicas measured with Qubit assay before and after purification and buffer exchange

Enzyme and CuCl$_2$ supplementation strategy	Average protein concentration (mg/mL) of	Average protein concentration (mg/mL) of three parallels of enzyme

122

	three parallels of cell extract before purification	solution after purification and buffer exchange
P11F6, strategy 1	0.487	0.127
P11F6, strategy 2	0.492	0.123
P11F6, strategy 3	0.49	0.148
P11G3, strategy 1	0.484	0.092
P11G3, strategy 2	0.483	0.122
P11G3, strategy 3	0.48	0.106
P2G3, strategy 1	0.476	0.038
P2G3, strategy 2	0.476	0.059
P2G3, strategy 3	0.476	0.056

7.4. Appendix D
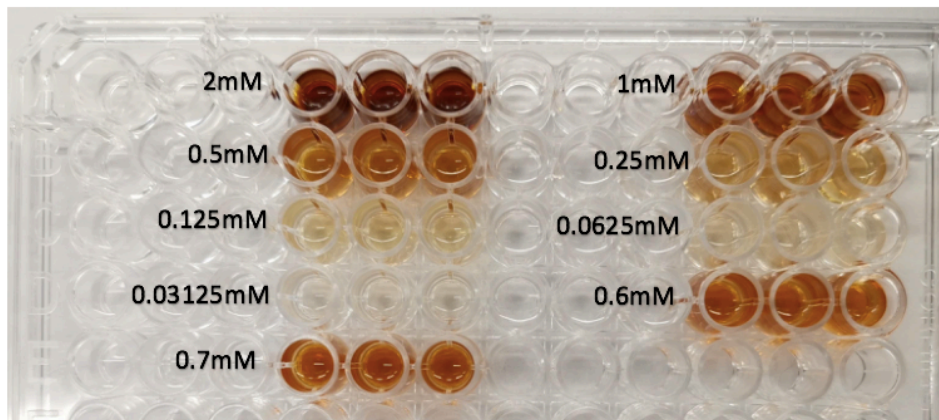
Figure 7.1. P20-F12 activity assay with sinapic acid. Color change in a CORNING 96-well plate after activity assay of the enzyme P20-F12 with different concentrations of sinapic acid. Control samples can be observed in the three wells to the left of each sinapic acid color change.

7.5. Appendix E

Multiple sequence alignment of the nucleotide sequences of the *Actinobacteria* laccases P01-C03, P01-E07, P06-A08 and P20-F12.

```
                                          1         10        20        30        40        50        60
                                          |         |         |         |         |         |         |
N-His_P01-C03 _pET-21a(+) extraction   CATATGCATCACCATCACCATCACAGCGAGGCGAACGGTAGCATCGGCCGTCGTGGTTTT
N-His_P01-E07 _pET-21a(+) extraction   CATATGCATCACCATCACCATCAC----------------------GACCGTCGTACCTTC
N-His_P06-A08 _pET-21a(+) extraction   CATATGCATCACCATCACCATCACC----CGCGTAGCGGT----CTGAGCCGTCGTAGCATT
N-His_P20-F12 _pET-21a(+) extraction   CATATGCATCACCATCACCATCACGATGATCATGCGGGTGGCCCGCACCGTC--ACCTGA

N-His_P01-C03 _pET-21a(+) extraction   C--ACCGTGGTCTGCTGGCGGGTGGCGCGGTTCTGGCGGCGGGTGGCCTGACCAGCATGA
N-His_P01-E07 _pET-21a(+) extraction   A--ACCGTCGTATGCTGGTTGGTGGTGGTGTGGCGGCGGCGACCGGTGTGACCAGCATGA
N-His_P06-A08 _pET-21a(+) extraction   CTGACCG--GTACCCTGGCGGGCCTGGTGGCGCCGACCGCG---GCGCTG---AGCCTGG
N-His_P20-F12 _pET-21a(+) extraction   G---CCGTCGTAGCCTGATTGCGACCGGTGCGCTGGCGGCGGGTGCGCTGGG-TGCGAGC

N-His_P01-C03 _pET-21a(+) extraction   GC-CAGAGC-------AGCGCG----GCGGCGGACACCCCGCCGAAGACCGCGCCGGCGGG
N-His_P01-E07 _pET-21a(+) extraction   GC-CTGGGTGCGGTTCAAGCGACCAGCG-CGGAGAACCCGGCGAAGACCGCGCCGGCGGG
N-His_P06-A08 _pET-21a(+) extraction   GCGCGGA--------TACCGCG----GCGGCGGCGAAACCGGGTCCGA-TTCGTCCGCTG-
N-His_P20-F12 _pET-21a(+) extraction   GCGCCGACCATTGGTACCGCGTTTGGTGGC-----AGCCCGGCGCG---TGCGGCGGCG--

N-His_P01-C03 _pET-21a(+) extraction   TGGCGAGGTTAAGCACCTGACCATGTACTGCGAAAAAATGGCGGATGGTATGACCGGTTA
N-His_P01-E07 _pET-21a(+) extraction   CGGTGCGGTGAAGCACCTGAAACTGTACGCGGAGAAACTGGCGGGCGGTCAACTGGGCTA
N-His_P06-A08 _pET-21a(+) extraction   -GGTACCACCCGTCACATCACCATTTTCGCGGAGGAACTGCCGGGTGGCCAATACGGTTA
N-His_P20-F12 _pET-21a(+) extraction   -GGCGTGACCAAGAAAATCACCATTTACGCGGAGCAGCTGCCGGGTAACCTGTTTGGTTA

N-His_P01-C03 _pET-21a(+) extraction   TGGCCTGGAGAAGGGCAAACCGAGCATCCCGGGTCCGCTGATTGAGCTGAACGAAGGTGA
N-His_P01-E07 _pET-21a(+) extraction   TGGTTTCGAAAAGGGCAAAGCGAGCGTGCCGGGTCCGCTGATCGAGATTACCGAAGGTGA
N-His_P06-A08 _pET-21a(+) extraction   TGGCCTGACCCCGGGTAAAGCGACCATTCCGGGTCCGCTGCTGGAGATGTGGGAAGGTGA
N-His_P20-F12 _pET-21a(+) extraction   TGGCCTGGCGCCGGGTCAAGCGACCGTTCCGGGTCCGATCCTGGAGATGTACGAAGGCGA

N-His_P01-C03 _pET-21a(+) extraction   CACCCTGCACATCGAATTCCACAACCTGCTGGATGTGGATGCGAGCCTGCATGCGCACGG
N-His_P01-E07 _pET-21a(+) extraction   CACCCTGCACATCGAGTTTGAAAACACCACCGACGTTGATGCGAGCCTGCACGTGCACGG
N-His_P06-A08 _pET-21a(+) extraction   TACCCTGCAAATCGAGCTGGTGAACAACACCGACCAGCGTCTGAGCATTCACCCGCACGG
N-His_P20-F12 _pET-21a(+) extraction   CACCCTGGAGATTACCCTGGTGAACACCACCAACCAGCGTCTGAGCATCCACCCGCACGG

N-His_P01-C03 _pET-21a(+) extraction   CGTTGACTACGAGATTAGCAGCGATGGTA-CCCGTCAAAGCAACAGCCACGTGGAACCGG
N-His_P01-E07 _pET-21a(+) extraction   TGTTGACTACGATATTGCGAGCGATGGCA-CCCGTATGAACCGTAGCCACGTTGAACCGG
N-His_P06-A08 _pET-21a(+) extraction   TGTTGACTACAAGACCGAAAGCGATGGCAGCCCGT-TCAACGACAGCTTTAACGAGCCGG
N-His_P20-F12 _pET-21a(+) extraction   TGTTGACTATAGCACCGAAAGCGATGGCAGCCCGT-TCAACGCGAGCTTTAACAACCCGG

N-His_P01-C03 _pET-21a(+) extraction   GTGGCAGCCGTACCTACACCTGGCGTACCCATGCGCCGG-GTCGTCGTAAGGATGGTACC
N-His_P01-E07 _pET-21a(+) extraction   GCGGTACCCGTACCTATACCTGGCGTACCCACACCCGG-GTCGTCGTAAAGATGGTACC
N-His_P06-A08 _pET-21a(+) extraction   GTGAAACCCGTACCTATACCTGGGGCACCCACGAGCAGC-AACAGCTGGATGATGGTCAT
N-His_P20-F12 _pET-21a(+) extraction   GCGAGACCCGTACCTACGTGTGGCGTAGCCATGAAATGGTGGCGGCG-GCGGGTCGTCGT

N-His_P01-C03 _pET-21a(+) extraction   TGGCGTCCGGGTAGCGCGGGTTACTGGAACTATCACGACCACGTGGTTGGCACCGATCAT
N-His_P01-E07 _pET-21a(+) extraction   TGGCAGGCGGGTAGCGCGGGTTACTGGCACTATCACGACCACGTGGTTGGCACCGATCAC
N-His_P06-A08 _pET-21a(+) extraction   TGGCTGCCGGGTAGCGCGGGTTACTGGCACTATCACGATCATGCGCTGGGTGGCGAACAT
N-His_P20-F12 _pET-21a(+) extraction   TATATGCCGGGTAGCGCGGGCTACTGGCACTATCACGACCACGCGATGGGTACCGATCAT

N-His_P01-C03 _pET-21a(+) extraction   GGTACCGGTGGCCTGCGTCAGGGTCTGTATGGTGGCCTGATCGTTCGTCGTAAGGGTGAC
N-His_P01-E07 _pET-21a(+) extraction   GGTACCGGCGGTATCCGTAAAGGCCTGTACGGTCCGCTGGTTGTGCGTCGTAAGGGTGAC
N-His_P06-A08 _pET-21a(+) extraction   GGTACCGCGGGCCTGCGTGCGGGTCTGTACGGTGGCCTGATCGTTCGTCGTAAGGGCGAC
N-His_P20-F12 _pET-21a(+) extraction   GGTACCGGTGGCGTGGCGAAGGGTCTGTATGGTGCGCTGATCGTTCGTCGTCGTGGTGAC
```

```
N-His_P01-C03 _pET-21a(+) extraction    ATTCTGCCGGATAAAACCTTTCA-AATCGTGTTCAACGACATGACCGTTAACAACAAGCC
N-His_P01-E07 _pET-21a(+) extraction    GTGCTGCCGGATAAAACC-CTGACCATCGTTTTCAACGACATGACCATTAACAACAAGGC
N-His_P06-A08 _pET-21a(+) extraction    ATTCTGCCGGATCGTACC-TTCACCGTGGTTTTCAACGATATGACCATCAACAACAAGAG
N-His_P20-F12 _pET-21a(+) extraction    ATTCTGCCG-AGCAAGCAATTCACCGCGGTGTTCCACGATATGATGATCAACAACAAGAT

N-His_P01-C03 _pET-21a(+) extraction    GGGCCACGAGAGCCCGAACTTTGAAGCGACCGTGGGTGATCGTATCGAGGTTCTGAGCAT
N-His_P01-E07 _pET-21a(+) extraction    GGCGCACGAGAGCCCGAACTTTGAAGCGACCGTGGGTGATCGTGTTGAGGTGGTTATGAT
N-His_P06-A08 _pET-21a(+) extraction    CGCGCCGGACACCCCGATGTTTGAGGCGAACCTGGGCGAGACCGTGGAATTTCTGGCGAT
N-His_P20-F12 _pET-21a(+) extraction    GGCGCCGGCGACCCCGATGTTCGAAGCGAACCTGGGCGAGCGTGTTGAATGGATCGCGAT

N-His_P01-C03 _pET-21a(+) extraction    TACCCACGGCGAATTTTATCACACCTTCCACATGCACGGTCACCGTTGGGCGGACAACCG
N-His_P01-E07 _pET-21a(+) extraction    CACCCACGGTGAATACTATCACACCTTTCACATTCATGGTCACCGTTGGGCGGACAACCG
N-His_P06-A08 _pET-21a(+) extraction    TGGTCACGGCGACCAACTGCACACCTTCCACGTTCACGCGCACCGTTGGGCGAACAACCG
N-His_P20-F12 _pET-21a(+) extraction    TGGTCACGGCAACCTGTTCCACACCTTTCACCTGCACGCGCACCGTTGGGCGGACAACCG

N-His_P01-C03 _pET-21a(+) extraction    TACCGGTCTGCTGACCGGTCCGGATGATCCGAGCCCGGTGATCGACAACAAAATTACCGG
N-His_P01-E07 _pET-21a(+) extraction    TACCGGTCTGCTGACCGGTCCGGATGATCCGAGCCGTGTGGTTGACACCAAGATTTGCGG
N-His_P06-A08 _pET-21a(+) extraction    TACCGGTTACCTGACCGGTCCGGATGATCCGAGCCAGATTGTGGACAACGCGGATCTGAA
N-His_P20-F12 _pET-21a(+) extraction    TACCGGTATGCTGGAGGGTCCGAGCGATCCGAGCCTGGTGGTTGACAACAAAGATCTGAA

N-His_P01-C03 _pET-21a(+) extraction    CCCGGCGGATAGCTTCGGTTTTCAGTTCATTGCGGGTGAAGGCGTGGGTGCGGGTGCGTG
N-His_P01-E07 _pET-21a(+) extraction    CCCGGCGGATAGCTTCGGTTTTCAAATTATTGCGGGTGAACATGTGGGTGCGGGTGCGTG
N-His_P06-A08 _pET-21a(+) extraction    CCCGGGTAGCAGCTTCGGCTTTCAAGTGAAGGCGGGTCAGAAAGTTGGTGCGGGCGCGTG
N-His_P20-F12 _pET-21a(+) extraction    CCCGGGTAGCAGCTTCGGCTTTCAGGTTCTGGCGGGTGAAGGCGTTGGTCCGGGTGCGTG

N-His_P01-C03 _pET-21a(+) extraction    GATGTACCACTGCCACGTTCAAAGCCACAGCGACATGGGCATGGCGGGTCTGTTCCTGAT
N-His_P01-E07 _pET-21a(+) extraction    GATGTACCACTGCCACGTTCAAAGCCACAGCGATATGGGCATGGCGGGTCTGCTGCTGGT
N-His_P06-A08 _pET-21a(+) extraction    GATGTATCACTGCCACGTTCAGTTCCACAGCGATGGTGGCATGGCGGGCGTGTTTCTGGT
N-His_P20-F12 _pET-21a(+) extraction    GATGTATCACTGCCACGTGCAAACCCACAGCGACGGTGGCATGGCGGGTATCTTCCTGGT

N-His_P01-C03 _pET-21a(+) extraction    CGCGAAGAAAGATGGCACCATTCCGGGGTTATGATCCGGATGCGCCGCACCACACCG-CGC
N-His_P01-E07 _pET-21a(+) extraction    TGCGAAACCGGACGGCACCGTTCCGGGGTTATGATC-------CGCCGCACCAC------G-
N-His_P06-A08 _pET-21a(+) extraction    TCGTAACGCGGATGGTAGCATGCCGGATGGTGCGCAAGAGGCGATTGACCGTTTTCACGA
N-His_P20-F12 _pET-21a(+) extraction    TCGTAACGCGGATGGTAGCATGCCGCCAGGTGCTGAGGAAGCGATTCACCGTTTT-----

N-His_P01-C03 _pET-21a(+) extraction    CGAAGAAAAGCAGCAAAGAGGCGGCGGAGGAAAAAGCTGCGGCGGAGAAGAAAGGCGAAG
N-His_P01-E07 _pET-21a(+) extraction    -------------------------CGGCGGCG-----------------G----------
N-His_P06-A08 _pET-21a(+) extraction    ACA----------------------CGGTGGCCACACCACCGGTG---ATGCGACCCAGAG
N-His_P20-F12 _pET-21a(+) extraction    -------------------------CAG-GGTCACA--------------------CCC----

N-His_P01-C03 _pET-21a(+) extraction    CGCAGAGCGGCAAGAGCAGCCAGGCGGAAAGC---GGTGGCCATGCGCACCACTAACTCG
N-His_P01-E07 _pET-21a(+) extraction    --------CGGACGATGC------GGCGGG----------TGCGCACG---AACACTAACTCG
N-His_P06-A08 _pET-21a(+) extraction    C-----GCGGACAAAACCGC--GGCGGGTAGCGCGGGTGGCCACGCGGGCCACTAACTCG
N-His_P20-F12 _pET-21a(+) extraction    -----------ACA---C------------------------CCACG---GCAGCTAACTCG

N-His_P01-C03 _pET-21a(+) extraction    AG
N-His_P01-E07 _pET-21a(+) extraction    AG
N-His_P06-A08 _pET-21a(+) extraction    AG
N-His_P20-F12 _pET-21a(+) extraction    AG
```

7.6. Appendix F

Amino acid sequence of N-His P01-C03 expressed from the pET-21 a(+) plasmid vector

```
1          10          20          30          40          50
|           |           |           |           |           |
HMHHHHHHSEANGSIGRRGFHRGLLAGGAVLAAGGLTSMSQSSAAADTPP
KTAPAGGEVKHLTMYCEKMADGMTGYGLEKGKPSIPGPLIELNEGDTLHI
EFHNLLDVDASLHAHGVDYEISSDGTRQSNSHVEPGGSRTYTWRTHAPGR
RKDGTWRPGSAGYWNYHDHVVGTDHGTGGLRQGLYGGLIVRRKGDILPDK
TFQIVFNDMTVNNKPGHESPNFEATVGDRIEVLSITHGEFYHTFHMHGHR
WADNRTGLLTGPDDPSPVIDNKITGPADSFGFQFIAGEGVGAGAWMYHCH
VQSHSDMGMAGLFLIAKKDGTIPGYDPDAPHHTAPKKSSKEAAEEKAAAE
KKGEAQSGKSSQAESGGHAHH*LE
```

Amino acid sequence of N-His P01-E07 expressed from the pET-21 a(+) plasmid vector

```
1          10          20          30          40          50
|           |           |           |           |           |
HMHHHHHHDRRTFNRRMLVGGGVAAATGVTSMSLGAVQATSAENPAKTAP
AGGAVKHLKLYAEKLAGGQLGYGFEKGKASVPGPLIEITEGDTLHIEFEN
TTDVDASLHVHGVDYDIASDGTRMNRSHVEPGGTRTYTWRTHTPGRRKDG
TWQAGSAGYWHYHDHVVGTDHGTGGIRKGLYGPLVVRRKGDVLPDKTLTI
VFNDMTINNKAAHESPNFEATVGDRVEVVMITHGEYYHTFHIHGHRWADN
RTGLLTGPDDPSRVVDTKICGPADSFGFQIIAGEHVGAGAWMYHCHVQSH
SDMGMAGLLLVAKPDGTVPGYDPPHHAAAADDAAGAHEH*LE
```

Amino acid sequence of N-His P06-A08 expressed from the pET-21 a(+) plasmid vector

```
1          10          20          30          40          50
|           |           |           |           |           |
HMHHHHHHPRSGLSRRSILTGTLAGLVAPTAALSLGADTAAAAKPGPIRP
LGTTRHITIFAEELPGGQYGYGLTPGKATIPGPLLEMWEGDTLQIELVNN
TDQRLSIHPHGVDYKTESDGSPFNDSFNEPGETRTYTWGTHEQQQLDDGH
WLPGSAGYWHYHDHALGGEHGTAGLRAGLYGGLIVRRKGDILPDRTFTVV
FNDMTINNKSAPDTPMFEANLGETVEFLAIGHGDQLHTFHVHAHRWANNR
TGYLTGPDDPSQIVDNADLNPGSSFGFQVKAGQKVGAGAWMYHCHVQFHS
DGGMAGVFLVRNADGSMPDGAQEAIDRFHEHGGHTTGDATQSADKTAAGS
AGGHAGH*LE
```

Amino acid sequence of N-His P20-F12 expressed from the pET-21 a(+) plasmid vector

```
1          10          20          30          40          50
|           |           |           |           |           |
HMHHHHHHDDHAGGPHRHLSRRSLIATGALAAGALGASAPTIGTAFGGSP
ARAAAGVTKKITIYAEQLPGNLFGYGLAPGQATVPGPILEMYEGDTLEIT
LVNTTNQRLSIHPHGVDYSTESDGSPFNASFNNPGETRTYVWRSHEMVAA
AGRRYMPGSAGYWHYHDHAMGTDHGTGGVAKGLYGALIVRRRGDILPSKQ
FTAVFHDMMINNKMAPATPMFEANLGERVEWIAIGHGNLFHTFHLHAHRW
ADNRTGMLEGPSDPSLVVDNKDLNPGSSFGFQVLAGEGVGPGAWMYHCHV
QTHSDGGMAGIFLVRNADGSMPPGAEEAIHRFQGHTHTHGS*LE
```

7.7. Appendix G

Table 7.4. PDB BLAST showing the best hit, query coverage, pairwise identity, and description of the best hit for P01-C03, P01-E07, P06-A08 and P20-F12. PDB BLAST was performed using the program Geneious.

Laccase	Best hit from PDB BLAST	Pairwise identity with PDB (%)	Query coverage (%)	Description of hits
P01-C03	*Streptomyces coelicolor*	80.4	40.44	Two-domain laccase
P01-E07	*Streptomyces coelicolor*	74.2	98.2	Laccase
P06-A08	*Streptomyces coelicolor*	54.6	89.8	Laccase
P20-F12	*Stremtomyces sviceus*	55.2	80.2	Small laccase